THE ROLE OF BRUTON'S TYROSINE KINASE AND PI3K p110δ IN MUTANT SHP2-INDUCED JUVENILE MYELOMONOCYTIC LEUKEMIA

Lisa Deng

Submitted to the faculty of the University Graduate School
in partial fulfillment of the requirements
for the degree
Doctor of Philosophy
in the Department of Medical and Molecular Genetics,
Indiana University

March 2018

Accepted by the Graduate Faculty of Indiana University, in partial fulfillment of the requirements for the degree of Doctor of Philosophy.

_____
Rebecca J. Chan, MD, PhD, Co-Chair

_____
Reuben Kapur, PhD, Co-Chair

Doctoral Committee

_____
Brittney-Shea Herbert, PhD

January 31, 2018

_____
Stephanie M. Ware, MD, PhD

_____
Mervin C. Yoder, MD

ACKNOWLEDGEMENTS

I give my heartfelt thanks to my mentor, Dr. Rebecca Chan. She welcomed me warmly into her lab and was a true mentor to me from the first day that I started my rotation. Under her tutelage, guidance, and encouragement, I have grown into a more careful and thorough scientist, and a more confident person. She sets a shining example of scientific rigor. I am thankful to have trained under such a kind and caring mentor.

I also thank my second mentor, Dr. Reuben Kapur, who made a great effort to make me feel welcome and well-supported in his lab during these last few months. He brought new insight to my project and proposed several key experiments at the end.

I thank the other members of my thesis committee, Dr. Mervin Yoder, Dr. Brittney-Shea Herbert, Dr. Stephanie Ware, and Dr. Nadia Carlesso, for taking the time and effort to give me sound scientific advice that has shaped my dissertation.

I thank the members of the Chan lab, past and present, who have helped me on my journey: Dr. Libby Virts, Dr. Victoria Jideonwo-Auman, Dr. Stefan Tarnawsky, Dr. Briana Richine, Dr. Charles Goodwin, and Dr. Xing-Jun Li. I also thank the members of the Kapur lab: Dr. Joydeep Ghosh, Dr. Anindo Chatterjee, Dr. Baskar Ramdas, Dr. Ping Hu, Dr. Reddy Palam, Dr. Ruchi Pandey, and Dr. Zhigang Cai.

I thank my collaborators, including Dr. Stacey Tannheimer at Gilead Sciences, Inc. and Dr. Cecile Krejsa at Acerta Pharma.

I thank the crucial people of the Herman B Wells Center whom keep it running, including Tracy Winkle, Les Lee, and Dave Schippnick. I thank the staff at the Laboratory Animal Resource Center, including Nancy Long, Dana Gonzales, and Dr. Keely Szilagyi. I

thank the technicians in the *In Vivo* Therapeutics Core, including Tony Sinn. I thank the technicians in the Flow Cytometry Facility, including Sue Rice.

I thank everyone in the Indiana University Medical Scientist Training Program, including Dr. Raghu Mirmira, Dr. Maureen Harrington, Jan Receuver, and my fellow student trainees.

I also specially acknowledge the many mice who I sacrificed for use in my experiments. They changed the way I live my life by inspiring me to avoid causing unnecessary harm and suffering to all animals. Their innocent lives, I sincerely hope, were not wasted but contributed to a meaningful cause.

I acknowledge my funding sources, the National Cancer Institute (National Research Service Award F30 CA210518), and the T32 HL0007910.

Finally, I give my deepest gratitude to my parents, Dr. Gary Deng and Dr. Soujuan Wang, who have given me everything I have. I thank my brother Albert Deng, my sister-in-law Dr. Zhichun Peng, and my niece Zoe Deng. Lastly, I thank Andrew Yuen for all his love and support. Thank you for brightening my life.

Lisa Deng

THE ROLE OF BRUTON'S TYROSINE KINASE AND PI3K p110δ IN MUTANT SHP2-INDUCED JUVENILE MYELOMONOCYTIC LEUKEMIA

Juvenile myelomonocytic leukemia (JMML) is an aggressive myeloproliferative neoplasm that lacks effective chemotherapies. Most commonly, patients have gain-of-function (GOF) oncogenic mutations in SHP2, leading to hyperactivation of ERK and AKT and hyperproliferation of cells in response to granulocyte macrophage-colony stimulating factor (GM-CSF). Our lab previously showed that p110δ, the hematopoietic-specific catalytic subunit of phosphoinositide 3-kinase, is a crucial mediator of mutant Shp2-induced GM-CSF hypersensitivity *in vitro*.

We treated oncogenic Shp2-expressing mice with a p110δ inhibitor and showed that the strong effect our lab observed *in vitro* translated into reduced splenomegaly and prolonged survival *in vivo*. We investigated molecules potentially cooperating with p110δ signaling and discovered that Bruton's tyrosine kinase (BTK) is hyperphosphorylated in GOF Shp2 myeloid cells. We used specific BTK and p110δ inhibitors to demonstrate that BTK cooperates with p110δ to hyperactivate Akt/Erk and to promote hyperproliferation. GOF Shp2-expressing mice treated *in vivo* with the drug combination targeting p110δ and BTK have significantly decreased splenomegaly and WBC counts.

We also explored the mechanism of BTK signaling and hypothesized that B cell adaptor for PI3K (BCAP) mediated BTK upregulation of PI3K activity. In mutant Shp2 macrophages, we observed BCAP phosphorylation specifically in the larger isoforms needed for PI3K activation, and BTK inhibition led to a dose-dependent reduction in this phosphorylation. We also demonstrated reduced interaction between BCAP and the PI3K regulatory p85α subunit bearing mutated SH2 domains.

Finally, we investigated the effects of mutated DNA methyltransferase 3A (*Dnmt3a*) in conjunction with GOF Shp2. Double mutant mice quickly became moribund with pronounced splenomegaly and leukocytosis. There was an expansion of mature myeloid cells in the periphery and myeloid progenitors in the bone marrow, plus anemia with evidence of compensatory erythropoiesis in the spleen.

Our findings show that the myeloproliferative neoplasm caused by GOF Shp2 is due to hyperactive p110δ, and this is further promoted by BTK, which forms a positive feedback loop with PI3K and BCAP, thus leading to more Akt/Erk hyperphosphorylation and more hyperproliferation in response to GM-CSF. The dual inhibition of p110δ and BTK represents a novel effective treatment strategy for JMML and other diseases induced by oncogenic Shp2.

Rebecca J. Chan, MD, PhD, Co-Chair

Reuben Kapur, PhD, Co-Chair

TABLE OF CONTENTS

LIST OF TABLES

LIST OF FIGURES

LIST OF ABBREVIATIONS

ALL……Acute Lymphoblastic Leukemia

AML……Acute Myeloid Leukemia

BCAP……B Cell Adaptor for PI3K

BCR……B Cell Receptor

BTK……Bruton's Tyrosine Kinase

CHIP……Clonal Hematopoiesis of Indeterminate Potential

CLL……Chronic Lymphocytic Leukemia

CML……Chronic Myelogenous Leukemia

CMP……Common Myeloid Progenitor

DNMT3A……DNA Methyltransferase 3A

EP……Erythroid Progenitor

FACS……Fluorescence-Assisted Cell Sorting

FBS……Fetal Bovine Serum

G-CSF……Granulocyte-Colony Stimulating Factor

GM-CSF……Granulocyte-Macrophage-Colony Stimulation Factor

GMP……Granulocyte Macrophage Progenitor

GVHD……Graft Versus Host Disease

HSC…… Hematopoietic Stem Cell

HSCT……Hematopoietic Stem Cell Transplant

IB……Immunoblot

IP……Immunoprecipitation

JMML……Juvenile Myelomonocytic Leukemia

LDMNC……Low-Density Mononuclear Cell

LRP……Lineage Restricted Progenitor

LSK……$Lineage^{-}Sca1^{+}cKit^{+}$

MAPK……Mitogen-Activated Protein Kinase

MCL……Mantle Cell Lymphoma

M-CSF……Macrophage-Colony Stimulating Factor

MEP……Megakaryocyte Erythrocyte Progenitor

MFI……Mean Fluorescent Intensity

MPN……Myeloproliferative Neoplasm

MDS……Myelodysplastic Syndrome

MPP……Multipotent Progenitor

MZL……Marginal Zone Lymphoma

PH……Plekstrin Homology

PI3K……Phosphoinositide 3-Kinase

PKC……Protein Kinase C

PLCγ2……Phospholipase C γ2

PTP……Protein Tyrosine Phosphatase

SCF……Stem Cell Factor

S.D……Standard Deviation

S.E.M……Standard Error of the Mean

SH2……Src Homology 2

SYK……Spleen Tyrosine Kinase

TEC……Tyrosine Kinase Expressed in Hepatocellular Carcinoma

TIR……Toll-IL-1 Receptor

TLR……Toll-like Receptor

TPO……Thrombopoietin

WBC……White Blood Cell

WM……Waldenström's Macroglobulinemia

WT……Wild Type

XID……X-linked Immunodeficiency

XLA……X-linked Agammaglobulinemia

YFP……Yellow Fluorescent Protein

CHAPTER ONE

INTRODUCTION

Juvenile Myelomonocytic Leukemia

Juvenile myelomonocytic leukemia (JMML) is an aggressive childhood myelodysplastic syndrome/myeloproliferative neoplasm (MDS/MPN). It is rare, with an incidence of about 1-2 cases per million, and makes up 2-3% of all childhood leukemias (Hasle, Wadsworth 1999, Passmore, Chessells 2003). The disease affects infants and young children, with a median age of 2 years. The typical presentation is notable for fever, failure to thrive, hepatosplenomegaly, thrombocytopenia, high white blood cell (WBC) count, and increased monocytes in the peripheral blood with some myeloid precursor cells (Loh 2011). The proper diagnosis of JMML can be difficult due to the rarity of the disease and because the presenting features are also associated with viral infections, such as cytomegalovirus, human herpesvirus-6, or Epstein-Barr virus (Lorenzana, Lyons 2002, Manabe, Yoshimasu 2004, Moritake, Ikeda 2009, Prabhu, Gupta 2010).

JMML (along with a few other diseases) bears features of both a myelodysplastic syndrome (MDS) as well as a myeloproliferative neoplasm (MPN). Thus, in 2001, the World Health Organization (WHO) created a separate category of mixed MDS and MPN for those leukemias that have characteristics of both. The WHO classification of myeloid tumors was revised in 2008 (Tefferi and Vardiman 2008) and again in 2016 (Arber, Orazi 2016), and the most up-to-date diagnostic criteria for JMML are listed in Table 1.1.

Table 1.1: Diagnostic criteria for JMML

I. Clinical and hematologic features (all 4 features mandatory)
• PB monocyte count ≥1 × 10^9/L (normal range = 0.2-1.0x10^9/L)
• Blast percentage in PB and BM <20%
• Splenomegaly
• Absence of Philadelphia chromosome (*BCR/ABL1* rearrangement)
II. Genetic studies (1 finding sufficient)
• Somatic mutation in *PTPN11* or *KRAS* or *NRAS* (germ line mutations must be excluded)
• Clinical diagnosis of NF1 or *NF1* mutation
• Germ line *CBL* mutation and loss of heterozygosity of CBL in BM and/or PB
III. For patients without genetic features, besides the clinical and hematologic features listed under I, the following criteria must be fulfilled:
• Monosomy 7 or any other chromosomal abnormality or at least 2 of the following criteria:
• Hemoglobin F increased for age
• Myeloid or erythroid precursors on PB smear
• GM-CSF hypersensitivity in colony assay
• Hyperphosphorylation of STAT5

Adapted from (Arber, Orazi 2016)

Patients over 4 years of age presenting with elevated fetal hemoglobin greater than 15% and platelets less than 33,000/uL fall into a poor prognosis category (Chan, Cooper 2009). For unknown reasons, there is a male predominance in JMML with a male to female ratio of 2.5:1 (Emanuel 2008).

The majority of JMML patients have mutations in the genes *PTPN11* (35%), *KRAS* or *NRAS* (35%), *NF1* (10%) and *CBL* (10%) (Chan, Cooper 2009, Hasle 2016). Of these, somatic *PTPN11* mutations tend to be the most aggressive and warrant immediate allogeneic hematopoietic stem cell transplant (HSCT). Conversely, a "watchful waiting" plan may be appropriate for cases with germline *PTPN11* and *CBL* mutations, and some somatic *NRAS* mutations, as cases with these mutations progress slowly and may even spontaneously resolve (Hasle 2016). However, these driver mutation classifications are not reliable indicators of disease aggressiveness. In recent years, whole-exome sequencing has been used to explore genomic differences between the aggressive and mild cases of JMML, and to identify previously unknown mutations involved in disease pathogenesis. Results from these studies provide additional information to resolve difficult decisions regarding treatment and offer strategies for developing novel therapies.

Sakaguchi et al. discovered from a cohort of 92 JMML patients that the genes *SETBP1* and *JAK3* are commonly involved as secondary somatic mutations (8% and 11%, respectively), especially in the presence of mutated *PTPN11* or *NF1*, and confer a much worse prognosis (Sakaguchi, Okuno 2013). Stieglitz et al. reported on a technique called droplet digital polymerase chain reaction that can be used to detect *SETBP1* mutations

in rare leukemia subclones at the time of diagnosis, thus identifying a much larger percentage of patients (30.3%) that harbor this aggressive form of JMML and should receive immediate HSCT (Stieglitz, Troup 2015). Furthermore, mutations in epigenetic modifiers were recently reported to be more common than previously believed, with the gene *DNMT3A* in particular found to be mutated in 3 of 100 JMML patients (Stieglitz, Taylor-Weiner 2015). These recent efforts reflect the drive to understand the underlying molecular mechanisms of JMML in an attempt to develop more personalized treatment plans and more targeted therapies for patients.

The current chemotherapeutic treatments for patients with JMML lack efficacy. Bergstrasser et al. demonstrated this conclusion by performing a retrospective study comparing various combination therapies, including interferon-alpha, etoposide, cytarabine, and 6-mercaptopurine/6-thioguanine. Importantly, in their analysis the authors standardized the definitions of disease regression using WBC count, platelet count, liver size, and spleen size. Although they found that certain agents resulted in partial responses, they concluded that all responses were transient and without improvement in overall survival (Bergstraesser, Hasle 2006). Because intensive chemotherapy is unable to significantly prolong survival, the only effective treatment is allogeneic HSCT, preferably from an HLA-matched donor, as the risk of relapse is higher if using unmatched donor HSCT or fetal cord blood. Cyclosporine-A, with or without methotrexate, is administered to prevent graft vs. host disease (GVHD), but may need to be reduced or discontinued to allow the graft vs. leukemia effect to occur. Because total body irradiation hampers this antileukemic effect and can lead to risk of infections, it is

recommended to be avoided as part of the conditioning regimen (Locatelli, Nöllke 2005).

Despite undergoing the aggressive intervention of allogeneic HSCT, about 50% of recipients will relapse with JMML, which is much higher than the 7% relapse rate seen in chronic myelogenous leukemia (CML) (Speck, Bortin 1984). Locatelli et al. reported that a cohort of 100 JMML patients, who were all conditioned identically with busulfan, cyclophosphamide, and melphalan, had a 64% 5-year overall survival and a 52% 5-year event-free survival. Thirty-four patients relapsed after HSCT at a median time of 6 months, and twenty-one patients had disease progression that resulted in death (Locatelli, Nöllke 2005). For patients who relapse, a second allogeneic HSCT with reduced amounts of immunosuppression has been recommended, but this intervention only rescues an additional one third of patients (Chang, Jou 2004, Inagaki, Fukano 2013, Yoshimi, Mohamed 2007). The ultimate cause of death is either transformation into acute myeloid leukemia (AML) or, more commonly, peripheral organ infiltration by monocytes and macrophages, leading to pulmonary failure, diarrhea, bleeding, and/or infection (Emanuel 2008).

Protein Tyrosine Phosphatase Non-Receptor Type 11 (*PTPN11*), SHP2

PTPN11 is the most commonly mutated gene in JMML at 35% of all cases. It encodes for SHP2, a non-receptor protein tyrosine phosphatase that is a positive regulator of many signaling pathways, including PDGFR, IRS1, JAK-STAT, and PI3K/AKT, among others (Mohi and Neel 2007, Ronnstrand, Arvidsson 1999). The protein structure

is notable for its N-Src homology 2 (N-SH2) domain and the protein tyrosine phosphatase (PTP) domain, which interact with each other to maintain the inactive conformation. Peptides with phospho-tyrosine residues bind to the N-SH2 and C-SH2 domains, causing SHP2 to open into its active form and allowing the PTP domain access to a substrate. Mutations in amino acid residues within these domains that preclude the folding of SHP2 into its inactive conformation lead to constitutive phosphatase activation, making *PTPN11* a *bona fide* proto-oncogene (Figure 1.1) (Chan and Feng 2007). Mutant *PTPN11* now has a well-established role as an oncogene in various leukemias such as JMML, AML, MDS, and acute lymphoblastic leukemia (Kratz, Niemeyer 2005, Loh, Reynolds 2004, Loh, Vattikuti 2004, Tartaglia, Martinelli 2004, Tartaglia, Niemeyer 2003), and in some solid tumors (Bentires-Alj, Paez 2004, Loh, Martinelli 2005, Martinelli, Carta 2006). SHP2's major role in promoting cancer lies in part in its ability to activate RAS-MAPK signaling, either by dephosphorylating (and thus inactivating) the RAS inhibitor, RAS-GAP, or dephosphorylating the SRC inhibitor, CSK, thus leading to more SRC activity and subsequent RAS activation (Chan and Feng 2007).

A recently published paper demonstrated that mutant SHP2 plays an oncogenic role even when expressed only in the bone marrow microenvironment. Dong et. al observed that mice developed myeloid leukemia when mutant *Ptpn11* was conditionally expressed only in bone marrow mesenchymal stem/progenitor cells using Nestin promoter-directed Cre expression. The authors also found that these mice developed a donor-derived myeloproliferative neoplasm after being transplanted with WT bone marrow cells (Dong, Yu 2016). This is the first study demonstrating that bone marrow

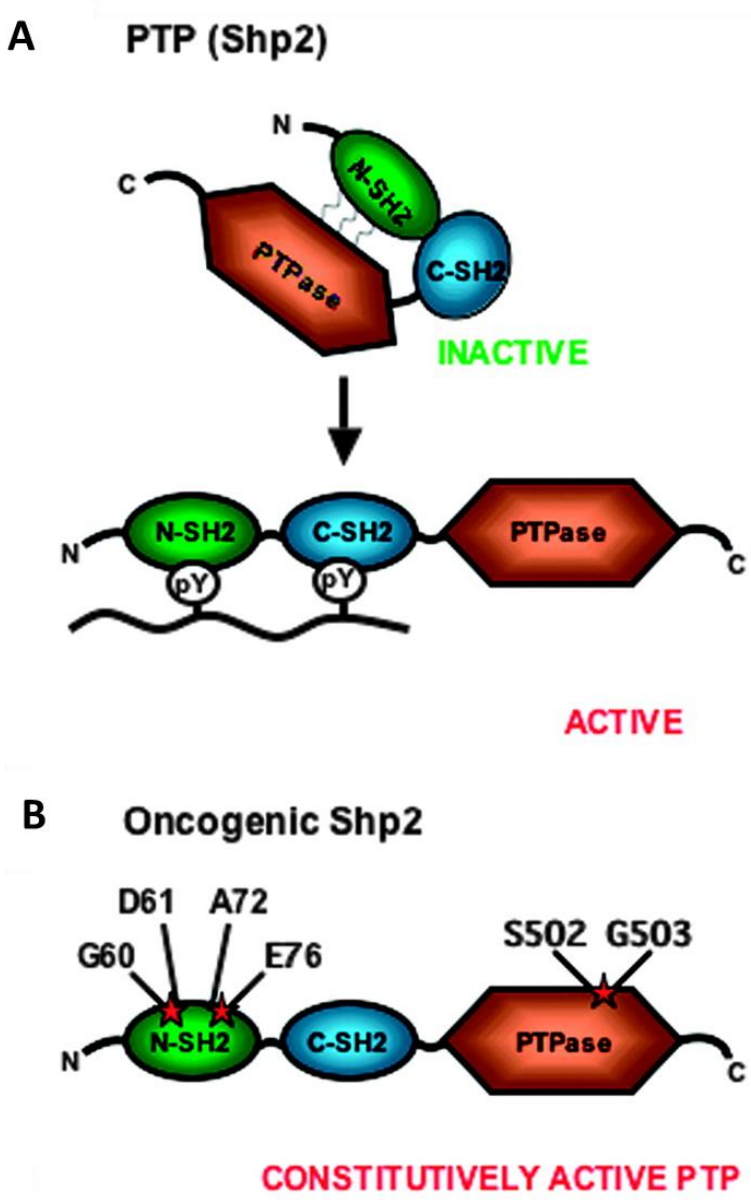

Figure 1.1: Schematic diagram of the normal SHP2 mechanism of activation and the result of common oncogenic mutations

(A) The closed, inactive state of SHP2 is stabilized by hydrophobic interactions between its N-SH2 and PTPase domains. When phospho-tyrosine residues bind to the N-SH2 and C-SH2 domains of SHP2, it transforms into its open, active conformation. This allows the PTPase domain to access and dephosphorylate a substrate. (B) Common oncogenic mutations in SHP2, found in the N-SH2 domain or in the PTPase domain, disrupt the interaction between the N-SH2 and PTPase domains. This destabilizes the inactive state and leads to SHP2 adopting a constitutively active conformation (adapted from (Chan and Feng 2007)).

niche-restricted expression of $Shp2^{E76K}$ is capable of inducing abnormal function of WT bone marrow cells and implies an explanation for the poor engraftment and relapse seen in JMML patients following allogeneic HSCT. The commonly observed resurgence of the JMML leukemic clone following transplantation may be due to the inability of the normal donor HSCs to engraft and remain in a quiescent state in the aberrant bone marrow microenvironment, permitting outgrowth of residual leukemic cells and thus patient relapse.

In addition to malignancies, activating mutations of *PTPN11* in the germline are found in 50% of patients with the autosomal dominant disorder Noonan syndrome (NS). This developmental disorder occurs in 1 in 1000-2500 live births and is characterized by growth retardation, dysmorphic facial features, congenital heart defects, and skeletal abnormalities (Tartaglia and Gelb 2005, Tartaglia, Mehler 2001). Noonan syndrome patients with *PTPN11* mutations are more susceptible to developing hematologic disorders, including JMML. The form of JMML affecting NS patients can follow an aggressive clinical course, but may also regress spontaneously, indicating that NS patients may not need immediate allogeneic HSCT intervention despite bearing a mutation in *PTPN11* (Kratz, Niemeyer 2005). This more indolent clinical course may be due to the particular germline *PTPN11* mutations commonly found in NS patients (N308S, A922G), which although located in the N-SH2 and PTP domains, are less activating than the somatic mutations most frequently found in JMML (D61Y, E76K) (Schubbert, Lieuw 2005, Tartaglia, Kalidas 2002). In a cohort of 91 NS patients and 27 JMML/MDS/AML patients, the most prevalent *PTPN11* mutations occurred at the N-SH2

residues E76 (33%) and D61 (26%), and the residue N308 (36%) in the PTPase domain (Schubbert, Lieuw 2005). Noonan syndrome with multiple lentigines (NSML), previously known as LEOPARD syndrome, is a similar disorder to NS characterized by Lentigines, Electrocardiogram abnormalities, Ocular hypertelorism, Pulmonary stenosis, Abnormal genitalia, Retardation of growth, and Deafness. It is interesting that both NS and NSML patients have similar clinical phenotypes, because NSML is caused by loss of phosphatase function mutations occurring in the PTP domain of SHP2 (Qiu, Wang 2014).

As previously stated, aberrant SHP2 activation has been established as a driver of various leukemias. Attempts to inhibit this upregulated signaling by direct targeting of SHP2 have been met with largely disappointing results. The difficulty lies in selective binding of small molecule inhibitors to the catalytic site, because this area is highly conserved among protein phosphatases (Barr 2010). Although there have been some promising preclinical results *in vitro* and *in vivo*, these successes have not held up in humans (Butterworth, Overduin 2014, Pathak and Yi 2001, Yi, Elson 2011). To bypass the non-specificity hurdles, more recent efforts have focused on creating allosteric inhibitors, which can be directed at unique domains of SHP2 to decrease the active site's affinity for substrate. SHP099 and IACS-13909 are two examples of small molecule allosteric SHP2 inhibitors that were recently developed (Chen, LaMarche 2016, Garcia Fortanet, Chen 2016). Also, a high-throughput compound screen identified benzothiazolopyrimidones as a chemical scaffold that interacts with the C-SH2 and PTP domains to allosterically stabilize SHP2's autoinhibited conformation (LaRochelle, Fodor 2017). However, these allosteric inhibitors have yet to be proven effective against

constitutively active leukemogenic SHP2, which is unable to sustain the self-inhibitory state. Therefore, until effective SHP2 drug inhibitors have been developed and tested, it is reasonable to also focus efforts on molecular targets downstream of SHP2.

Phosphoinositide 3-kinase (PI3K)

One particular downstream effector that has been identified as an important player in SHP2 signaling is phosphoinositide 3-kinase (PI3K). Class Ia PI3K is a lipid kinase that acts on a component of the plasma membrane, phosphatidylinositol-4,5-bisphosphate [$PI(4,5)P_2$], to phosphorylate it into phosphatidylinositol-3,4,5-trisphosphate [$PI(3,4,5)P_3$] (Cantley 2002). Signaling kinases that contain Plekstrin Homology (PH) domains are recruited to the membrane by direct binding to this $PI(3,4,5)P_3$ phosphorylated lipid product. These proteins then become activated and can signal to their downstream effectors (Cantley 2002, Wang and Shaw 1995). One noteworthy example of PH domain protein signaling is PDK1 and its direct downstream target AKT, both of which contain PH domains and are thus brought into close proximity of each other by $PI(3,4,5)P_3$. The phosphorylation of AKT by PDK1 allows key signaling downstream to promote cell survival and growth (Lawlor and Alessi 2001). Another PH domain-containing protein is Bruton's tyrosine kinase (BTK), which will be further discussed below.

Structurally, class Ia PI3K is a heterodimer made up of one of three catalytic subunits (p110α, p110β, or p110δ) and a regulatory subunit (p85α or its splice variants

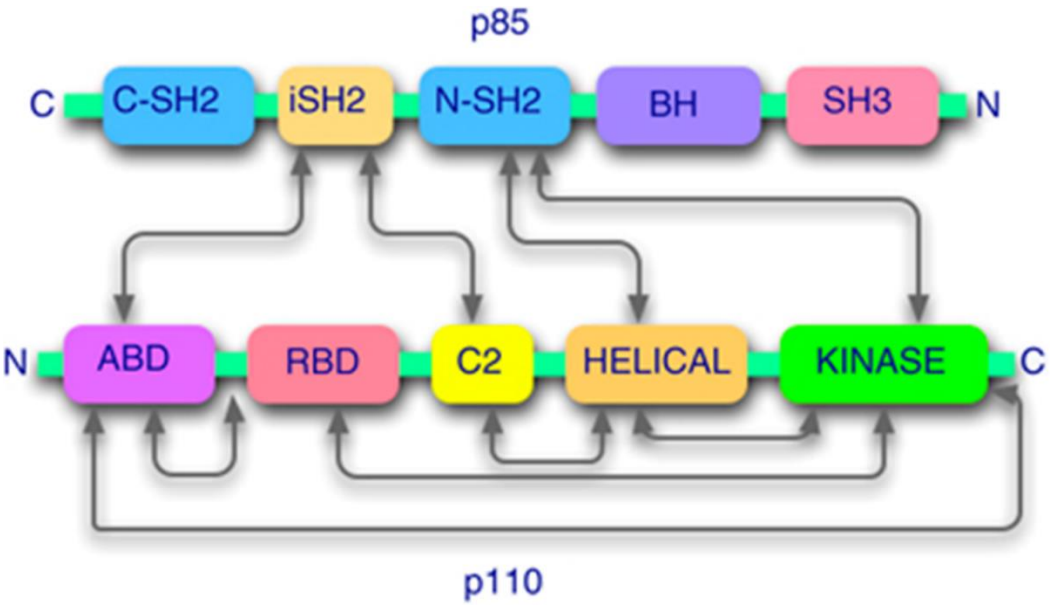

Figure 1.2: Schematic diagram of the functional domains and intramolecular interactions between a catalytic subunit and a regulatory subunit of PI3K

PI3K is a heterodimer made up of a regulatory subunit (p85) and a catalytic subunit (p110). The regulatory subunit has two Src Homology-2 domains (N-SH2 and C-SH2), which interact with phospho-tyrosine residues; an inter-SH2 (iSH2) in between the two SH2 domains, which interacts with the catalytic subunit; a Src Homology-3 (SH3) domain, which interacts with proline-rich domains; and a Breakpoint clustered Homology (BH) domain. The catalytic subunit contains an Adapter-Binding Domain (ABD), which mediates the major interaction with the regulatory subunit; a Ras-Binding Domain (RBD), where Ras binds and promotes the activation of PI3K; a protein-kinase-C homology-2 (C2) domain, which mediates interactions with lipid membranes; and the Kinase domain, which performs the lipid phosphorylation activity (adapted from (Zhao and Vogt 2008)).

p55α and p50α, p85β, or p55γ) (Vanhaesebroeck, Guillermet-Guibert 2010). Each of the p110 subunits are encoded by a separate gene (*PIK3CA* for p110α, *PIK3CB* for p110β, and *PIK3CD* for p110δ) and the regulatory subunits are encoded by *PIK3R1* (p85α, p55α, p50α), *PIK3R2* (p85β), and *PIK3R3* (p55γ) (Jean and Kiger 2014). The regulatory subunits contain an N-terminal and a C-terminal Src homology 2 domain (N-SH2 and C-SH2), between which lies an intervening region (iSH2). The iSH2 region binds to the N-terminal adaptor-binding domain (ABD) on the p110 catalytic subunit, thus allowing constitutive interaction between the two subunits (Figure 1.2). This interaction stabilizes the catalytic subunits and protects them from degradation (Fruman 2010). p85 also acts as an adaptor whereby the SH2 domains recruit the PI3K complex to phosphorylated tyrosine residues on activated signaling proteins, normally downstream of receptor tyrosine kinases (Vadas, Burke 2011).

As mentioned above, PI3K has roles in the regulation of cell proliferation, growth, and survival. Therefore, it is unsurprising that upregulated PI3K signaling is found in numerous human cancers. Most frequently, PI3K signaling is aberrantly upregulated due to an oncogenic upstream effector or due to loss of activity of phosphatase and tensin homolog (PTEN), the functional antagonist of PI3K (Luo, Manning 2003). Although less common, the genes encoding the p110 subunits themselves can also play important roles in human cancer when they become constitutively active or are erroneously overexpressed. The p110α gene, *PIK3CA*, is one of the most commonly mutated oncogenes in breast cancer (Lawrence, Stojanov 2014) and mutations in *PIK3CD* lead to activated PI3Kδ syndrome (APDS), a primary

immunodeficiency syndrome which sharply increases the risk of developing B cell lymphomas (Crank, Grossman 2014, Kracker, Curtis 2014). Thus, PI3K is recognized as a promising drug target, with various inhibitors already developed and tested preclinically and clinically. For example, the p110δ inhibitor umbralisib is currently in clinical trials for relapsed/refractory Hodgkin and non-Hodgkin lymphoma following favorable preclinical data and phase II trials (Deng, Lipstein 2017). Duvelisib is a p110δ and p110γ inhibitor that has shown activity against chronic lymphocytic leukemia (CLL) cells *in vitro* and is now in a phase III trial for treatment of relapsed/refractory CLL (Balakrishnan, Peluso 2015, Flinn, Jäger 2014). FDA approval was recently granted to copanlisib (Aliqopa®), an inhibitor of the α- and δ-isoforms of PI3K, for the treatment of patients with relapsed follicular lymphoma (Dreyling, Morschhauser 2017). Finally, a specific p110δ inhibitor, idelalisib (Zydelig®), has been FDA approved for use in patients with relapsed chronic lymphocytic leukemia, follicular B-cell non-Hodgkin lymphoma, and small lymphocytic lymphoma (Furman, Sharman 2014, Gopal, Kahl 2014).

Pan-PI3K inhibitors, such as wortmannin and LY294002, although quite useful as research tools, have little clinical usefulness due to poor selectivity and thus low tolerability (Gharbi, Zvelebil 2007, Liu, Shreder 2005). However, isoform-specific inhibitors have proven more successful because a higher efficacy-to-toxicity ratio can be achieved. Of the catalytic subunits, p110δ in particular has been identified as a good target for leukemia therapies because its expression is predominantly in hematopoietic cells, whereas p110α and p110β are ubiquitously expressed (Zhao and Vogt 2008). A genetic mouse model with mutated kinase inactive p110δ ($p110\delta^{D910A/D910A}$)

demonstrated that the complete loss of p110δ activity does not cause lethality or developmental defects except for reduced numbers and function of B cells, and of T cells to a lesser extent (Okkenhaug, Bilancio 2002). These findings further strengthen the rationale for targeting p110δ, as there would be minimal side effects upon inhibition.

The majority of p110δ research has been performed in lymphoid malignancies, and in 2014 idelalisib (previously called CAL-101 and GS-1101) became the first PI3K inhibitor approved by the FDA for three B cell neoplasms: relapsed/refractory CLL (in combination with the anti-CD20 antibody rituximab), relapsed follicular lymphoma, and relapsed small lymphocytic lymphoma (Yang, Modi 2015). Idelalisib is a potent and specific p110δ inhibitor, with an IC_{50} of 19nM and 110-fold selectivity over p110γ, 210-fold over p110β, and 453-fold over p110α (Somoza, Koditek 2015). Although the focus has mainly been in lymphoid diseases, recently there has been growing evidence that p110δ also plays an important role in myeloid cell lineages as well. For instance, the p110δ isoform was found to be consistently overexpressed in AML patient blast cells (Sujobert, Bardet 2005). Furthermore, in a mouse model of JMML bearing the gain-of-function Shp2 mutation, D61Y, p110δ activity was shown to be vital for *in vitro* hyperproliferation of bone marrow low-density mononuclear cells, hyperactivation of the downstream cell growth/survival regulators Akt and Erk, and progenitor hypersensitivity to GM-CSF. Goodwin et al. demonstrated these findings using mice bearing genetic inactivation of *Pik3cd* ($p110\delta^{D910A/D910A}$), the p110δ inhibitor, GS-9820, against $Shp2^{D61Y}$-expressing murine cells, and idelalisib against primary leukemia cells

from JMML patients (Goodwin, Li 2014). Therefore, p110δ inhibitors have recently gained relevance for JMML and other myeloid leukemias in addition to lymphoid malignancies.

Bruton's Tyrosine Kinase (BTK): Structure and Signaling

Bruton's tyrosine kinase (BTK) is another Plekstrin Homology domain-containing signaling kinase activated downstream of PI3K. BTK plays a key role in B cell receptor (BCR) signaling as evidenced by the immunodeficiency disease X-linked agammaglobulinemia (XLA), where patients have inherited mutations causing loss of BTK function. In affected males, there is an almost complete lack of mature B cells and serum immunoglobulins, making these patients susceptible to severe and recurrent bacterial infections. The immune cell developmental defects are limited to the B cell lineage, and do not cause deficiencies in T cells or myeloid cells. BTK was identified in 1993 as the non-receptor protein tyrosine kinase responsible for XLA, so it has long been known to be a key player in regulating B cell proliferation and survival (Hendriks, Bredius 2011, Tsukada, Saffran 1993, Vetrie, Vorechovsky 1993). There also exists a mouse strain with a point mutation in *Btk*, which causes the disease X-linked immunodeficiency (XID). Interestingly, XID mice have a somewhat less severe phenotype than humans affected with XLA (Rawlings, Saffran 1993, Thomas, Sideras 1993).

BTK is one of the members of the TEC kinase family, which also includes four other non-receptor tyrosine kinases: tyrosine kinase expressed in hepatocellular carcinoma (TEC), interleukin-2-inducible T cell kinase (ITK), resting lymphocyte kinase

(RLK) and bone marrow-expressed kinase (BMX) (Bradshaw 2010). The TEC family members are expressed in various cell types, with ITK and RLK expressed in T cells, TEC expressed in B and T cells, and BMX expressed in myeloid cells. Loss of TEC in mice does not cause any apparent immunological defects, but the combined deletion of both *Tec* and *Btk* results in a more severe B cell development arrest than that seen in $Btk^{-/-}$ mice. Therefore, it has been postulated that TEC is able to compensate for BTK in mice to a certain extent, lessening the B cell phenotype seen in XID mice (Ellmeier, Jung 2000).

The structure of BTK contains multiple domains that allow it to function as a key signaling molecule. It contains the SRC homology domains SH2 and SH3, a catalytic domain, the aforementioned PH domain, and a TEC homology domain (Figure 1.3) (Bradshaw 2010). BTK is predominantly cytoplasmic and requires PH domain-to-$PI(3,4,5)P_3$ binding in order to be recruited to the membrane. BTK is activated downstream of B cell receptors after antigen binding and activation. To become active, BTK first associates with the membrane, and is then phosphorylated at tyrosine 551 (Y551) by spleen tyrosine kinase (SYK) or a SRC family kinase, which leads to autophosphorylation of Y223 (Park, Wahl 1996, Rawlings, Scharenberg 1996).

Once phosphorylated, BTK is stimulated to signal to its downstream targets, and research has focused mainly on its role in BCR signaling. The major known function of BTK is direct phosphorylation of phospholipase C γ2 (PLCγ2) at Y753 and Y759, leading to the activation of PLCγ2 lipase activity (Kim, Sekiya 2004). PLCγ2 then cleaves $PI(4,5)P_2$ into the two second messengers inositol triphosphate (IP_3) and diacylglycerol (DAG). IP_3 goes on to regulate intracellular Ca^{2+} levels, while DAG promotes the activation of

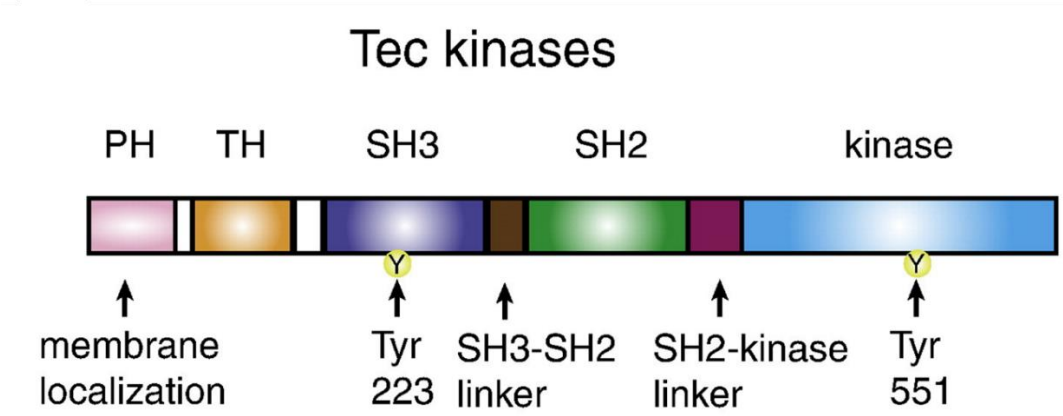

Figure 1.3: Schematic diagram of the functional domains of Tec kinases, including BTK

BTK, a member of the Tec kinase family, contains multiple functional domains. The Plekstrin Homology (PH) domain is needed for binding to PI(3,4,5)P_3 at the plasma membrane; the Tec homology (TH) domain is an extension of the PH domain; the Src Homology-3 (SH3) domain, which has Y223, is the site of autophosphorylation; the Src Homology-2 (SH2) domain; and the kinase domain, which has Y551, is the residue phosphorylated by SYK after BCR cross-linking (adapted from (Bradshaw 2010)).

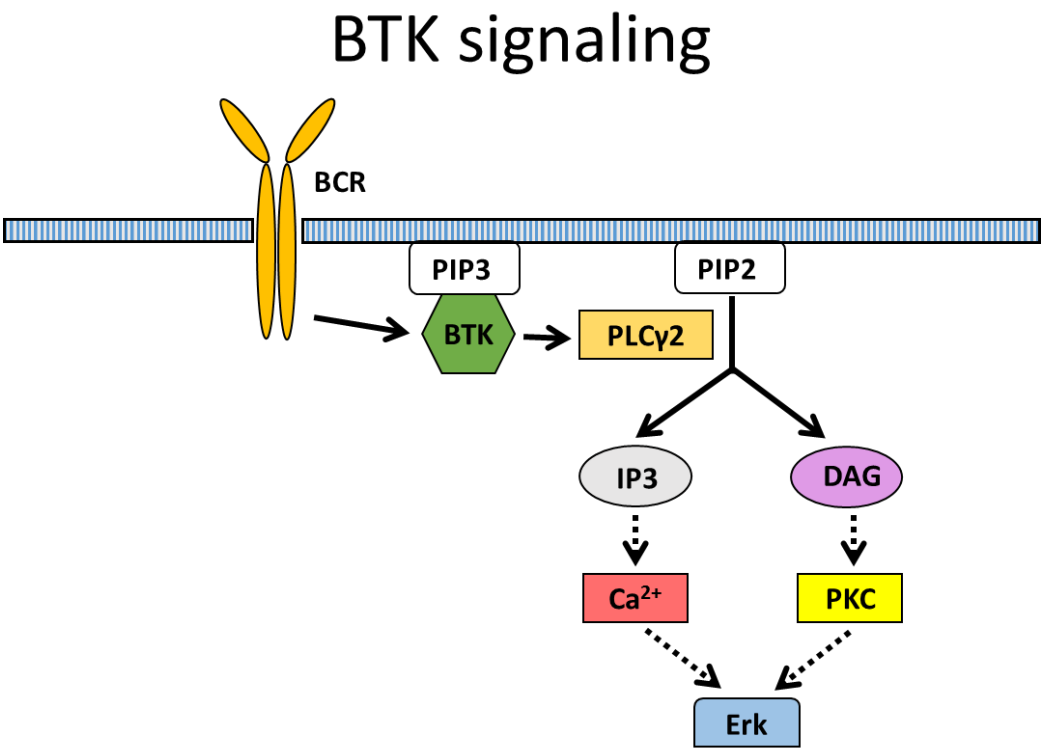

Figure 1.4: Schematic diagram of the signaling pathway of BTK in B cells

BTK is phosphorylated downstream of B cell receptors (BCR) after antigen stimulation and cross-linking. The activated BTK, which is recruited to $PI(3,4,5)P_3$ in the membrane, directly phosphorylates PLCγ2. PLCγ2 then hydrolyzes $PI(4,5)P_2$ into IP_3 and DAG. IP_3 leads to the release of intracellular calcium and DAG promotes the activation of PKC. Both of these events increase ERK activity, and thus cell survival and proliferation. Solid arrows indicate activation by direct interactions; dotted arrows indicate indirect activation.

protein kinase C (PKC) and then ERK, which is also dependent on RAS signaling (Figure 1.4) (Hashimoto, Okada 1998). Beyond its role downstream of the B cell receptor, BTK is also involved in chemokine receptor and toll-like receptor signaling in B cells. Interestingly, there has been some evidence that BTK can act independently of its kinase activity. As an adaptor protein, BTK can recruit phosphatidylinositol 4-phosphate 5-kinase (PI4P5K) to the plasma membrane, which promotes the production of $PI(4,5)P_2$ from phosphatidylinositol 4-phosphate. This forms a positive-feedback loop whereby BTK enhances the generation of the $PI(3,4,5)P_3$ needed for its own activation (Saito, Tolias 2003).

Bruton's Tyrosine Kinase: Role in Malignancies and Pharmacologic Inhibition

BTK is expressed in various B cell leukemias and lymphomas which, combined with the isolated effects to the B cell lineage upon complete loss of BTK, makes it an attractive target for inhibition. The first rationally designed small-molecule inhibitor of BTK, LFM-A13, was described in 1999 to have anti-leukemic activity *in vitro* (Mahajan, Ghosh 1999). However, the first BTK inhibitor to enter clinical trials was ibrutinib (PCI-32765, trade name Imbruvica®), and it went on to receive accelerated FDA-approval for the treatment of patients with relapsed mantle cell lymphoma (MCL) in 2013 (Dreyling, Jurczak 2016). In 2014, ibrutinib approval was expanded to include patients with relapsed chronic lymphocytic leukemia (CLL) following the success of the RESONATE trial, and then for use as first-line CLL treatment in 2016 based on the results of the RESONATE-2 study (Barr, Robak 2016, Burger, Tedeschi 2015, Byrd, Brown 2014). It was

also approved for the treatment of Waldenström's macroglobulinemia (WM) in 2015, relapsed/refractory marginal zone lymphoma (MZL) in January 2017, and chronic graft versus host disease (GVHD) in August 2017 (Dimopoulos, Trotman 2017, Miklos, Cutler 2017, Noy, Vos 2016). Ibrutinib has also been shown to improve overall response rate when used in combination with other agents, namely with ofatumumab in CLL (Jaglowski, Jones 2015), and with rituximab in high-risk CLL (Burger, Keating 2014) and relapsed/refractory MCL (Wang, Lee 2016).

Part of ibrutinib's success as an anti-tumor agent is due to activity beyond its role in BCR signaling. BTK is also important for B cell chemokine receptor signaling involving CXCR4. CXC-chemokine ligand 12 (CXCL12), the ligand for CXCR4, activates BTK, and BTK plays a major role in normal B cell trafficking and tissue homing (de Gorter, Beuling 2007). As such, BTK signaling promotes CLL cell migration to the proliferative centers in lymph nodes and spleens as well as retention in this protective microenvironment. In fact, there is a phenomenon of ibrutinib-induced lymphocytosis in CLL patients, as inhibition of BTK disrupts multiple pathways needed for CLL cell retention in protective microenvironments and results in rapid mobilization into the peripheral circulation (Byrd, Furman 2013).

Despite ibrutinib's impressive performance against multiple B cell diseases, it is not without its problems. Ibrutinib's mechanism of action involves covalent binding to cysteine 481 (C481) inside BTK's ATP binding pocket, but it also has off-target irreversible binding to epidermal growth factor receptor (EGFR), TEC, ITK, and T-cell X chromosome kinase (TXK) (Honigberg, Smith 2010), which can lead to undesirable

adverse events of increased bleeding and atrial fibrillation. Furthermore, although XLA patients have abnormalities limited to the B cell lineage, ibrutinib administration leads to the broader chemotherapy toxicities of neutropenia, anemia, thrombocytopenia, diarrhea, nausea, rash, bruising, fatigue, pyrexia, and hemorrhage (Khan, Gibbons 2017). Surprisingly because of the irreversible inhibition of BTK and the immunodeficiency phenotype of XLA patients, the amount of immunosuppression actually decreases over time with continued use of ibrutinib. A clinical study showed that the reduction in average infection rate of patients treated with ibrutinib could be explained by a corresponding rise in IgA levels (Byrd, Furman 2013). As mentioned previously, two more serious complications of ibrutinib involve the development of atrial fibrillation and bleeding, indicating that consideration must be taken prior to giving patients anticoagulation or performing surgery (Yun, Vincelette 2017).

Several second-generation inhibitors have been developed that are improved upon ibrutinib. Acalabrutinib, ONO/GS-4059, and BGB-3111 are all irreversible BTK inhibitors with higher selectivity for BTK than other kinases such as EGFR, ITK, and others (Sarkissian and O'Brien 2017). Of these, FDA approval was recently granted to acalabrutinib (ACP-196, trade name Calquence®) for use in patients with relapsed mantle cell lymphoma based on results of the ACE-LY-004 phase II trial (NCT02213926). Like ibrutinib, ACP-196 also covalently binds to C481, and although the IC_{50} of ACP-196 for BTK is 3-fold greater than that of ibrutinib, its IC_{50} for other kinases is much higher. ACP-196 also has better pharmacologic features, namely improved plasma exposure, more rapid oral absorption, and a shorter half-life. These compound characteristics

allow more frequent dosing and continuous BTK binding while eliciting fewer toxic effects from off-target binding to other kinases (Byrd, Harrington 2016). These improvements in acalabrutinib are highly notable because the development of side effects is the most common reason that patients discontinue ibrutinib treatment. The phase I/II trial results of 61 relapsed/refractory CLL patients revealed that prolonged and continuous ACP-196 treatment led to minor adverse events that self-resolved over time with few patients developing more serious adverse events (diarrhea, arthralgia, pyrexia, fatigue, hypertension) and only 1 patient experiencing disease progression (Byrd, Harrington 2016). A phase III trial comparing ACP-196 to ibrutinib in relapsed/refractory CLL is currently recruiting patients to evaluate progression-free survival (NCT02477696).

In addition to toxicity, another problem that can occur under ibrutinib treatment is the development of resistance by the malignant cells. This can occur by either a substitution of cysteine to serine at the BTK binding site, leading to reversibility of ibrutinib binding, or by acquiring activating mutations in PLCγ2 (Woyach, Furman 2014). Second-generation inhibitors like ACP-196 do not circumvent this problem, so an alternate strategy is to target other molecules in the signaling pathway, such as p110δ, PLCγ2, and/or others.

Because BTK's major function was found to be downstream of BCR signaling, prior research on BTK has largely focused on its role in normal B cell development and in B cell malignancies. However, despite the apparently B cell-restricted phenotype in XLA, BTK is expressed in all hematopoietic cell types except for T lymphocytes and plasma

cells (Smith, Baskin 1994), so it is likely to function in the signaling of the other cell types as well. Therefore, BTK may also be a good target in myeloid leukemias.

B-cell adaptor for phosphoinositide 3-kinase (BCAP)

One of the known downstream direct targets of BTK in B cells is B cell adaptor for phosphoinositide 3-kinase (BCAP), encoded by the *Pik3ap1* gene. BCAP was discovered in 2000 as a novel protein that connects the B cell receptor to PI3K activation. Okada et al. first isolated BCAP using the immobilized N-terminal SH2 domain in chicken DT40 B cells, then cloned the murine counterpart from a spleen cDNA library (Okada, Maeda 2000). The chicken BCAP contains four YxxM motifs, which is the motif that binds to PI3K's p85α subunit, and the mouse BCAP protein contains three YxxM motifs (YESM, YESM, and YVEM). In the mouse, BCAP is highly expressed in the spleen, but small amounts of BCAP are also present in the thymus, lung, and liver. As for cell types, BCAP is expressed predominantly in hematopoietic cells, particularly B cells and macrophages (Okada, Maeda 2000), but is also expressed in dendritic cells, natural killer cells (MacFarlane, Yamazaki 2008), and hematopoietic stem and progenitor cells (Duggan, Buechler 2017). In B cells, BCAP is phosphorylated directly by BTK and SYK (spleen tyrosine kinase) following BCR activation. Once tyrosine phosphorylated at the YxxM motifs, phospho-BCAP can then bind to the two SH2 domains of the p85α regulatory subunit of PI3K (Fruman, Meyers 1998, Shoelson, Sivaraja 1993). This association between BCAP and p85α promotes the activity of PI3K in two distinct manners: 1) it increases the kinase activity of the catalytic p110 domain and 2) it recruits PI3K to

glycolipid-enriched microdomains (GEMs) at the plasma membrane, thus localizing PI3K to its PI(4,5)P_2 substrate. Without the p85α subunit, B cells cannot develop properly in response to BCR stimulation because PI3K is integral to cell proliferation and survival (Fruman, Snapper 1999).

Originally four different isoforms of BCAP were isolated with molecular weights of 70, 72, 98, and 100 kDa, termed BCAP1, BCAP2, BCAP3, and BCAP4, respectively. All four isoforms are encoded by the same *Pik3ap1* gene, and screening of a cDNA library showed that BCAP1 and BCAP2 are generated by an alternative sequence truncated at the N-terminal end (BCAP-S) while the full-length transcript (BCAP-L) gives rise to BCAP3 and BCAP4 (Okada, Maeda 2000). The difference between BCAP-S and BCAP-L is likely due to alternative start sites of transcription, and the smaller differences within the isoform sizes (BCAP1 vs. BCAP2 and BCAP3 vs. BCAP4) are likely due to post-translational modifications. Following BCR activation, two additional larger BCAP isoforms were visible (BCAP5 and BCAP6), so these may be less prevalently expressed species that only become visible after stimulation (Okada, Maeda 2000). It is unknown if these larger isoforms result from further post-translational modifications or from another alternative transcript.

Architecturally, BCAP is made up of several well-defined motifs necessary for protein-protein interactions (Figure 1.5). It contains two ankyrin repeats and a coiled coil, similar to that found in the Drosophila version of BCAP, Dof, where these motifs were first reported. Just upstream in the BCAP protein is a Dof/BANK/BCAP (DBB) domain, named because it is a conserved sequence also found in Dof and another B cell

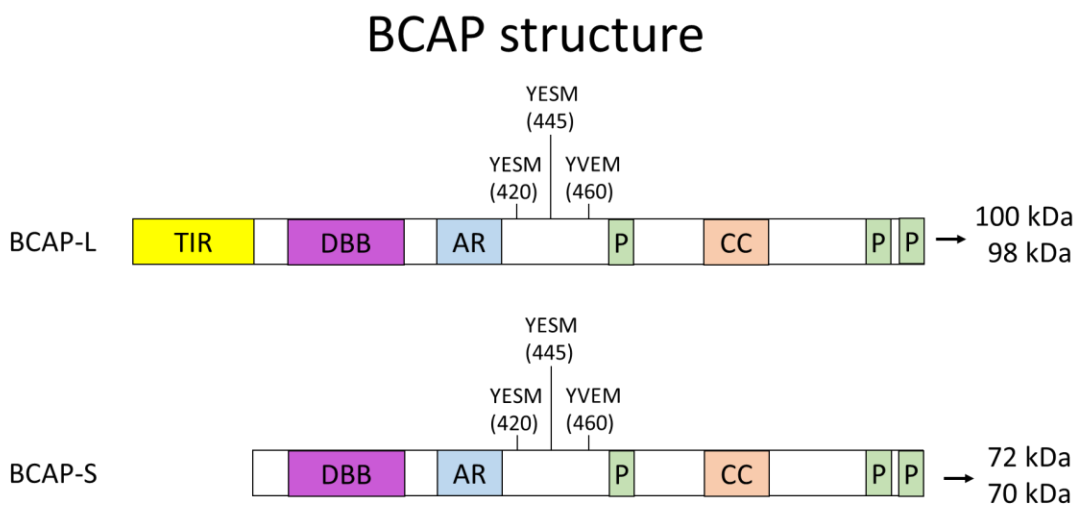

Figure 1.5: Schematic diagram of the structure of BCAP

BCAP is encoded by a full-length transcript (BCAP-L) that gives rise to 100kDa and 98kDa proteins, and a truncated BCAP-S transcript that encodes the 72kDa and 70kDa species. The shortened transcript lacks the N-terminal Toll-IL-1 receptor (TIR) domain, which has been shown to interact with PI3K to downregulate the TLR inflammatory response. All isoforms of BCAP contain a Dof/BANK/BCAP (DBB) domain, which is necessary for dimerization; the double ankyrin repeat (AR) motif and the coiled coil (CC) motif, which are two protein folding motifs important for protein-protein interactions; and the proline-rich regions (P), which are also commonly involved in protein-protein interactions.

signaling molecule, B cell scaffold with ankyrin repeat (BANK). Previous work has shown that this DBB domain is required in Dof for FGF-dependent signaling and for both Dof and BCAP to form homodimers (Battersby, Csiszar 2003). While BCAP is not involved in FGF-dependent signaling, it was recently reported that BCAP-L exists as a homodimer (Halabi, Sekine 2017).

In 2011, Troutman et. al reported that the N-terminal end of BCAP was homologous to the Toll-IL-1 receptor (TIR) domain and functioned to negatively regulate toll-like receptor (TLR) signaling by activating PI3K. The structure of the N-terminal domain of BCAP was recently confirmed to be a TIR domain by protein crystallization (Halabi, Sekine 2017). TLRs are activated as a component of the innate immune response to microbial infections by agonists such as lipopolysaccharide (LPS) from Gram-negative bacteria. However, the activation of TLR signaling also activates PI3K, which inhibits proinflammatory events and thus negatively regulates TLR signaling as a negative feedback mechanism (Hazeki, Nigorikawa 2007). Macrophages lacking BCAP have decreased PI3K activation and are hyperresponsive to TLR agonists (Ni, MacFarlane 2012), which also renders them more vulnerable to ER stress-induced apoptosis (Song, Chew 2011). Finally, as previously mentioned, BCAP contains YxxM motifs that enable interaction with p85α's SH2 domains once tyrosine-phosphorylated (Okada, Maeda 2000).

As stated above, BCAP is an important downstream target of BTK. Similar to BTK loss, the loss of BCAP results in defective B cell development and attenuates the humoral immune response, as demonstrated by Yamazaki et. al in $BCAP^{-/-}$ mice

(Yamazaki, Takeda 2002). However, although macrophages also have high BCAP expression, BCAP$^{-/-}$ mice demonstrate no defects in macrophage development compared to their wild-type littermates (Yamazaki, Takeda 2002). There is evidence that the signaling pathways involving BCAP also differ between cell types. For example, in mouse B cells, SYK initiates and BTK sustains the phosphorylation of BCAP; however, SYK does not function in a parallel fashion in myeloid cells. In fact, Ni et al. demonstrated that bone marrow-derived macrophages lacking SYK have increased phosphorylation of BCAP-L, suggesting that SYK functions to decrease BCAP phosphorylation in myeloid cells (Ni, MacFarlane 2012).

Due to the incongruous functions of BCAP in various cell types, it is unknown if BCAP acts as a connector from BTK to PI3K signaling in myeloid cells as it does in B cells. Some evidence suggests that BCAP has this ability, as bone marrow-derived macrophages lacking both *Btk* and *Tec* expression demonstrated decreased BCAP phosphorylation (Tampella, Kerns 2015). Because of the role that PI3K plays in cell survival, proliferation, and malignancies, the potential role of BCAP as a possible molecule-of-interest in cancer is worth exploring. The importance of BCAP in Akt activation after BCR cross-linking is well-established (Castello, Gaya 2013, Qin and Chock 2003), but its role in malignancies is largely unknown. As stated earlier, BCAP has a small amount of expression in the lung, and a recent study found that BCAP expression was increased in tumor tissues of lung cancer patients. These studies also identified miR-486 as a direct inhibitor of BCAP, which led to inhibition of Akt and induction of autophagy

(Xu, Wang 2017). These findings suggest a possible clinical application of BCAP inhibition in cancer, including in myeloid malignancies.

DNA Methyltransferase 3A (DNMT3A)

The addition of a methyl group to cytosine in DNA, called DNA methylation, is an epigenetic modification that affects embryonic development, genomic imprinting, stem cell behavior, and malignancies (Yang, Rau 2015). DNA methyltransferase 3A (DNMT3A) is an enzyme that catalyzes cytosine methylation at CpG dinucleotide sites. Typically, methylation in a promoter region is associated with silencing of gene expression (You and Jones 2012). Aberrant DNA methylation has long been observed in cancer (Baylin and Herman 2000) and *DNMT3A* has recently been identified as a commonly mutated gene in hematologic malignancies.

The mechanism of DNMT3A activity, such as how it is regulated, recruited to chromatin, and targeted to specific sites, is still poorly understood. Experiments using mouse models have provided new insight into the function of DNMT3A. Complete and ubiquitous loss of *Dnmt3a* expression in mice results in failure to thrive and death one month after birth (Okano, Bell 1999), reflecting the important role of DNA methylation during development. Mice with conditional deletion of *Dnmt3a* in hematopoietic stem cells (HSCs) have normal development, but their HSCs aberrantly favor self-renewal over differentiation, leading to accumulation of *Dnmt3a*-null HSCs in the bone marrow (Challen, Sun 2011). Genome-wide methylation studies have been performed to study the mechanism of how DNMT3A loss leads to increased self-renewal. These studies

found that HSCs lacking *Dnmt3a* expression have an overall hypomethylated profile, but especially affected areas of the genome are the edges of large canyon regions, which are enriched for genes related to self-renewal and cancer (Jeong, Sun 2014).

Although abnormal methylation patterns have long been recognized to be associated with cancer, mutations in *DNMT3A* were only identified in 2010, specifically in acute myeloid leukemia (AML) patients. *DNMT3A* is now known to be mutated in over 20% of AML patients (Ley, Ding 2010), in 8% of myelodysplastic syndrome (MDS) patients (Walter, Ding 2011), and in smaller frequencies in other leukemias. Multiple different mutations throughout *DNMT3A* have been observed, but the R882 codon in particular is a mutational hotspot, making up 60% of *DNMT3A* mutations found in AML patients. R882 mutations are dominant-negative, resulting in less than 80% of DNMT3A enzymatic activity (Kim, Zhao 2013).

One of the critical steps in the development of malignancy is the clonal expansion of HSCs bearing somatic mutations. Multiple studies have found *DNMT3A* to be one of the recurrently mutated epigenetic regulators found in clonal hematopoiesis of normal individuals with no signs of hematologic malignancy, a phenomenon called clonal hematopoiesis of indeterminate potential (CHIP) (Xie, Lu 2014). In this preleukemic state, almost all *DNMT3A* mutations are nonsynonymous, truncating, or splicing, and mutations in R882 are rare (Young, Challen 2016). These healthy individuals are at an increased risk of developing hematologic malignancy and will have a poorer overall prognosis (Genovese, Jaiswal 2015, Jaiswal, Fontanillas 2014). It is not surprising

that *DNMT3A* is among the first genes to acquire a preleukemic lesion since HSCs with mutated *DNMT3A* have enhanced self-renewal and expand over time.

DNMT3A mutations have also been identified in JMML patients as secondary mutations, most commonly in conjunction with *PTPN11* mutations, which is important given the increasing recognition that secondary mutations lead to much poorer prognosis in JMML patients (Stieglitz, Taylor-Weiner 2015). Furthermore, the DNA methylation profile of JMML patients has recently been found to be predictive of disease outcome. Using unsupervised hierarchical clustering, Stieglitz et. al observed that JMML patients could be clustered into low, intermediate, and high genome-wide methylation. Those in the low methylation cluster had the highest survival rate, with almost all patients experiencing spontaneous resolution of disease (Stieglitz, Mazor 2017). Consistent with these findings, there is a case report describing a JMML patient treated with azacitidine, a DNA methyltransferase inhibitor, who had impressive resolution of hepatosplenomegaly and monocytosis even prior to allogeneic HSCT (Furlan, Batz 2009). Based on the prediction that patients exhibiting hypermethylated profiles would respond to DNA hypomethylating agents, there is an ongoing phase I/II clinical trial testing the effect of azacitidine in JMML patients (NCT02447666). Although mutations in *DNMT3A* lead to decreased methyltransferase activity and thus focal areas of CpG hypomethylation, the presence of secondary mutations in patients are associated with an overall hypermethylated state (Stieglitz, Mazor 2017). These findings suggest that DNMT3A activity significantly affects disease progression and overall prognosis in JMML.

Summary and Significance

JMML is a childhood disease that, albeit rare, is extremely aggressive and currently lacks effective therapies and thus has a pressing need for more investigation. The only curative treatment is allogeneic hematopoietic stem cell transplant (Loh 2011), yet even this aggressive intervention elicits a 5-year event-free survival of only 50% (Bergstraesser, Hasle 2006, Locatelli, Nöllke 2005). This is in stark contrast to other pediatric leukemias, such as acute lymphoblastic leukemia (ALL), which have made great strides forward in improving care with overall survival over 80% (Gaynon, Angiolillo 2010). In recent years, JMML researchers have made efforts to better genetically define JMML patients, with whole genome studies performed to find secondary mutations (Stieglitz, Taylor-Weiner 2015). The hope is that, by understanding the underlying molecular mechanisms, patients can receive more personalized and targeted therapeutics.

For the five causative gene mutations that make up 90% of JMML cases, the underlying signaling abnormality in common is hyperactivated RAS signaling. Either RAS itself is mutated (*KRAS* or *NRAS*) or *NF1*, the RAS-GAP protein responsible for hydrolyzing RAS-GTP into RAS-GDP, acquires a genetic lesion. CBL and the most commonly mutated protein, SHP2, also have upregulated RAS signaling, but the mechanism for these two proteins is still unknown. Targeting aberrant RAS signaling, which is also seen in many other malignancies, has proven difficult. The strategy of GTP-competitive inhibitors against RAS has not been successful because of the high affinity RAS has for GTP (Gysin, Salt 2011). Because RAS must traffic to the plasma membrane to

function as a signal transducer, another protein called farnesyl-transferase normally adds hydrophobic farnesyl groups to the mature RAS protein. Therefore, farnesyl-transferase inhibitors have been developed as an alternate strategy to GTP-competitive inhibitors for RAS inhibition. Tipifarnib is one such inhibitor whose mechanism-of-action is to inhibit prenylation of the tail motif of RAS. Unfortunately for JMML patients, tipifarnib's initial success *in vitro* did not translate in clinical trials (Stieglitz, Ward 2015). The failure of tipifarnib is believed to be due to geranylgeranylation, another form of post-translational modification prenylation, that allows RAS to continue to interact with the membrane even lacking farnesylation (Epling-Burnette and Loughran 2010).

Because of the difficulties in targeting RAS itself, the next best strategy is to target an effector in a downstream signaling pathway, such as in the MAPK pathway or the PI3K/Akt pathway. For the MAPK pathway, there is an ongoing phase II clinical trial in patients with relapsed/refractory JMML using trametinib, a MEK inhibitor (NCT03190915). In addition to the MAPK pathway, PI3K is known to be hyperactivated in a multitude of malignancies with many drugs developed for clinical use, as described earlier. The pan-PI3K inhibitors have proven to be too toxic for use in humans, but isoform-specific inhibitors are more tolerable. Our lab has previously shown that *in vitro* inhibition of the hematopoietic-specific catalytic subunit, p110δ, using GS-9820 significantly reduced GM-CSF-stimulated phosphorylation of Akt and Erk and cell hyperproliferation in the context of gain-of-function (GOF) mutant Shp2. However, promising findings *in vitro* do not always translate *in vivo*. Furthermore, single-agent therapy is unlikely to be effective because of the development of resistance and the

upregulation of parallel signaling pathways. With this in mind, we moved forward with studies employing GS-9820 *in vivo* in GOF Shp2-bearing mice and further explored the p110δ signaling pathway to find other potential targets.

In the following work, we used pharmacologic inhibitors of p110δ and BTK in mice conditionally expressing a GOF Shp2 mutation in cells of the myeloid lineage. We first treated mice with GS-9820 and showed that the strong effect on signaling in bone marrow-derived macrophages and the reduction in low-density mononuclear cell hyperproliferation that our laboratory had previously seen *in vitro* translated into reduced spleen size and prolonged survival *in vivo* (Chapter Three). We also found that drug-treated mice had reduced stem/progenitor cells in the bone marrow and increased mature myeloid cells in the peripheral blood, suggesting that the inhibition of p110δ signaling may disrupt the nurturing microenvironment for progenitors and induce myeloid differentiation (Chapter Three).

In our search for molecules potentially cooperating with p110δ signaling, we focused our efforts on BTK, as BTK has recently emerged as a highly successful target of inhibition in B cell malignancies. First, we demonstrated that BTK and the known downstream target, PLCγ2, are both hyperphosphorylated in GOF Shp2 myeloid cells (Chapter Four). We next used BTK and p110δ inhibitors to demonstrate that PI3K is upstream of BTK and that BTK cooperates with p110δ to cause hyperactivation of Akt and Erk in mutant Shp2-expressing macrophages (Chapter Four). We further found that the two inhibitors cooperate to reduce GM-CSF-stimulated hyperproliferation of mutant Shp2-expressing bone marrow low-density mononuclear cells. We next treated mice *in*

vivo with the drugs as single-agents or as a combination therapy and observed significantly decreased splenomegaly and peripheral blood WBC counts in the dual inhibitor-treated group (Chapter Four). Here again, we noticed decreased stem/progenitor cells in the bone marrow compartment with an increase in terminally differentiated myeloid cells in the peripheral blood compartment. Despite these significant results, however, we did not observe any change in phospho-PLCγ2 in the presence of the BTK inhibitor (Chapter Four). This finding is inconsistent with the function of PLCγ2 in B cell receptor signaling, where it is the downstream target of BTK that leads to the activation of Erk (Hashimoto, Okada 1998, Kim, Sekiya 2004).

In order to obtain a better understanding of the mechanism of signaling from BTK to Akt and Erk in myeloid cells, we performed a literature search for other targets of BTK that could potentially lead to activation of these downstream effectors. We found that BCAP had recently been identified as a protein with reduced phosphorylation in bone marrow-derived macrophages lacking *Btk* and *Tec* expression (Tampella, Kerns 2015) and that it had long been known to connect BTK to PI3K in B cells (Okada, Maeda 2000). As PI3K certainly positively signals to activate Akt and Erk, we hypothesized that BCAP connects BTK to the upregulation of PI3K activity in GOF Shp2-expressing myeloid cells. When we tested this hypothesis, we found that BCAP is phosphorylated in mutant Shp2 macrophages specifically in the two larger isoforms that are needed for PI3K activation (Chapter Five). We further demonstrated that BTK inhibition leads to a dose-dependent reduction in this phosphorylation (Chapter Five), suggesting that BTK is signaling upstream of BCAP in myeloid cells as well as B cells. Since one of the ways that

BCAP increases PI3K catalytic activity is by binding to the regulatory p85α domain, we explored the mechanism of this interaction using p85α constructs with mutated SH2 domains. We found reduced interaction between BCAP and p85α after mutating the two SH2 domains, indicating that one or both of these domains are necessary for BCAP binding (Chapter Five).

Finally, we explored the consequences of concurrent expression of the *Shp2*^{D61Y} mutation and *Dnmt3a* haploinsufficiency. We observed that mice bearing both mutations had accelerated development of leukemia and earlier mortality (Chapter Six). The double mutant mice had increased myeloid cells in the periphery and granulocyte macrophage progenitors in the bone marrow. We also saw evidence for a novel phenotype of defective erythrocyte maturation leading to anemia in the double mutant mice, with compensatory erythropoiesis in the spleen (Chapter Six).

From our results, we propose that the myeloproliferative neoplasm caused by GOF Shp2 mutations is facilitated by hyperactivated PI3K, particularly the catalytic subunit p110δ, and significant improvements can be made by treatment with a p110δ inhibitor *in vivo*. Our findings also suggest that in mutant Shp2-expressing myeloid cells, BTK promotes p110δ activity by forming a positive feedback loop with PI3K and BCAP, thus leading to augmented hyperphosphorylation of Akt and Erk and enhanced hyperproliferation in response to GM-CSF. The dual inhibition of p110δ and BTK represents a novel effective treatment strategy for JMML and other myeloid diseases induced by oncogenic Shp2. In addition to targeting GM-CSF-stimulated signaling proteins p110δ and BTK, our findings also provide a functional mechanism underlying

the observed inferior prognosis for JMML patients bearing mutations in both *PTPN11* and *DNMT3A* and support the use of hypomethylating agents in JMML.

CHAPTER TWO

MATERIALS AND METHODS

Materials

Plasmids

pMIEG3

WT Shp2 and Shp2 E76K constructs in tandem with enhanced green fluorescent protein (eGFP) were expressed in pMIEG3 plasmid. These constructs were previously made in our laboratory (Chan, Leedy 2005).

pQCXIN

WT Shp2 and Shp2 E76K constructs were expressed in the pQCXIN plasmid. This plasmid has the neomycin resistance cassette with an IRES sequence. cDNA from murine WT Shp2 and mutated Shp2 E76K were obtained from previously made constructs in pCMV2 plasmid from our laboratory.

pMSCV

WT p85α, p85α R358A, p85α R649A, and p85α R358A/R649A constructs were expressed using pMSCV plasmid. cDNA from murine p85α and the mutated forms of p85α were previously generated by site-directed mutagenesis and fused in-frame to the DNA sequence for yellow fluorescent protein (YFP) as a marker.

pCMV6

BCAP construct was expressed using pCMV6 plasmid. cDNA from murine BCAP (purchased from Origene) was fused in-frame to the DNA sequence for mCherry as a marker.

Primers

Standard polymerase chain reactions (PCRs) were performed using oligonucleotides synthesized by Invitrogen. The primers used for genotyping are listed in Table 2.1.

Table 2.1: Genotyping primers

Gene	Forward (5' – 3')	Reverse (3' – 5')
Shp2 Exon 3 (*Shp2^{D61Y}*)	5'-CAAGGTGAGTGGGCGTTTCATTTTAAC-3'	5'-ACCTTTCAGAGGTAGGGTCTGCAC-3'
Mx1-cre	5'-GCCTGCATTACCGGTCGATGCAACGAGTG-3'	5'-CTGGCAATTTCGGCTATACGTAACAGGGTG-3'
Neo cassette (*Shp2^{E76K}*)	5'-TGGGAAGACAATAGCAGGCA-3'	5'-CCCACTCACCTTGTCATGTA-3'
LysM-cre	5'-CCCAGAAATGCCAGATTACG-3'	5'-CTTGGGCTGCCAGGATTTCTC-3'
Dnmt3a loxP	5'-CTGTGGCATCTCAGGGTGATGAGCA-3'	5'-AAGCCTCAGGCCCTCTAGGCAAGA-3'

Mice

LSL-Shp2$^{D61Y/+}$

LoxP-STOP-LoxP (LSL)-Shp2$^{D61Y/+}$ mice were a gift from Dr. Benjamin G. Neel. The *Ptpn11* gene has insertion of an LSL cassette in order the express the allele containing the knock-in D61Y mutation only after cre-mediated recombination. These mice were crossed with Mx1-cre mice (Chan, Kalaitzidis 2009).

Mx1-cre

Mx1-cre transgenic mice were a gift from Dr. Reuben Kapur (Kuhn, Schwenk 1995). The Mx1 promoter is induced by three intraperitoneal injections of 300ug polyI:polyC to stimulate the γ-interferon response.

LSL-Shp2$^{E76K/+}$

LSL-Shp2$^{E76K/+}$ mice were a gift from Dr. Cheng-Kui Qu. The *Ptpn11* gene has insertion of an LSL cassette in order the express the allele containing the knock-in E76K mutation only after cre-mediated recombination. These mice were crossed with LysM-cre mice (Xu, Liu 2011).

LysM-cre

LysM-cre mice were purchased from The Jackson Laboratory (Clausen, Burkhardt 1999). Cre recombinase is inserted into the first coding ATG of the lysozyme 2 gene (*Lyz2*) and therefore is expressed under the control of the *Lyz2* promoter. This results in targeted expression in the myeloid cell lineage, particularly in mature macrophages and granulocytes.

Dnmt3a$^{flox/flox}$

Mice with a conditional knockout *Dnmt3a* allele were a gift from Dr. Reuben Kapur (Yu, Zhou 2012).

Antibodies

Immunoprecipitation and immunoblot

Table 2.2: Primary antibodies for immunoblot

Primary antibody	Vendor	Clone
Total Akt	Cell Signaling	N/A
Phospho-Akt (S473)	Cell Signaling	587F11
Phospho-Akt (S473)	Cell Signaling	D9E
Total Erk	Cell Signaling	N/A
Phospho-Erk (T202/T204)	Cell Signaling	N/A
Total BTK	Cell Signaling	C82B8

Table 2.2: Primary antibodies for immunoblot (continued)

Primary antibody	Vendor	Clone
Phospho-BTK (Y223)	Cell Signaling	N/A
Total PLCγ2	Cell Signaling	N/A
Phospho-PLCγ2 (Y759)	Cell Signaling	N/A
Phospho-PLCγ2 (Y1217)	Cell Signaling	N/A
p85α	Cell Signaling	6G10
BCAP	R&D Systems	501813
BCAP	R&D Systems	N/A
Phospho-tyrosine	Millipore	4G10
GAPDH	Biodesign International	6C5

Table 2.3: HRP Secondary antibodies

Secondary antibody	Vendor
Goat Anti-Rabbit IgG HRP	Santa Cruz
Goat Anti-Mouse IgG HRP	Santa Cruz
Goat Anti-Rabbit IgG HRP	Cell Signaling
Horse Anti-Mouse IgG HRP	Cell Signaling
Donkey Anti-Goat IgG HRP	R&D Systems

Table 2.4: Immunoprecipitation antibodies

Antibody	Vendor	Concentration
BCAP	R&D Systems	5μg/μL
p85α	Cell Signaling	1:25

Flow cytometry

Table 2.5: Primary antibodies for flow cytometry

Primary antibody	Fluorophore	Vendor
Sca1	PE	BD Biosciences
cKit	APC	BD Biosciences
Gr1	FITC	eBioscience
Mac1	APC	BD Biosciences
B220	PE	BD Biosciences
CD4	N/A – biotinylated	BD Biosciences
CD8	N/A – biotinylated	BD Biosciences

Table 2.5: Primary antibodies for flow cytometry (continued)

Primary antibody	Fluorophore	Vendor
Mac1	N/A – biotinylated	BD Biosciences
Gr1	N/A – biotinylated	BD Biosciences
CD4	N/A – biotinylated	BD Biosciences
CD8	N/A – biotinylated	BD Biosciences
B220	N/A – biotinylated	BD Biosciences
Ter119	N/A – biotinylated	BD Biosciences
IL7Rα	N/A – biotinylated	BD Biosciences
CD19	N/A – biotinylated	BD Biosciences
CD3	N/A – biotinylated	BD Biosciences
CD71	FITC	BD Biosciences
CD36	APC	BD Biosciences

Table 2.6: Secondary antibodies

Streptavidin fluorophore	Vendor
Streptavidin-PerCPcy5.5	eBioscience
Streptavidin-APC	eBioscience

Inhibitors

Table 2.7: Inhibitors

Inhibitor	Vendor/Source	Target
GS-9820	Gift from Gilead Sciences	p110δ
ACP-196	Gift from Acerta Pharma	BTK
ACP-319	Gift from Acerta Pharma	p110δ

Kits

Table 2.8: Kits

Kit	Vendor	Catalog Number
SuperSignal West Dura Extended Duration Substrate	Thermo Scientific	34076
Profection Mammalian Transfection	Promega	E1200
Plasmid Maxi-Prep Kit	Invitrogen	K210007
Mini-prep kit	Qiagen	27106

Methods

Cell Culture

Primary Murine Bone Marrow-Derived Low-Density Mononuclear Cells (LDMNCs)

Primary murine bone marrow-derived LDMNCs were isolated from total bone marrow cells by Histopaque ficoll gradient (Sigma-Aldrich) and cultured in IMDM (Invitrogen), 20% FBS (Hyclone), 2% penicillin/streptomycin (Invitrogen), granulocyte-colony-stimulating factor (G-CSF), stem cell factor (SCF), and thrombopoietin (TPO) at 100ng/mL concentration each. LDMNCs were maintained at 37°C and 5% CO_2 for a maximum of 5 days.

Adherent Macrophage Progenitor Cells

Primary murine LDMNCs were cultured in IMDM, 20% FBS, 2% penicillin/streptomycin, and 25ng/mL macrophage-colony-stimulating factor (M-CSF) for 7-10 days at 37°C and 5% CO_2 to generate adherent macrophage progenitors. The media was changed after cells became adherent at day 5 and every 2 days thereafter.

Eco-Phoenix Packaging Cells

Eco-Phoenix packaging cell were cultured in DMEM (Invitrogen), 10% FBS, 1% Penicillin/Streptomycin, 1% L-glutamine (Invitrogen), and 1% sodium pyruvate (Invitrogen) at 37°C and 5% CO_2. Cells were split every 2-3 days.

NIH3T3 cells

Native NIH3T3 cells were cultured in DMEM, 10% FBS, 1% penicillin/streptomycin, 1% L-glutamine, and 1% sodium pyruvate at 37°C and 5% CO_2. Cells were split every 2-3 days.

Following transduction with the pQCXIN-Shp2 plasmid containing neomycin resistance, cells were cultured in media containing 600µg/mL of neomycin (G418) for selection.

Retroviral Supernatant Production

Retroviral supernatant were produced by transfecting the Eco-Phoenix cells with retroviral vector plasmids using calcium phosphate transfection (ProFection® Mammalian Transfection System, Promega). Supernatants, collected at 48 and 72 hours post-transfection were filtered through 0.45µm filters.

Retroviral Transduction of NIH3T3 cells

NIH3T3 cells were transduced with 1mL of pQCXIN-Shp2, pQCXIN-Shp2^{E76K}, pMSCV-p85α, pMSCV-p85α R358A, pMSCV-p85α R649A, pMSCV-p85α R358A/R649A, or pCMV6-Bcap retroviral supernatant in one well of a 6-well non-tissue culture plate, with 8ug of polybrene (Sigma). Plates were incubated for 24 hours at 37°C, then viral supernatant was replaced with DMEM, 10% FBS, 1% penicillin/streptomycin, 1% L-glutamine, and 1% sodium pyruvate, and plates were incubated for another 24 hours. At 72 hours after the start of transduction, cells were started on selection media (neomycin) or collected for fluorescence-activated cell sorting (FACS).

Cell Sorting

Retrovirally transduced cells were sorted using FACS to collect yellow fluorescent protein- and mCherry-positive (YFP$^+$mCherry$^+$) cells.

Generation of NIH3T3 cells expressing constructs of Shp2, p85α, and BCAP

Native NIH3T3 cells were first transduced with either WT Shp2 or $Shp2^{E76K}$ plasmid and cultured in neomycin-containing selection media. NIH3T3 cells stably expressing Shp2-neoR were used as recipients for p85α transduction, and sorted on YFP^+ cells. NIH3T3 cells stably expressing both Shp2-neoR and p85α-YFP were used as recipients for transduction with BCAP-mCherry, and sorted on $mCherry^+$ cells. This resulted in four NIH3T3 cell lines: 1) WT Shp2, WT p85α, BCAP; 2) WT Shp2, R358A/R649A p85α, BCAP; 3) $Shp2^{E76K}$, WT p85α, BCAP; and 4) $Shp2^{E76K}$, R358A/R649A p85α, BCAP (Figure 5.5).

Isolation of Total Cellular Protein Lysates

Cells were washed twice in cold PBS and incubated on ice for 5-10 minutes in a lysis buffer containing 50mM Hepes, 150mM NaCl, 10% Glycerol, 1% Triton X, 1.5mM $MgCl_2$, 1mM EGTA, 100mM NaF, and 10mM NaPPi with Na_3VO_4, $ZnCl_2$, PMSF, and protease inhibitor cocktail (Sigma). Protein lysates were collected by scraping, then centrifuged at 13,200 rpm for 15 minutes at 4°C and quantified using Bradford reagent.

Immunoblot Analysis

Protein lysates were separated by SDS-Polyacrylamide Gel Electrophoresis (SDS-PAGE) and transferred to nitrocellulose membrane, which was then incubated with shaking overnight in primary antibody (see Table 2.2) at 4°C. The membrane was then washed and incubated with HRP-conjugated secondary antibody (see Table 2.3), developed with SuperSignal (see Table 2.8), and exposed by using a Bio-Rad Imager.

Immunoprecipitation

Equal amounts of fresh protein lysates per sample were aliquoted into 1.5mL Eppendorf tubes, volumes were equalized with lysis buffer, HNTG buffer (1% Triton X, 50mM Hepes, 50mM NaCl, 5mM EDTA, 0.1% BSA, 50mM NaF with Na_3VO_4, $ZnCl_2$, PMSF, and protease inhibitor cocktail) was added to bring total volume to 500µL, and anti-BCAP or anti-p85α antibody was added (see Table 2.4). Tubes were rotated at 4°C for 2 hours, then 25µL of HNTG-washed Protein A/G PLUS-Agarose beads (Santa Cruz) were added per tube. Tubes were rotated at 4°C overnight, then washed three times with wash buffer (1% Triton X, 50mM Hepes, 120mM NaCl, 5mM EDTA, 50mM NaF with Na_3VO_4, $ZnCl_2$, PMSF, and protease inhibitor cocktail) for 15 minutes at 4°C rotating, spinning down at 3000rpm for 30 seconds in between washes, and used for immunoblot analysis.

[^{3}H]-Thymidine Incorporation Assay

Cells were starved for 4-5 hours in IMDM containing 0.2% Bovine Serum Albumin (BSA) (Roche) and then plated in 96-well plates (200µL IMDM with 2% penicillin/streptomycin per well) for [^{3}H]-thymidine incorporation assays (2 x 10^4 cells/well) either at baseline (no growth factor) or in the presence of 10ng/mL granulocyte macrophage-colony-stimulating factor (GM-CSF), with or without indicated inhibitors, and incubated overnight at 37°C. The following morning, cells were pulsed with 1µCi of [^{3}H]-thymidine and incubated for 5-6 hours at 37°C. [^{3}H]-thymidine incorporation was measured using an automated 96-well cell harvester and scintillation counter (Brandel, Gaithersburg, MD).

Methylcellulose Colony-Forming Assay

Bone marrow low-density mononuclear cells (1.0×10^5) were plated in triplicate in 1mL progenitor assays containing 1% methylcellulose (ES-Cult® M3120, Stem Cell Technologies), 30% FBS, 2% penicillin/streptomycin, 1% glutamine, and 80μM β-mercaptoethanol in the presence of increasing concentrations of GM-CSF (0, 0.01, 0.1, or 10ng/mL). Methylcellulose plates were incubated at 37°C for 7 days before total number of colonies were counted.

***In vivo* drug treatment of mice**

A solution of 0.5% w/v methylcellulose (Sigma) and 0.1% v/v Tween-80 (Sigma) was made in water. Using this solution, a stock of drug inhibitor (GS-9820, ACP-196, or ACP-319; see Table 2.7) was made, aliquoted into 1mL aliquots, and stored at 4°C during the 21 days of treatment. Prior to each dosing, the necessary amount of drug and vehicle were brought to room temperature and mixed thoroughly. Mice were dosed BID (twice a day) via oral gavage.

Flow Cytometry Analysis

Cell suspensions were incubated for 5 minutes with 10% rat serum (MP Biomedicals) and 0.2% BSA (Roche) in PBS, stained for 30 minutes at 4°C with primary antibody (see Table 2.5), washed with PBS, then stained for 15 minutes at 4°C with secondary antibody (see Table 2.6). The analyzer used for flow cytometry was a BD LSR II or a BD FACSCanto II and data was analyzed using CellQuest.

Complete Blood Counts

Peripheral blood was collected from the saphenous vein of mice and complete blood counts were measured using a Hemavet 950 (Drew Scientific Group) or an Element HT5 Hematology Analyzer (Heska).

Statistical Analysis

Statistics for Figures 3.8 and 4.5 were done using log-rank (Mantel-Cox) test. Statistics for all other experiments were performed using unpaired, two-tailed Student's t test. Figures show mean +/- standard deviation (S.D.) or mean +/- standard error of the mean (S.E.M.) as indicated in the figure.

CHAPTER THREE

PHARMACOLOGIC INHIBITION OF PI3K p110δ REDUCES SPLENOMEGALY AND PROLONGS SURVIVAL IN MUTANT Shp2^{E76K}-EXPRESSING MICE

Introduction

When studying gain-of-function (GOF) mutations in Shp2, which is the most common mutation found in juvenile myelomonocytic leukemia (JMML) patients, our laboratory has focused on the downstream target phosphoinositide 3-kinase (PI3K). We previously found that genetic and pharmacologic inhibition of the hematopoietic-specific catalytic subunit of PI3K, p110δ, is uniquely important in promoting GOF Shp2-induced leukemia (Goodwin, Li 2014). A mouse model of JMML with a GOF Shp2 mutation (*Shp2$^{D61Y/+}$*;Mx1-cre^{+}) was crossed with mice bearing a mutated p110δ with complete loss of catalytic activity. These *Shp2$^{D61Y/+}$*;*Pik3cd$^{D910A/D910A}$*;Mx1-cre^{+} mice had reduced splenomegaly, decreased phosphorylation of Akt and Erk, and decreased progenitor cell hypersensitivity to GM-CSF compared to the *Shp2$^{D61Y/+}$*;Mx1-cre^{+} mice. A similar mouse model with the same GOF Shp2, but with complete loss of p110α expression (*Shp2$^{D61Y/+}$*;*Pik3ca$^{flox/flox}$*;Mx1-cre^{+}), had no differences in comparison to the *Shp2$^{D61Y/+}$*;Mx1-cre^{+} mice. These findings demonstrated that the hematopoietic-specific p110δ subunit, and not the ubiquitously expressed p110α subunit, is essential for GOF Shp2-induced myeloproliferative neoplasm. Furthermore, pharmacologic inhibition of p110δ *in vitro* using the Gilead Sciences small molecule GS-9820, or the FDA-approved inhibitor idelalisib, decreased phospho-Akt and –Erk, proliferation of *Shp2$^{D61Y/+}$* cells,

and GM-CSF hypersensitivity of primary mononuclear cells from JMML patients (Goodwin, Li 2014).

The PI3K p110δ-specific inhibitor idelalisib was FDA-approved in 2014 for the treatment of patients with relapsed chronic lymphocytic leukemia and follicular lymphoma (Miller, Przepiorka 2015). However, the effectiveness of p110δ inhibition in JMML, a disease that lacks effective chemotherapies, has not yet been studied. Therefore, following our laboratory's promising results demonstrating reduced GM-CSF hypersensitivity and proliferation of GOF Shp2-expressing murine cells and primary JMML cells *in vitro*, we assessed the effect of p110δ inhibition on GOF Shp2-expressing mice *in vivo* as the next step in exploring p110δ inhibition as a potential treatment strategy for JMML. We utilized the p110δ inhibitor GS-9820 (hereafter PI3Kδ inhibitor), which has superior pharmacokinetics in murine models compared to idelalisib (Dr. Stacey Tannheimer, personal communication) (Carter, Cox 2017).

Results

Pharmacologic inhibition of PI3Kδ using the specific and potent inhibitor, GS-9820, significantly reduces gain-of-function mutant Shp2-induced splenomegaly

Having seen the effectiveness of p110δ inhibition *in vitro* for correcting GOF Shp2-induced leukemia characteristics, we next wished to test the usefulness of treatment with a p110δ inhibitor *in vivo*. To do this, we used mice expressing the Shp2 mutation E76K, which is the most frequent and the most active SHP2 mutation in JMML patients. The E76K mutant allele is conditionally expressed by Cre recombinase under

the control of the promoter of the lysozyme 2 gene. The LysMcre^{+} mice express Cre only in cells of the myeloid lineage, including monocytes, mature macrophages, and granulocytes (Clausen, Burkhardt 1999). *Shp2*$^{E76K/+}$;LysMcre^{+} mice have been previously reported to reliably develop a myeloid expansion and myeloproliferative neoplasm that closely mimics human JMML. These animals begin to die at 28 weeks of age and have a median survival of 36 weeks (Xu, Liu 2011). Thus, we determined 12-20 weeks of age to be an ideal treatment window, as this period provides sufficient time for the development of disease but typically precedes MPN-induced mortality. We treated *Shp2*$^{E76K/+}$;LysMcre^{+} mice between 12 and 20 weeks of age with 30mg/kg of PI3Kδ inhibitor (GS-9820) or vehicle (0.5% w/v methylcellulose + 0.1% v/v Tween 80) BID via oral gavage for 21 days. In our first of two cohorts, we had seven mice per treatment group and euthanized all fourteen mice 16 hours following the final dose of PI3Kδ inhibitor or vehicle.

When euthanized directly after completing 21 days of treatment, the PI3Kδ inhibitor-treated mice had significantly reduced spleen-to-body weight ratio in comparison to the vehicle-treated mice (Figure 3.1). To test the hypersensitivity of hematopoietic progenitors to GM-CSF, a hallmark feature of JMML, we measured the colony-forming ability of bone marrow low-density mononuclear cells (LDMNCs) in response to increasing concentrations of GM-CSF. 100,000 LDMNCs from each mouse were plated in semi-solid methylcellulose media containing 0, 0.01, 0.1, or 10ng/mL GM-CSF and colonies were counted 7 days later. LDMNCs isolated from PI3Kδ inhibitor-

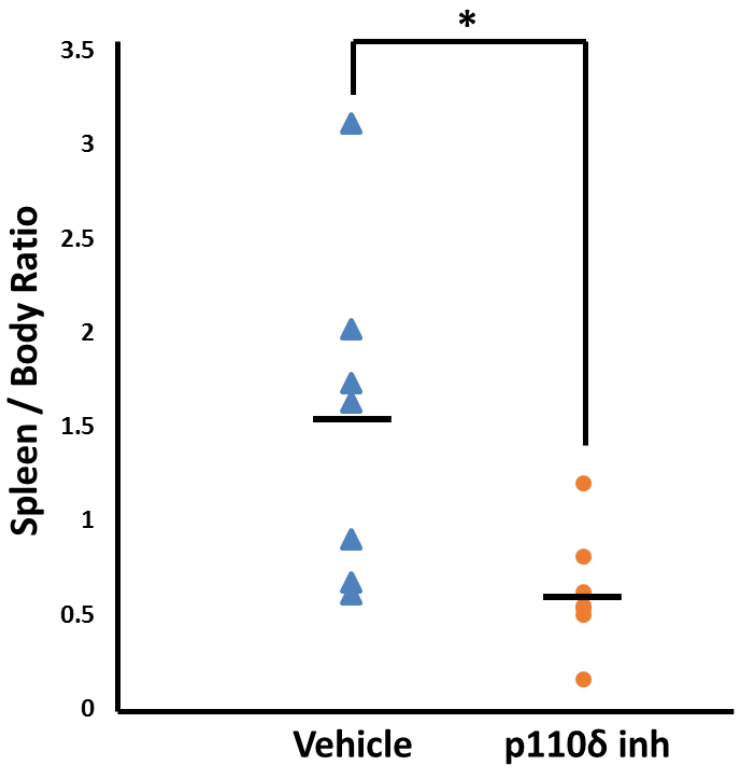

Figure 3.1: PI3Kδ inhibition *in vivo* decreases splenomegaly in *Shp2*$^{E76K/+}$;LysMcre^{+} mice

The spleen to body weight ratio of mice at the end of 21 days of treatment. Mice between the ages of 12-20 weeks were treated via oral gavage BID with either vehicle or 30mg/kg of PI3Kδ inhibitor. n=7 per group, *p=0.03 comparing the PI3Kδ inhibitor-treated mice to vehicle-treated mice, statistical analyses performed by unpaired, two-tailed, Student's t-test.

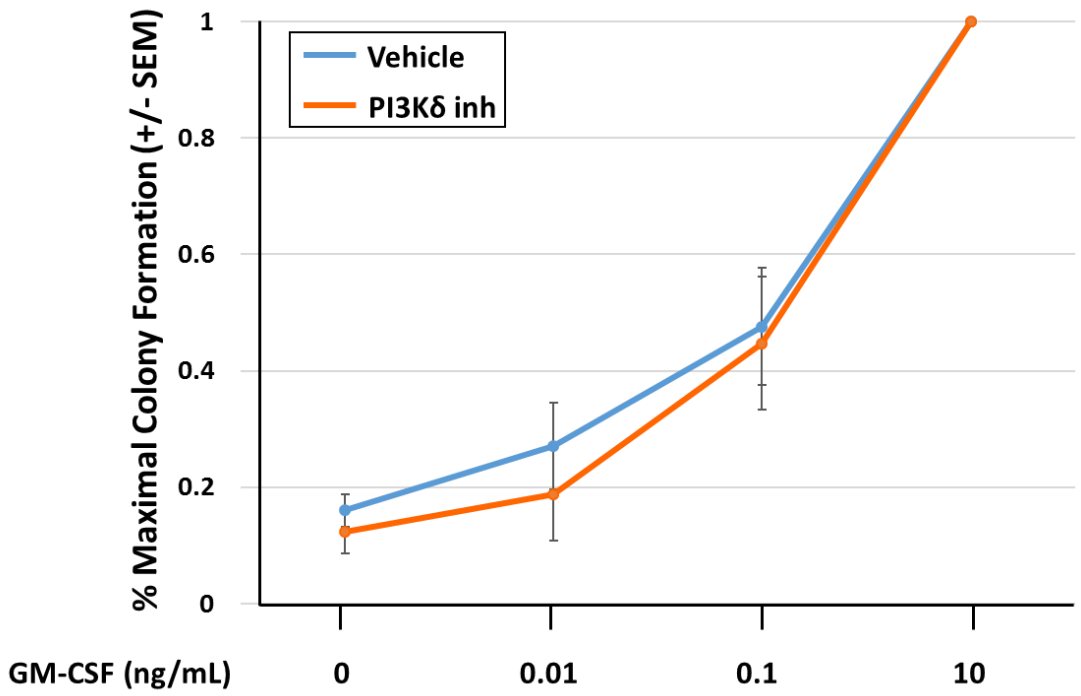

Figure 3.2: Time-limited PI3Kδ inhibition *in vivo* does not permanently correct GM-CSF hypersensitivity of bone marrow progenitors in *Shp2*$^{E76K/+}$;LysMcre^{+} mice

Number of colonies formed in methylcellulose colony forming assays, shown as a percentage of total colonies at maximum GM-CSF concentration. Bone marrow LDMNCs were collected from 7 PI3Kδ inhibitor-treated mice and 7 vehicle-treated mice and plated in triplicate per each concentration of GM-CSF. Colonies were counted 7 days after plating.

treated mice demonstrated similar GM-CSF hypersensitivity compared to the vehicle-treated mice, indicating that pharmacologic inhibition of PI3K p110δ does not permanently correct GM-CSF hypersensitivity of GOF Shp2-expressing cells (Figure 3.2).

Pharmacologic inhibition of PI3Kδ reduces bone marrow hematopoietic stem/progenitor cells and increases mature myeloid cells in the periphery of gain-of-function Shp2-expressing mice

To investigate how PI3Kδ inhibitor treatment induced the functional effect of reduced spleen size, we phenotypically analyzed the bone marrow, spleen, and peripheral blood for hematopoietic stem/progenitor cells (lineage$^-$Sca1$^+$cKit$^+$, LSK) and for terminally differentiated hematopoietic cells. The frequency of LSK cells was significantly reduced in the bone marrow of PI3Kδ inhibitor-treated mice and trended lower in the spleen and peripheral blood (Figure 3.3). When examining hematopoietic differentiation, we found no significant difference in myeloid progenitor populations (CMPs, GMPs, or MEPS, data not shown) or in the frequency of terminally differentiated CD4$^+$, CD8$^+$ (T cells), B220$^+$ (B cells), and Gr1$^+$Mac1$^+$ (myeloid cells) in the bone marrow (Figure 3.4) and spleen compartments (Figure 3.5). However, the frequency of peripheral blood Gr1$^+$Mac1$^+$ cells was significantly increased in the PI3Kδ inhibitor-treated mice compared to vehicle-treated mice (Figure 3.6). Furthermore, the Mac1$^+$ mean fluorescence intensity (MFI) in the peripheral blood was significantly higher in PI3Kδ inhibitor-treated mice (Figures 3.7). Collectively, these findings suggest that PI3K

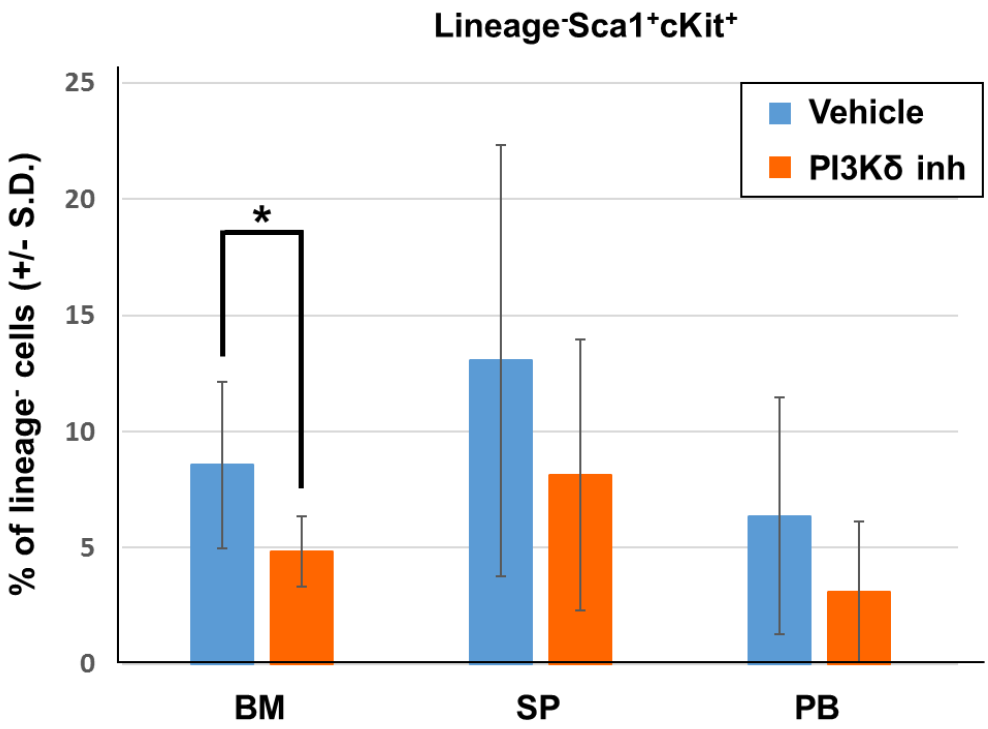

Figure 3.3: PI3Kδ inhibition *in vivo* decreases Lin$^-$Sca1$^+$Kit$^+$ progenitor cells in the bone marrow of *Shp2*$^{E76K/+}$;LysMcre$^+$ mice

Average percentage of Lin$^-$Sca1$^+$Kit$^+$ (LSK) cells in bone marrow (BM), spleen (SP), and peripheral blood (PB), n=7 per group, *p=0.026 comparing LSK cells in the bone marrow of PI3Kδ inhibitor-treated mice to vehicle-treated mice, statistical analyses performed by unpaired, two-tailed, Student's t-test.

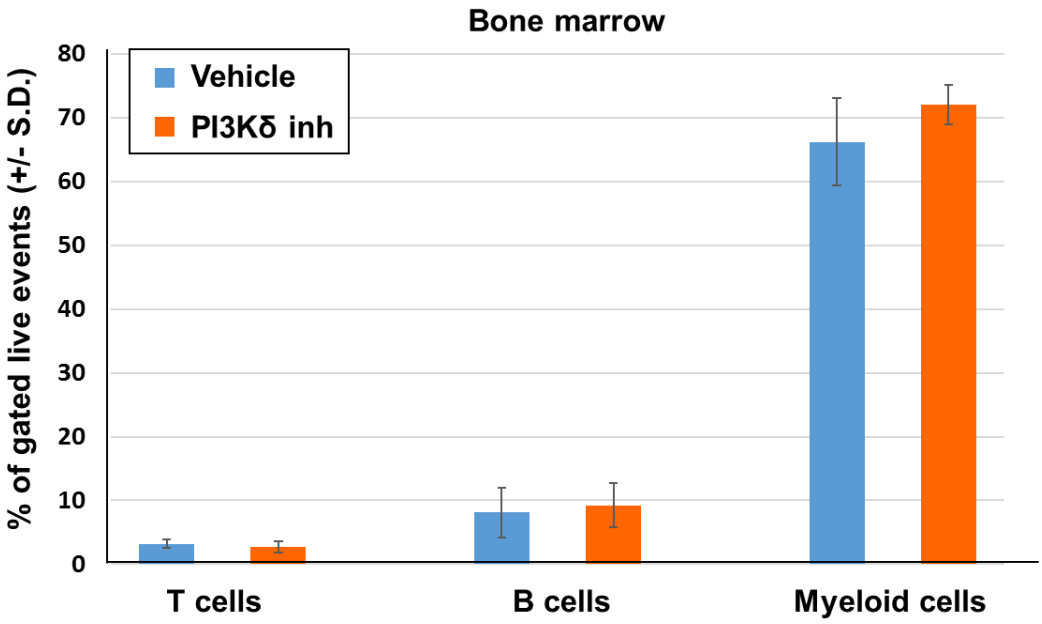

Figure 3.4: PI3Kδ inhibition *in vivo* does not affect terminally differentiated hematopoietic cell populations in the bone marrow of *Shp2*$^{E76K/+}$;LysMcre^{+} mice

Average percentage of bone marrow T cells (CD4^{+}CD8^{+}), B cells (B220^{+}), and myeloid cells (Gr1^{+}Mac1^{+}) gated on live events, n=7 per treatment group.

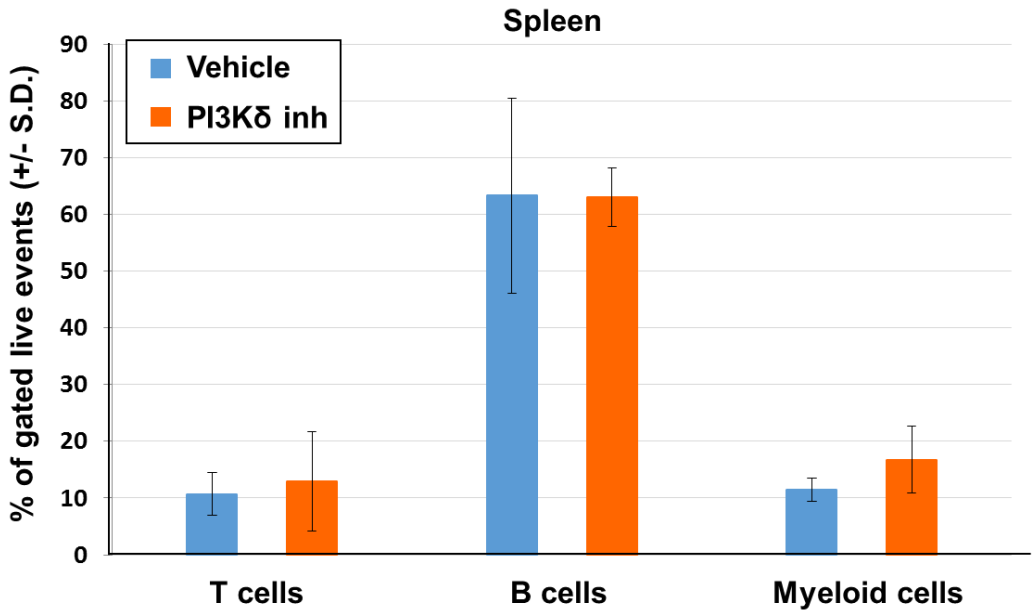

Figure 3.5: PI3Kδ inhibition *in vivo* does not affect terminally differentiated hematopoietic cell populations in the spleen of *Shp2*$^{E76K/+}$;LysMcre^{+} mice

Average percentage of spleen T cells (CD4^{+}CD8^{+}), B cells (B220^{+}), and myeloid cells (Gr1^{+}Mac1^{+}) gated on live events, n=7 per treatment group.

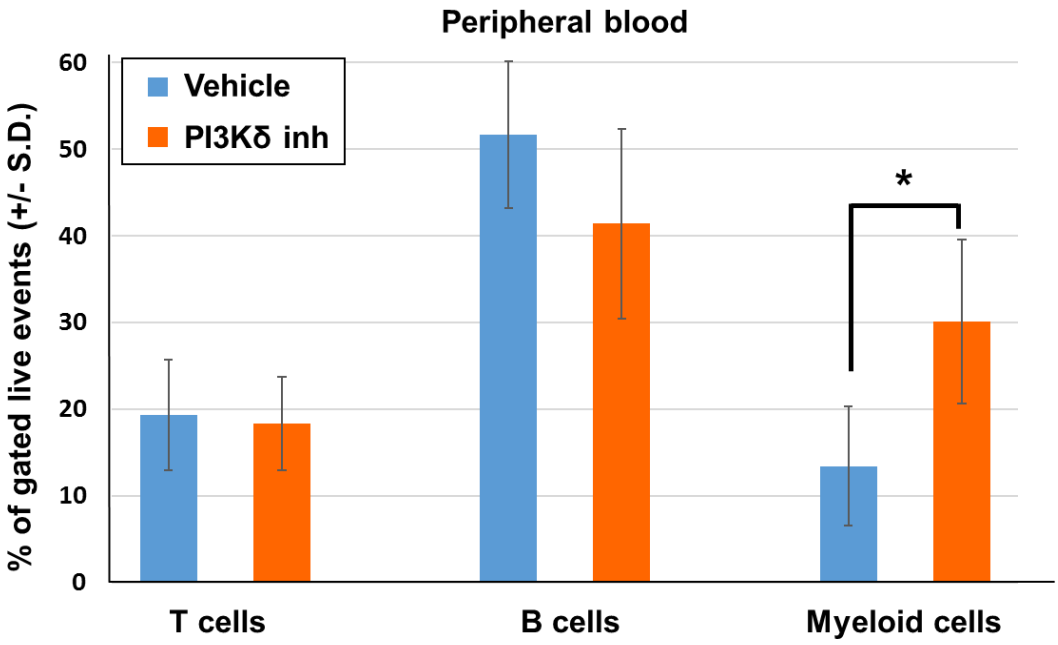

Figure 3.6: PI3Kδ inhibition *in vivo* increases the terminally differentiated myeloid cells in the peripheral blood of *Shp2*$^{E76K/+}$;LysMcre^{+} mice

Average percentage of peripheral blood T cells (CD4^{+}CD8^{+}), B cells (B220^{+}), and myeloid cells (Gr1^{+}Mac1^{+}) gated on live events, n=7 per treatment group, *p=0.05 comparing the percentage of myeloid cells in the peripheral blood of PI3Kδ inhibitor-treated mice to vehicle-treated mice, statistical analyses performed by unpaired, two-tailed, Student's t-test.

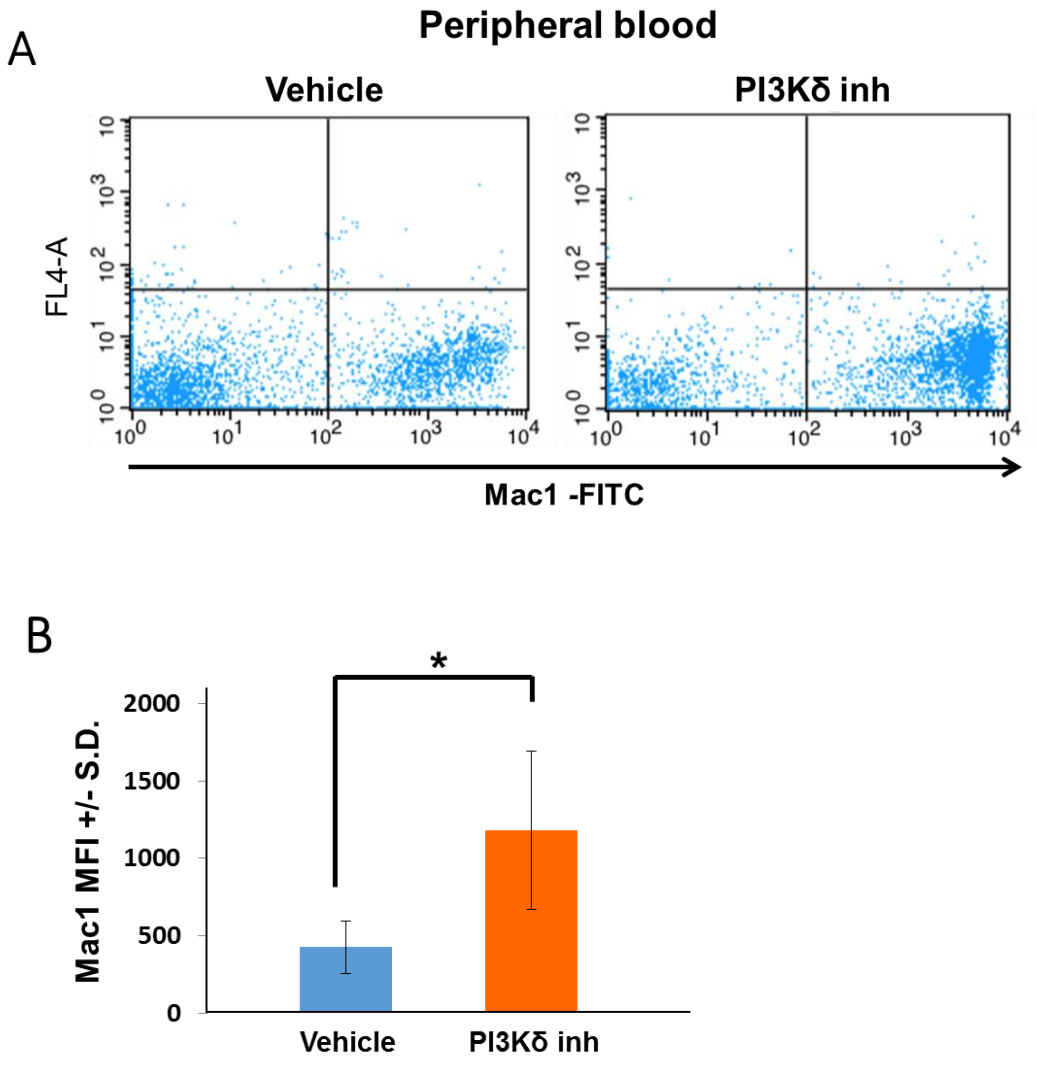

Figure 3.7: PI3Kδ inhibition *in vivo* increases the mean fluorescent intensity of Mac1 in the peripheral blood of *Shp2*$^{E76K/+}$;LysMcre^{+} mice

(A) Representative flow cytometry diagrams showing Mac1 brightness in the peripheral blood of vehicle-treated and PI3Kδ inhibitor-treated mice. (B) Average Mac1 mean fluorescent intensity (MFI) in peripheral blood, n=7 per group, *p=0.0029 comparing PI3Kδ inhibitor-treated to vehicle-treated mice, statistical analyses performed by unpaired, two-tailed, Student's t-test.

p110δ inhibition induced stem/progenitor terminal differentiation and reduced the self-renewal and hyperproliferation of immature myeloid cells.

Pharmacologic inhibition of PI3Kδ significantly prolongs survival of gain-of-function mutant Shp2-expressing mice

A second cohort of *Shp2*$^{E76K/+}$;LysMcre^{+} mice was made up of 15 mice per treatment group that were treated with PI3Kδ inhibitor or vehicle as described above. The second cohort of mice was followed long-term for overall survival with peripheral blood counts assessed every 4 to 6 weeks. Each treatment group consisted of 6 male mice and 9 female mice, and groups were age-matched with an average age of 114 days for the vehicle-treated mice and 109 days for the PI3Kδ inhibitor-treated mice. Survival of the PI3Kδ inhibitor-treated mice was significantly prolonged compared to their vehicle-treated counterparts (Figure 3.8). Serial peripheral blood WBC counts were similar between the two groups until approximately 18 weeks following the start of treatment, when WBC counts in the vehicle-treated animals started increasing compared to the PI3Kδ inhibitor-treated mice (Figure 3.9). Notably, the period of time of increasing WBC counts in the vehicle-treated animals coincided with the period of time when the survival curves started to separate (20 – 35 weeks). Later at 37 weeks, the drug-treated mice also demonstrated an increase in WBC counts, which corresponded to this group's cluster of deaths between 38 – 40 weeks.

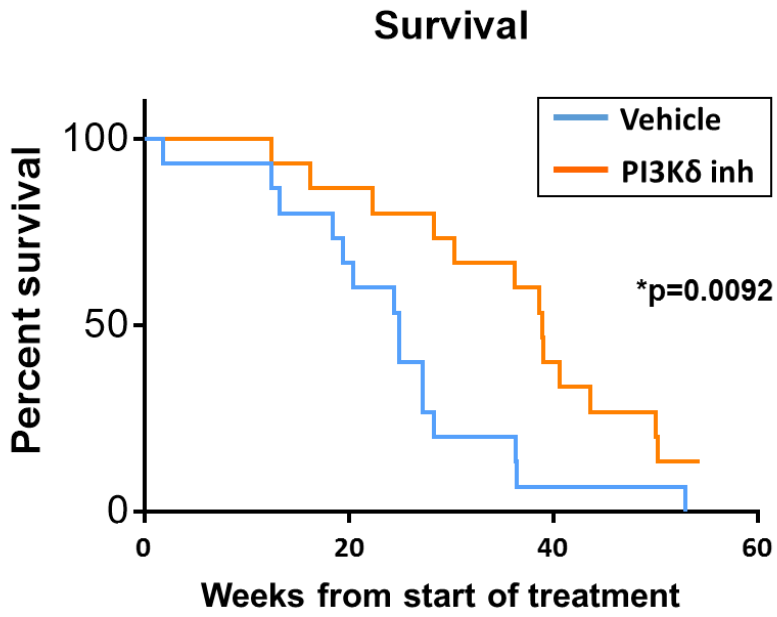

Figure 3.8: PI3Kδ inhibitor-treated *Shp2*$^{E76K/+}$;LysMcre^{+} mice have prolonged survival compared to vehicle-treated mice

Kaplan-Meier survival curve of days elapsed from start of treatment until death, n=15 per treatment group, *p=0.0092 comparing survival after treatment for PI3Kδ inhibitor-treated mice and vehicle-treated mice, statistical analyses performed by log-rank (Mantel-Cox) test.

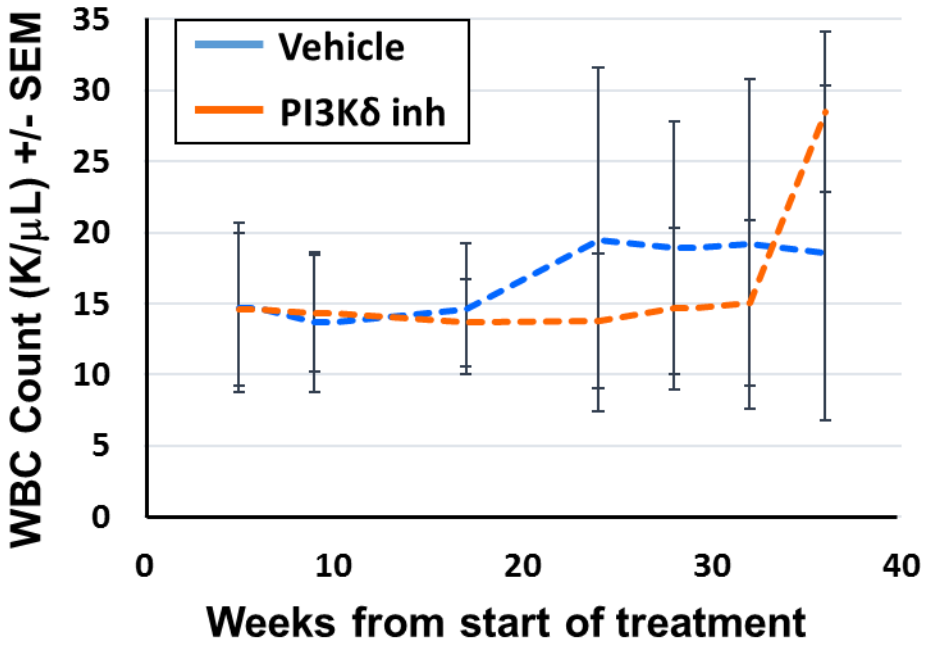

Figure 3.9: Vehicle- and PI3Kδ inhibitor-treated *Shp2*$^{E76K/+}$;LysMcre^{+} mice have a sharp increase in average peripheral blood WBC count prior to a cluster of deaths

Average WBC count (K/μL) in peripheral blood of mice.

Time-limited PI3Kδ inhibition does not alter the ultimate course of disease in gain-of-function mutant Shp2-expressing mice

Whenever possible, moribund mice were euthanized for analysis to assess the cause of death. Although the PI3Kδ inhibitor-treated animals demonstrated prolonged survival, at the time of euthanasia, these animals demonstrated similar levels of splenomegaly and elevated peripheral leukocyte counts compared to the vehicle-treated animals (Figure 3.10). Furthermore, composition of the bone marrow and spleen in moribund animals was not significantly different between the two groups (Figures 3.11 and 3.12). Most animals in both groups succumbed to a myeloid disease; however, both groups did demonstrate the emergence of T cell leukemia in a small number of mice, indicated by elevated levels of $CD4^+CD8^+$ cells in the bone marrow and spleen. Taken together, these findings suggest that time-limited PI3Kδ inhibition delays mortality due to Shp2-induced leukemia, but does not alter the ultimate course of disease. These findings imply that PI3Kδ activity resumes after termination of treatment and that continued or intermittent inhibition may be needed for optimal treatment of disease.

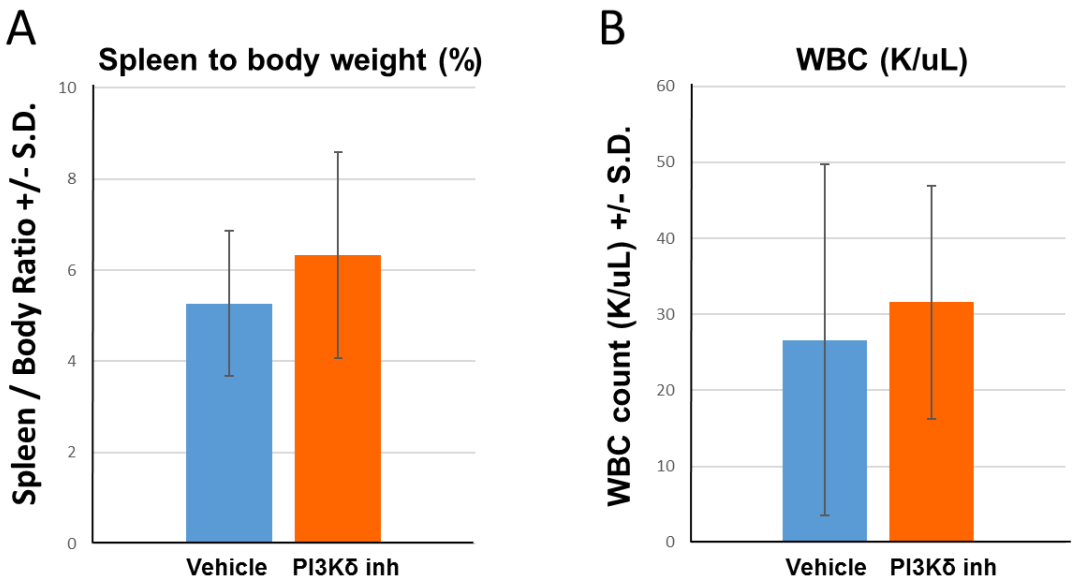

Figure 3.10: Vehicle- and PI3Kδ inhibitor-treated *Shp2*$^{E76K/+}$;LysMcre^{+} mice have no differences in degree of splenomegaly or leukocytosis when moribund

(A) Average spleen to body weight percentage at the time of death, n=14 for vehicle group, n=12 for PI3Kδ inhibitor group. (B) Average WBC count (K/μL) in peripheral blood at the time of death, n=9 for vehicle group, n=6 for PI3Kδ inhibitor group.

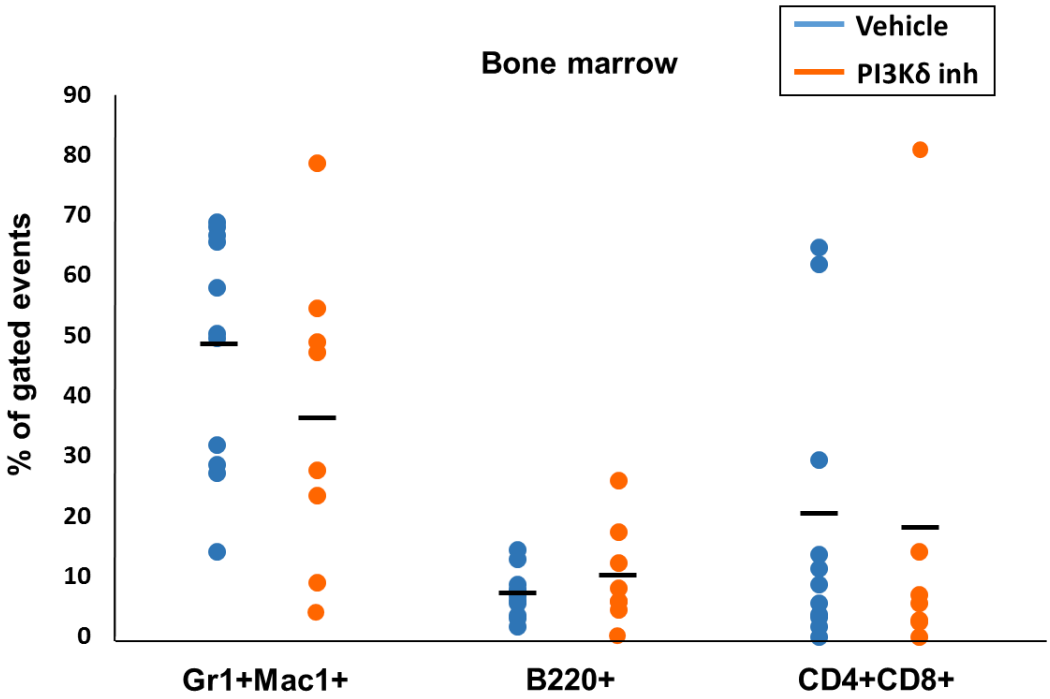

Figure 3.11: Vehicle- and PI3Kδ inhibitor-treated *Shp2*$^{E76K/+}$;LysMcre^{+} mice have no differences in terminally differentiated hematopoietic cell populations in the bone marrow when moribund

Percentage of bone marrow myeloid cells (Gr1^{+}Mac1^{+}), B cells (B220^{+}), and T cells (CD4^{+}CD8^{+}) at the time of death, gated on live events. n=13 for vehicle group, n=8 for PI3Kδ inhibitor group.

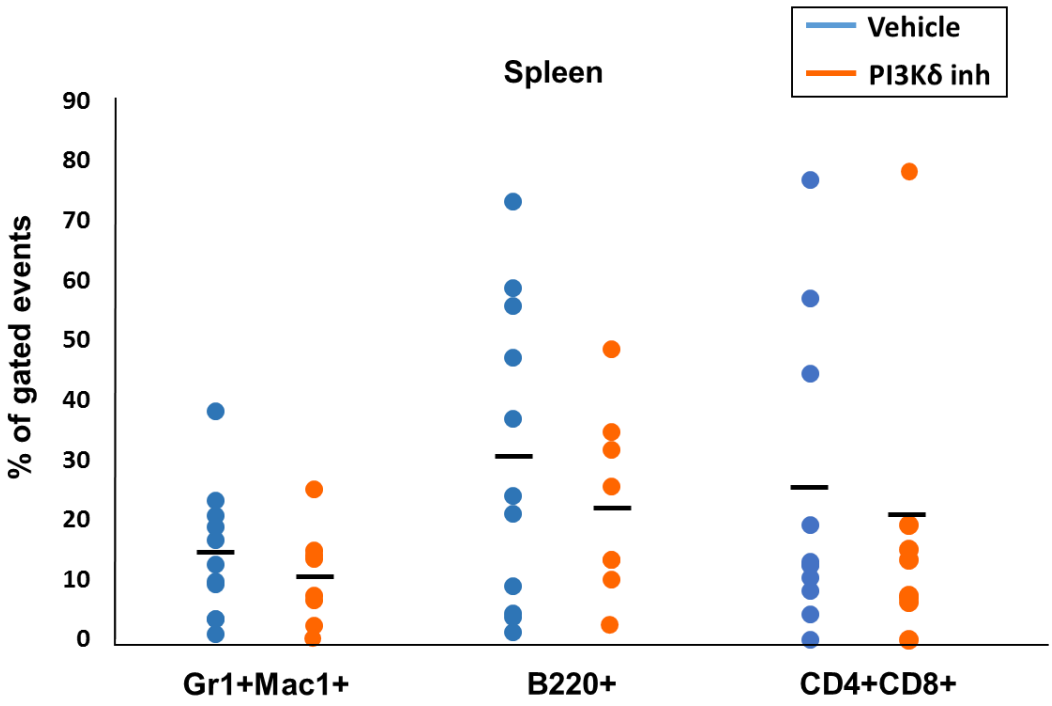

Figure 3.12: Vehicle- and PI3Kδ inhibitor-treated *Shp2*$^{E76K/+}$;LysMcre^{+} mice have no differences in terminally differentiated hematopoietic cell populations in the spleen when moribund

Percentage of spleen myeloid cells (Gr1^{+}Mac1^{+}), B cells (B220^{+}), and T cells (CD4^{+}CD8^{+}) at the time of death, gated on live events. n=13 for vehicle group, n=8 for PI3Kδ inhibitor group.

Discussion

We previously found that genetic and pharmacologic inhibition of PI3K p110δ *in vitro* normalizes hypersensitivity to GM-CSF and reduces GM-CSF-stimulated hyperproliferation of GOF Shp2-expressing murine and human cells (Goodwin, Li 2014). We now demonstrate that *in vivo* inhibition of PI3K p110δ increases the survival of GOF Shp2-expressing mice. One notable observation was increased terminally differentiated myeloid cells ($Gr1^+Mac1^+$) in the peripheral blood of PI3Kδ inhibitor-treated animals (Figure 3.6). A potential explanation for this observation is the recently-appreciated role of PI3K p110δ in regulatory T cell function with the resulting disruption of the protective tumor cell microenvironment and peripheral distribution of tumor cells upon PI3K p110δ inhibition (Fruman, Chiu 2017). In the context of this JMML model, it is possible that PI3K p110δ inhibition leads to redistribution and increased differentiation of mutant myeloid cells.

In both the vehicle- and PI3Kδ inhibitor-treated animals, we observed increased peripheral blood WBC counts that temporally preceded a precipitous drop in survival (Figures 3.8 and 3.9). The WBC spike in the PI3Kδ inhibitor-treated animals was more pronounced than that observed in the vehicle-treated group (Figure 3.9). One possibility accounting for this difference is that we simply "missed" a similarly high spike in the vehicle-treated mice, which might have occurred between the 18 week and 24 week scheduled blood draws (Figure 3.9). An alternative explanation is that treatment with the PI3K p110δ inhibitor allowed animals to tolerate higher circulating WBC counts before succumbing to disease.

As the armamentarium of molecularly targeted therapies continues to grow, potential application to difficult-to-treat diseases such as JMML is a valuable priority. Previous work conducted in the Braun lab demonstrated that treatment of GOF Kras- and GOF Nras-expressing mice with the pan-PI3K inhibitor, GDC-0941, or the allosteric Akt inhibitor, MK-2206, effectively ameliorated hyperactive Ras-induced disease (Akutagawa, Huang 2016). The effectiveness of single pathway inhibition is likely limited, as drug resistance to PI3K/Akt inhibition can develop due to aberrant upregulation of the Ras-Erk pathway. However, an analysis of clinical trials found that patients receiving Ras/MEK/Erk pathway inhibitors combined with pan-PI3K inhibitors commonly experienced toxic adverse effects (Shimizu, Tolcher 2012). The differential and potentially more limited side effect profile of PI3Kδ inhibition compared to pan-PI3K inhibition (Brown, Byrd 2014, Fruman, Chiu 2017) may provide a therapeutic window to simultaneously target both the Ras-Erk and PI3K-Akt pathways in the treatment of JMML. There is a clear need for improved chemotherapeutic treatments for JMML, as the current treatment options are limited with only variable efficacy. This work supports the rationale of using PI3Kδ inhibitors in the treatment of patients with JMML and possibly other myeloid cell malignancies.

CHAPTER FOUR

PHARMACOLOGIC INHIBITION OF BTK AND OF PI3K p110δ COOPERATE TO REDUCE GAIN-OF-FUNCTION MUTANT SHP2-INDUCED GM-CSF HYPERSENSITIVITY AND THE DEVELOPMENT OF MYELOID LEUKEMIA

Introduction

Having shown the effectiveness of PI3K p110δ inhibition in correcting gain-of-function mutant Shp2-induced leukemia phenotypes *in vitro* and in prolonging survival of mice *in vivo*, we next wanted to explore signaling molecules with which p110δ may be interacting to promote the aberrant Shp2 signaling in myeloid cells. In recent years, a key player in B cell receptor (BCR) signaling, Bruton's tyrosine kinase (BTK), has come under intense study in the field of lymphocytic leukemia and lymphoma research. Ibrutinib, a small molecule inhibitor targeting BTK, has proven to be very effective and has received FDA-approval for the treatment of a variety of B cell malignancies, including mantle cell lymphoma, chronic lymphocytic leukemia, Waldenström's macroglobulinemia, and marginal zone lymphoma (Barr, Robak 2016, Burger, Tedeschi 2015, Byrd, Brown 2014, Dimopoulos, Trotman 2017, Dreyling, Jurczak 2016, Noy, Vos 2016).

BTK's main function is to promote normal B cell development, as demonstrated by individuals with the disease X-linked agammaglobulinemia (XLA), who have inactivating mutations in BTK and lack mature B lymphocytes due to failure of immunoglobulin heavy chain rearrangement. Therefore, up until this point, all research on BTK has focused on B cell malignancies. However, although XLA patients have no

deficiencies beyond those affecting the B cell-mediated immune system response, BTK expression is not limited solely to the B cell lineage. BTK is also highly expressed in myeloid cells, and mice lacking BTK are defective in many myeloid cell functions, such as the generation of reactive oxygen species by macrophages (Mangla, Khare 2004). Furthermore, BTK has been found to be highly expressed and phosphorylated in AML patient samples (Rushworth, Murray 2014). Thus, it is possible that BTK signaling may also play an important role in myeloid malignancies, such as JMML.

Following antigen-mediated BCR cross-linking and activation, BTK is phosphorylated by spleen tyrosine kinase (SYK) and, once activated, signals downstream to phospholipase C γ2 (PLCγ2), protein kinase C (PKC), and ERK for proper B cell development and maturation (Hashimoto, Okada 1998, Kim, Sekiya 2004). BTK activation depends on its recruitment to the plasma membrane by $PI(3,4,5)P_3$, the phospho-lipid product of PI3K p110δ. Thus, it has been hypothesized that dual inhibition with a BTK and a p110δ inhibitor may have an additive effect in the treatment of CLL (Brown 2014). In line with this notion, Acerta Pharma is currently recruiting for a phase I clinical trial to test the combination of a second-generation BTK inhibitor (ACP-196) with a specific p110δ inhibitor (ACP-319) in B cell malignancies (NCT02328014). ACP-196, also called acalabrutinib and marketed under the name Calquence®, is FDA approved for the treatment of relapsed mantle cell lymphoma. Given the collaboration of BTK and p110δ in BCR signaling, the key role of p110δ in GOF Shp2-induced leukemia, and the high expression of BTK in myeloid cells, we hypothesized that BTK and p110δ function cooperatively in GOF Shp2-expressing myeloid cells to promote MPN. To test this

hypothesis, we examined the potential collaboration of GM-CSF-stimulated BTK and p110δ in GOF Shp2-expressing myeloid cells and tested the inhibitor combination *in vivo* in mice to test their effectiveness for correcting leukemia phenotypes and increasing survival.

For these studies, we used ACP-196 (BTK inhibitor) and ACP-319 (p110δ inhibitor), which were generously provided to us by Acerta Pharma. For the *in vitro* studies, we utilized bone marrow low-density mononuclear cells (LDMNCs) from *Shp2*$^{E76K/+}$;LysMcre^{+} mice, which express the most common and active SHP2 mutation (E76K) conditionally in cells of the myeloid lineage (Xu, Liu 2011) or from polyI:polyC-treated *Shp2*$^{D61Y/+}$;Mx1-cre^{+} mice (Chan, Kalaitzidis 2009). For the *in vivo* experiments, we used ACP-196 and ACP-319 either singly or in combination to treat *Shp2*$^{E76K/+}$;LysMcre^{+} mice between 12 and 20 weeks of age to allow sufficient time for the development of disease prior to the initiation of therapy. We predicted that the treatment of GOF Shp2-expressing myeloid cells with ACP-196 and ACP-319 would reduce progenitor cell hyperproliferation and hyperphosphorylation of Akt and Erk in response to GM-CSF stimulation. We further predicted that the combination of inhibitors would correct leukemia features, such as splenomegaly and leukocytosis, and prolong the overall survival of *Shp2*$^{E76K/+}$;LysMcre^{+} mice.

Results

BTK is hyperactivated in gain-of-function mutant Shp2 expressing macrophages and is downstream of PI3K p110δ in myeloid cell signaling

BTK's role in malignancies has previously only been studied in B cell leukemia and lymphoma. Therefore, we initially performed an experiment to determine if BTK is hyperactivated in mutant Shp2 myeloid cells. We isolated LDMNCs from the bone marrow of *Shp2*$^{D61Y/+}$;Mx1-cre^{+} mice 8-12 weeks after polyI:polyC treatment to allow for disease onset. The cells were cultured in media containing 25ng/mL of macrophage colony-stimulating factor (M-CSF) for 1 week to generate bone marrow-derived macrophages. Once fully differentiated, the macrophages were starved overnight, treated for 1 hour with 0ng/mL or 10ng/mL of GM-CSF, and lysed for immunoblot analysis. We found that BTK was indeed hyperphosphorylated in the Shp2^{D61Y}-expressing cells compared to WT Shp2, both with and without GM-CSF stimulation (Figure 4.1). Furthermore, we also observed increased phosphorylation of BTK's known downstream target in B cell receptor signaling, PLCγ2, at two different tyrosine phosphorylation sites in the GOF Shp2-expressing macrophages (Figure 4.1).

Knowing that BTK is hyperactivated in GOF Shp2-expressing macrophages, we next tested the hypothesis that BTK is activated downstream of p110δ in the GM-CSF-stimulated signaling pathway using the BTK and p110δ inhibitors. We treated bone marrow-derived macrophages from *Shp2*$^{E76K/+}$;LysMcre^{+} mice with GM-CSF (0ng/mL or 10ng/mL) and ACP-196 (0.05uM or 0.1uM) or ACP-319 (0.5uM or 1uM) or no inhibitor at all, followed by examination of BTK and PLCγ2 phosphorylation levels via immunoblot. We saw, as expected, a dose-dependent decrease in BTK phosphorylation at Y223, the autophosphorylation site, when treated with the BTK inhibitor (Figure 4.2, compare lanes 2, 3, and 4). More interestingly, there was likewise a dose-dependent reduction in

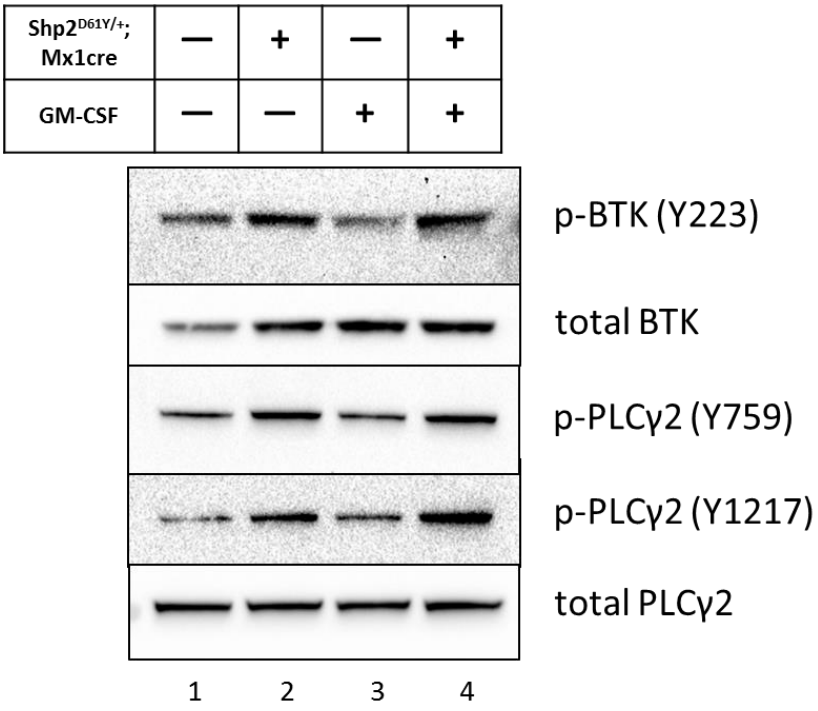

Figure 4.1: BTK and PLCγ2 are hyperphosphorylated in gain-of-function mutant Shp2-expressing macrophages

Immunoblot analysis of phospho- and total BTK and PLCγ2 protein levels in bone marrow-derived macrophages from WT Shp2 and Shp2^{D61Y}-expressing mice in the absence and presence of 10ng/mL GM-CSF.

phospho-BTK with the p110δ inhibitor, indicating that p110δ does function as an upstream activator of BTK (Figure 4.2, compare lanes 2, 5, and 6). This finding is consistent with the known BCR-stimulated signaling pathway in B cells, where PI3K's phospholipid product $PI(3,4,5)P_3$ recruits BTK to the plasma membrane by BTK's Plekstrin Homology domain to facilitate its phosphorylation (Bradshaw 2010). However, notably unlike the BCR signaling pathway, neither inhibitor had any effect on the levels of phospho-PLCγ2 at Y759 or Y1217, two tyrosine phosphorylation sites known to be direct BTK targets in B cells.

Next, we wished to test if the BTK and p110δ inhibitors reduced GM-CSF-induced hyperphosphorylation of Akt and Erk. We again treated bone marrow-derived macrophages with GM-CSF (0ng/mL or 10ng/mL) and two different concentrations of ACP-319 (0.1uM and 0.5uM), and also included the presence or absence of 0.05uM ACP-196 for each condition. Upon treatment with the p110δ inhibitor ACP-319, similar to that observed with GS-9820 (Goodwin, Li 2014), there was a dose dependent decrease in phospho-Akt and phospho-Erk (Figure 4.3, compare lanes 2, 3, and 4). With the BTK inhibitor alone at the 0.05uM dose, we observed only modest reductions in Akt and Erk phosphorylation (Figure 4.3, compare lanes 2 and 5). However, when ACP-319 was added to this dose of ACP-196, there was a pronounced reduction in both phospho-Akt and –Erk compared to either the same dose of ACP-319 or ACP-196 alone (Figure 4.3, compare lanes 3 and 4 to lanes 6 and 7, or lane 5 to lanes 6 and 7, respectively). These findings demonstrate that BTK cooperates with p110δ in promoting the hyperactivation of Akt and Erk in GOF Shp2-expressing macrophages and strengthens the idea that dual

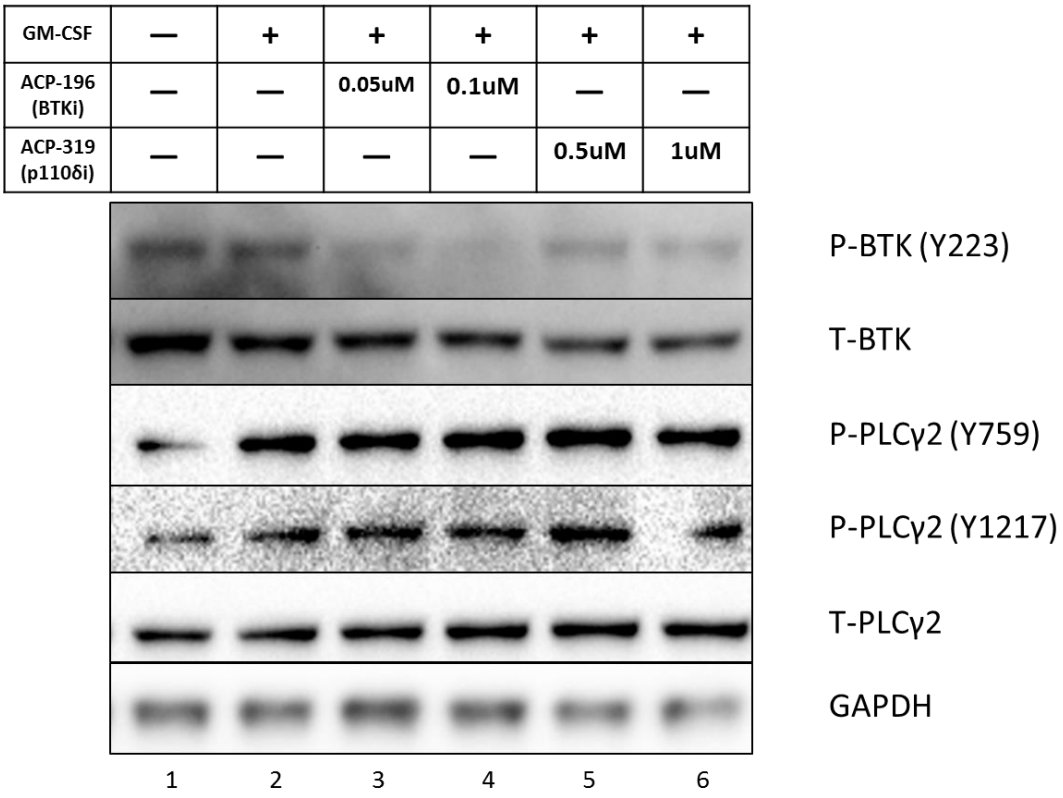

Figure 4.2: Inhibition of BTK and p110δ independently decrease BTK phosphorylation in a dose-dependent manner in gain-of-function mutant Shp2-expressing macrophages

Immunoblot showing phospho- and total BTK and PLCγ2 protein levels in $Shp2^{E76K}$-expressing bone marrow-derived macrophages in the absence or presence of 10ng/mL GM-CSF and the indicated concentrations of BTK and p110δ inhibitor.

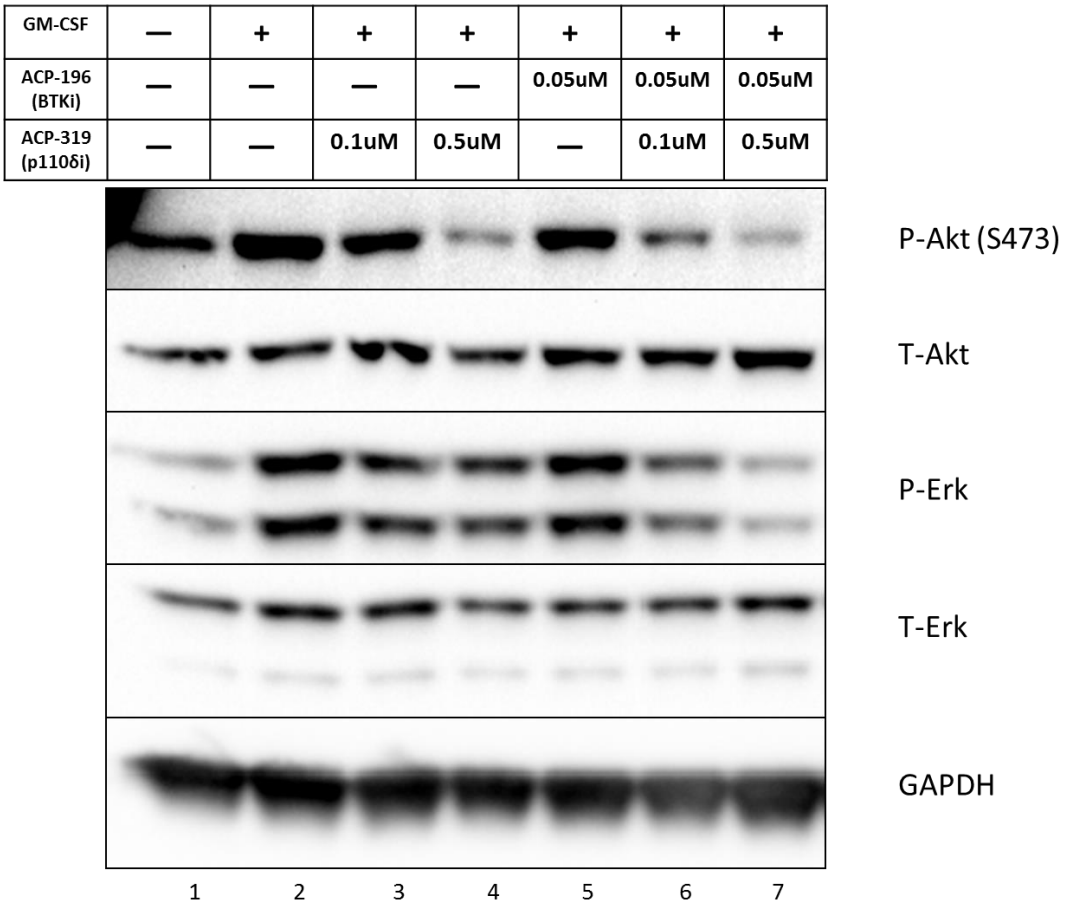

Figure 4.3: Inhibition of BTK and p110δ independently decrease Akt and Erk phosphorylation in a dose-dependent manner in gain-of-function mutant Shp2-expressing macrophages

Immunoblot showing phospho- and total Akt and Erk protein levels in $Shp2^{D61Y}$-expressing bone marrow-derived macrophages in the absence or presence of 10ng/mL GM-CSF and the indicated concentrations of BTK and p110δ inhibitor.

inhibition may be effective for myeloid malignancies. Along with data presented in Figure 4.2, which show that p110δ and BTK inhibition both fail to reduce phospho-PLCγ2 levels, these findings highlight the novel observation that p110δ and BTK positively signal to Erk and Akt in a PLCγ2-independent manner in GOF Shp2-expressing myeloid cells.

Inhibition of BTK and PI3K p110δ cooperatively reduce GM-CSF-stimulated hyperproliferation in bone marrow progenitor cells from gain-of-function mutant Shp2 expressing mice

With the signaling pathway of p110δ to BTK demonstrated to be intact in myeloid cells, we next went on to test the effectiveness of the Acerta Pharma p110δ and BTK inhibitors at reducing GM-CSF-stimulated hyperproliferation *in vitro*. We isolated bone marrow LDMNCs from *Shp2*$^{E76K/+}$;LysMcre^{-} or *Shp2*$^{E76K/+}$;LysMcre^{+} mice and performed [^{3}H]-thymidine incorporation assays to measure proliferation in the presence of 10ng/mL of GM-CSF. While 1uM and 5uM of ACP-319 induced a dose-dependent decrease in cell proliferation, ACP-196 at concentrations of 1uM and 5uM had no effect on cell proliferation (Figure 4.4). However, there was a significantly greater reduction in proliferation when 5uM of ACP-319 was combined with 1uM of ACP-196 compared to that of 5uM ACP-319 alone (Figure 4.4). These proliferation data are consistent with the results of the biochemical studies, where we observed only a modest reduction in Akt or Erk phosphorylation in response to ACP-196 treatment alone, but a cooperative effect in

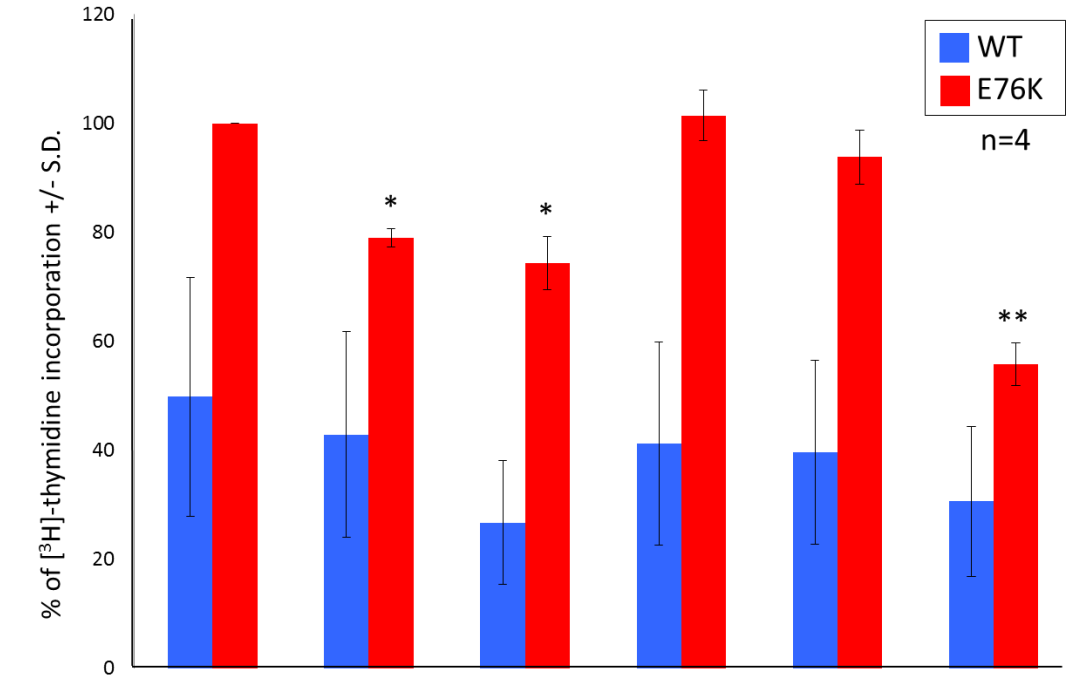

ACP-319 (p110δi)	**—**	**1uM**	**5uM**	**—**	**—**	**5uM**
ACP-196 (BTKi)	**—**	**—**	**—**	**1uM**	**5uM**	**1uM**

Figure 4.4: Proliferation is cooperatively decreased by BTK and p110δ dual inhibition in bone marrow LDMNCs from *Shp2^{E76K}*;LysMcre^{+} mice

WT Shp2 and E76K-expressing murine bone marrow LDMNCs were subjected to [^{3}H]-thymidine incorporation assays in the presence of 1ng/mL GM-CSF, n=4 independent experiments, *p<0.05 for E76K treated with 1μM or 5μM ACP-319 compared to E76K untreated, **p<0.05 for E76K treated with 5μM ACP-319 plus 1μM ACP-196 compared to E76K treated with 5μM ACP-319 alone and compared to E76K treated with 1μM ACP-196 alone, statistical analyses performed using unpaired, two-tailed, Student's t-test.

response to the combination of ACP-196 with ACP-319 (Figure 4.3). This finding provides further evidence that dual inhibition of p110δ and BTK is a viable strategy in the treatment of mutant Shp2-induced myeloid leukemia.

Pharmacologic inhibition of BTK and PI3K p110δ in vivo *using 15mg/kg of ACP-196 and 15mg/kg of ACP-319 trends towards prolonged survival in gain-of-function mutant Shp2-expressing mice*

With the promising performance of the combination of ACP-196 plus ACP-319 *in vitro*, our next step was to treat *Shp2*$^{E76K/+}$;LysMcre^{+} mice with these inhibitors *in vivo*. Twelve mice were assigned to each of four different treatment groups: vehicle (0.5% w/v methylcellulose + 0.1% v/v Tween 80), 15mg/kg ACP-196, 15mg/kg ACP-319, and 15mg/kg ACP-196 plus 15mg/kg ACP-319. The average ages of each group at the start of treatment, respectively, were 146 days, 141 days, 136 days, and 141 days. There were six females and six males in each group except for the vehicle group, which had five females and seven males. The dosing protocol was previously tested in mice and recommended by collaborators at Acerta Pharma (Dr. Cecile Krejsa, personal communication). After completion of treatment, these 48 mice were followed for overall survival.

We observed no differences in survival after treatment with either ACP-196 or ACP-319 alone, with these survival curves overlapping with and often crossing that of the vehicle group (Figure 4.5). In contrast, the drug combination-treated mice demonstrated an improved survival compared to the other three treatment groups, and

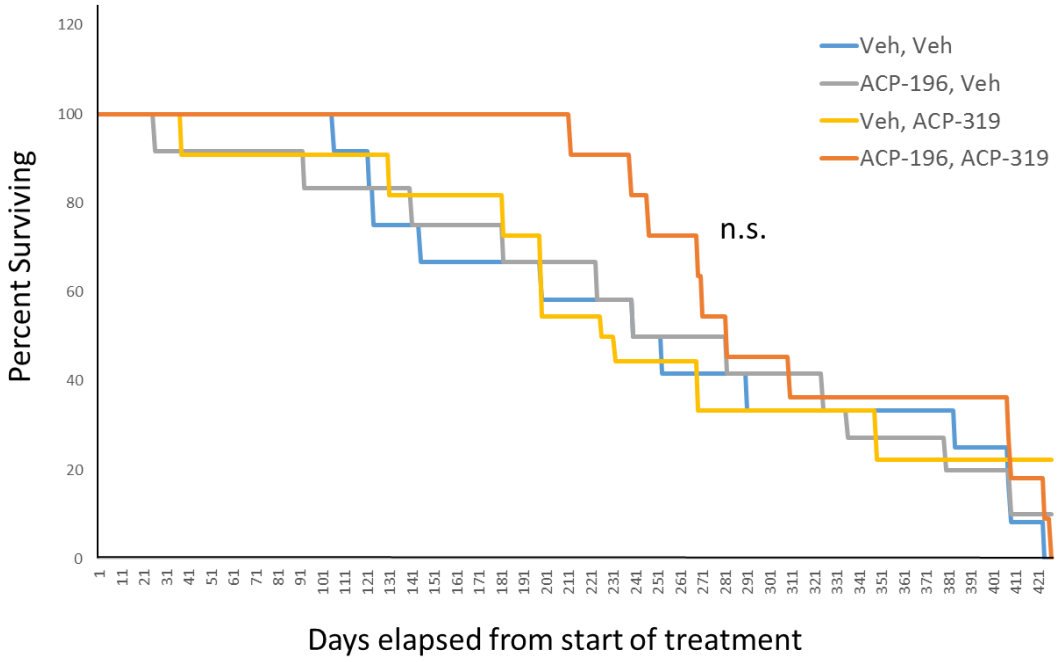

Figure 4.5: BTK and p110δ dual inhibitor-treated *Shp2*$^{E76K/+}$;LysMcre^{+} mice show a trend towards prolonged survival compared to vehicle-treated and single agent-treated mice

Kaplan-Meier survival curve of days elapsed from start of treatment until death, n=12 per treatment group, p=0.112 comparing survival after treatment for BTK plus p110δ inhibitor-treated mice and vehicle-treated mice, statistical analyses performed by log-rank (Mantel-Cox) test.

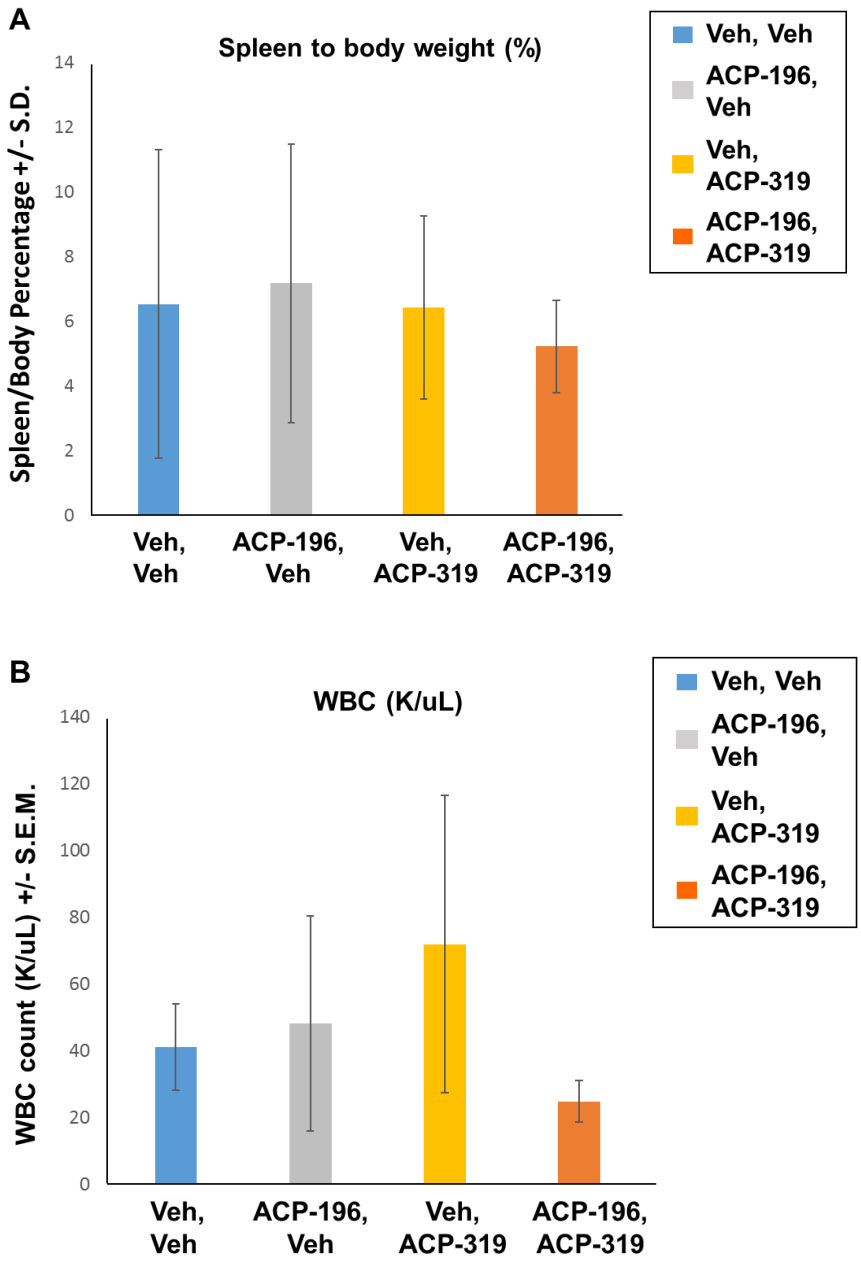

Figure 4.6: Vehicle-, BTK inhibitor-, and p110δ inhibitor-treated *Shp2*$^{E76K/+}$;LysMcre^{+} mice have no differences in degree of splenomegaly or leukocytosis when moribund

(A) Average spleen to body weight percentage at the time of death; n=10 for Veh, Veh; n=8 for ACP-196, Veh; n=8 for Veh, ACP-319; n=7 for ACP-196, ACP-319. (B) Average WBC count (K/μL) in peripheral blood at the time of death; n=6 for Veh, Veh; n=5 for ACP-196, Veh; n=6 for Veh, ACP-319; n=3 for ACP-196, ACP-319.

its curve never crossed the vehicle group curve (Figure 4.5). However, the difference in survival was not statistically significant, with a logrank p-value of 0.112 comparing the ACP-196 plus ACP-319 group to the vehicle group. Every effort was made to analyze the mice in this survival study as they became moribund. We did not observe any differences in spleen to body weight percentage or peripheral blood WBC values between any of the four groups (Figure 4.6). There was also no change in the bone marrow, spleen, or peripheral blood populations of myeloid cells, B cells, or T cells (data not shown).

Pharmacologic inhibition of BTK and PI3K p110δ in vivo *using 15mg/kg of ACP-196 and 15mg/kg of ACP-319 elicited a modest reduction in splenomegaly and leukocytosis in gain-of-function mutant Shp2-expressing mice*

Another cohort of four *Shp2*$^{E76K/+}$;LysMcre^{+} mice in each treatment group were treated in the same manner as described above. The average ages at the start of treatment were as follows: vehicle = 120 days, ACP-196 = 117 days, ACP-319 = 117 days, ACP-196 plus ACP-319 = 119 days. Each group had three males and one female except for the ACP-319 group, which consisted of one male and three females. All sixteen mice were euthanized on the morning directly following administration of the final drug dose in order to analyze the extent of disease progression.

With the 15mg/kg combination drug dose, we observed favorable but non-significant trends in several measures of leukemia. The spleen to body weight percentage was unchanged by administration of ACP-196 alone, but there was a small

decrease in the ACP-319 group and a greater decrease in the dual inhibitor-treated group of mice (Figure 4.7). The combination-treated mice also had the greatest reduction in peripheral blood WBC count, as calculated by subtracting the WBC count immediately before beginning treatment from the WBC count immediately before euthanasia (Figure 4.8).

We analyzed the hematopoietic stem/progenitor cells (lineage$^-$Sca1$^+$cKit$^+$, LSK), granulocyte monocyte progenitors (GMP, CD34$^+$CD16/32$^+$), common myeloid progenitors (CMP, CD34$^+$CD16/32$^-$), megakaryocyte erythrocyte progenitors (MEP, CD34$^-$CD16/32$^-$), and the SLAM marker populations of hematopoietic stem cells (HSC, CD150$^+$CD48$^-$), multipotent progenitor cells (MPP, CD150$^-$CD48$^-$), and lineage-restricted progenitor cells (LRP, CD150$^-$CD48$^+$). We found no significant changes in the bone marrow, spleen, or peripheral blood of the mice for these stem/progenitor populations (data not shown). Consistent with no changes in the phenotypically-defined progenitor populations, we found no differences in the GM-CSF hypersensitivity of the bone marrow hematopoietic progenitors from the drug-treated mice in methylcellulose colony-forming assays (data not shown).

The terminally differentiated hematopoietic cell populations were also analyzed in each of these three hematopoietic compartments. The B220$^+$ B cells and CD4$^+$CD8$^+$ T cells were unchanged among the four treatment groups; however, we found that the Gr1$^+$Mac1$^+$ myeloid cells were significantly increased in the peripheral blood of the ACP-319-treated and trended higher in the ACP-196 + ACP-319-treated groups (Figure 4.9).

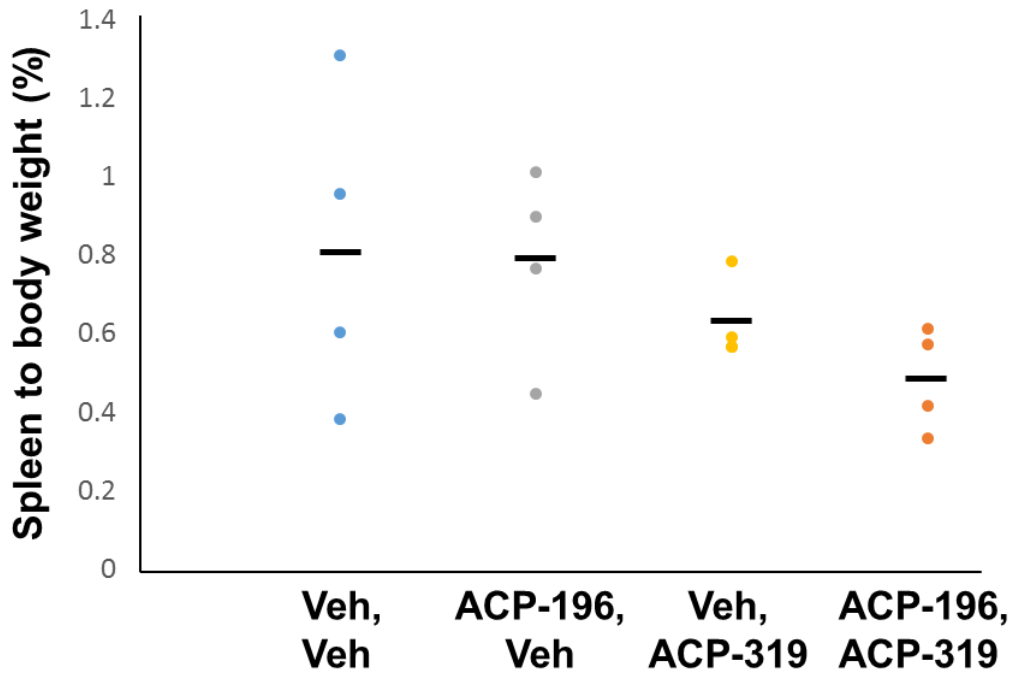

Figure 4.7: Dual inhibition of BTK and p110δ *in vivo* trends towards decreased splenomegaly in *Shp2*$^{E76K/+}$;LysMcre^{+} mice

The spleen to body weight ratio of mice at the end of 21 days of 15mg/kg treatment, n=4 per group, p=0.1742 comparing the BTK plus p110δ inhibitor-treated mice to vehicle-treated mice, statistical analyses performed by unpaired, two-tailed, Student's t-test.

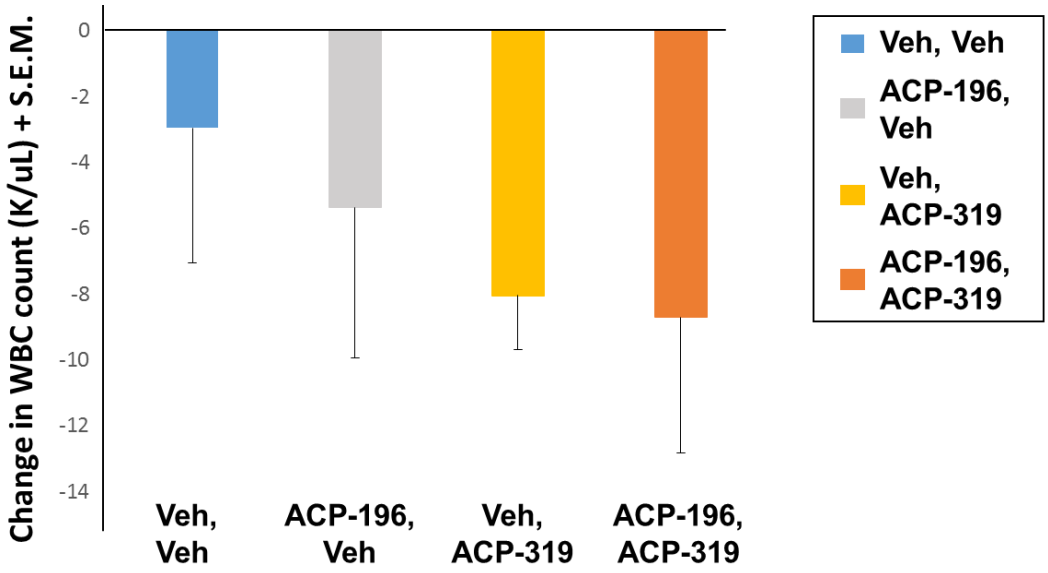

Figure 4.8: BTK and p110δ dual inhibition *in vivo* trends towards a reduction in peripheral blood WBC count in *Shp2*$^{E76K/+}$;LysMcre^{+} mice

The average values of peripheral blood WBC count prior to treatment subtracted from the WBC count at the end of 21 days of 15mg/kg treatment, n=4 mice per group.

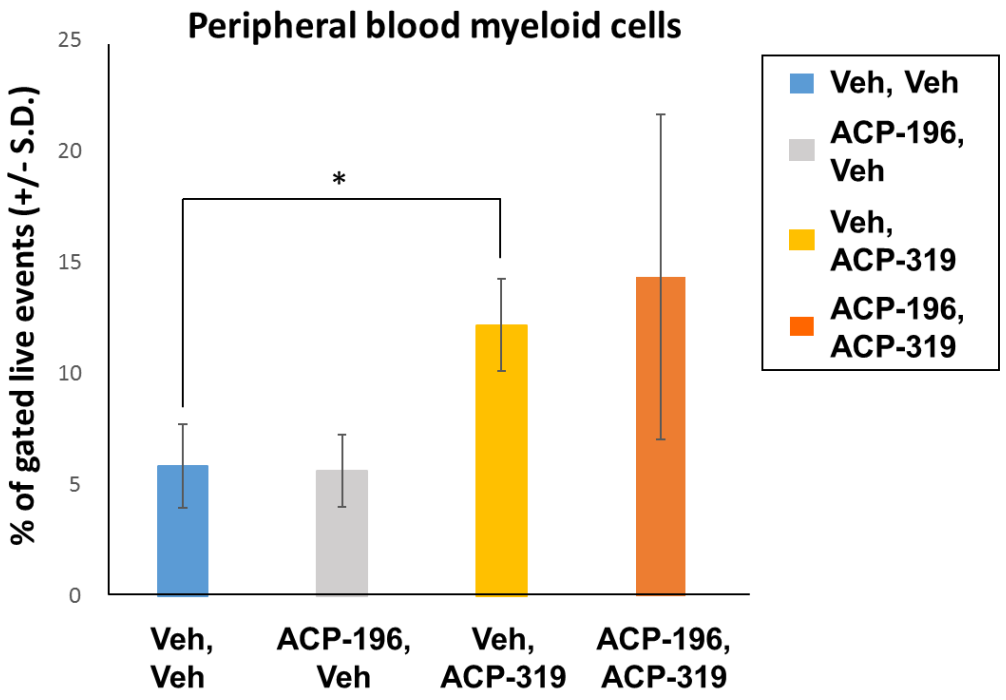

Figure 4.9: BTK and p110δ dual inhibition *in vivo* trends towards increased terminally differentiated myeloid cells in the peripheral blood of *Shp2*$^{E76K/+}$;LysMcre^{+} mice

Average percentage of peripheral blood myeloid cells (Gr1^{+}Mac1^{+}) gated on live events, n=4 per treatment group, *p=0.004 comparing the percentage of myeloid cells in the peripheral blood of 15mg/kg ACP-319-treated mice to vehicle-treated mice, p=0.065 comparing the percentage of myeloid cells of 15mg/kg ACP-196 + ACP-319-treated mice to vehicle-treated mice, statistical analyses performed by unpaired, two-tailed, Student's t-test.

Pharmacologic inhibition of BTK and PI3K p110δ in vivo *using 20mg/kg of ACP-196 and 20mg/kg of ACP-319 significantly reduced splenomegaly and leukocytosis in gain-of-function mutant Shp2-expressing mice*

Because we had observed promising trends in the 15mg/kg drug combination group, we sought to determine if increasing the dose of each drug to 20mg/kg would produce a greater normalization of leukemic parameters. We focused on the ACP-196 plus ACP-319 combination because neither ACP-196 alone nor ACP-319 alone induced favorable trends compared to the vehicle group. The ACP-196 inhibitor had previously been tested at this higher concentration, but ACP-319 had never been used above 15mg/kg (Dr. Cecile Krejsa, personal communication). Therefore, we closely observed the mice each day during treatment and were prepared to scale back the dosing of one or both inhibitors if any signs of toxicity developed. However, the mice appeared healthy throughout the entire course of treatment, with no major changes in weight or activity level. We treated seven *Shp2*$^{E76K/+}$;LysMcre^{+} mice per group (vehicle or ACP-196 plus ACP-319) for 21 days BID via oral gavage. The vehicle group had an average age of 129 days and the drug combination group had an average age of 125 days at the start of treatment. Both groups consisted of four females and three males each. At the end of the 21 days, the fourteen mice were euthanized for analysis.

With the increased dose of 20mg/kg of each drug, there was a significant reduction in splenomegaly compared to the vehicle-treated mice (Figure 4.10). Prior to treatment, the peripheral blood WBC count was not significantly different between the two groups, but the treatment group was slightly higher than the vehicle group (Figure

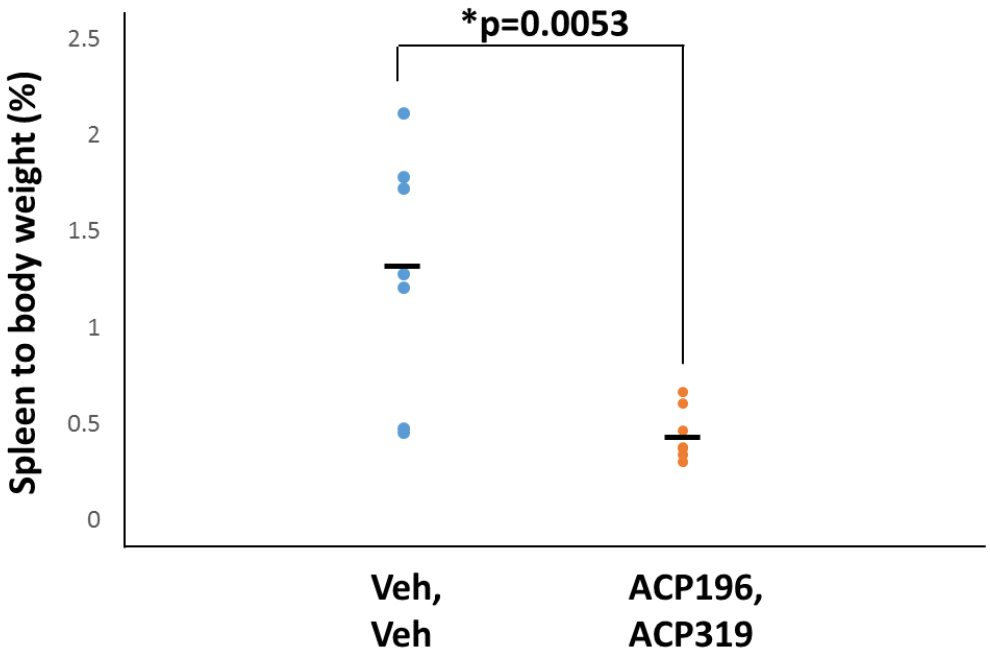

Figure 4.10: BTK and p110δ dual inhibition *in vivo* decreases splenomegaly in *Shp2*$^{E76K/+}$;LysMcre^{+} mice

The spleen to body weight ratio of mice at the end of 21 days of treatment with 20mg/kg of inhibitors, n=7 per group, *p=0.0053 comparing the inhibitor-treated mice to vehicle-treated mice, statistical analyses performed by unpaired, two-tailed, Student's t-test.

4.11A). After the completion of treatment, however, the ACP-196 plus ACP-319 treated mice had significantly lower WBC count (Figure 4.11B).

We also phenotypically characterized the composition of the cell populations in the bone marrow, spleen, and peripheral blood by flow cytometry analysis. Similar to what we observed with GS-9820 treatment (Chapter Three, Figure 3.3), the LSK cells were significantly reduced in the bone marrow of the inhibitor-treated mice (Figure 4.12). For the hematopoietic progenitor populations, we found no significant differences in the CMPs, GMPs, or MEPS (data not shown) or in the frequency of the HSC, MPP, and LRP populations as determined by SLAM markers (data not shown). Regarding the terminally differentiated myeloid cells, B cells, and T cells, the frequencies were the same between treatment groups in the bone marrow (Figure 4.13) and spleen compartments (Figure 4.14). However, the peripheral blood had significantly more terminally differentiated myeloid cells and fewer B cells in the drug-treated mice compared to vehicle (Figure 4.15). These findings suggest that the combination of BTK and p110δ inhibition promote myeloid differentiation and mobilization of mature myeloid cells into the peripheral circulation. The decreased peripheral blood B cell population is likely due to the action of BTK inhibition, as B cell differentiation and maturation is a well-documented function of BTK.

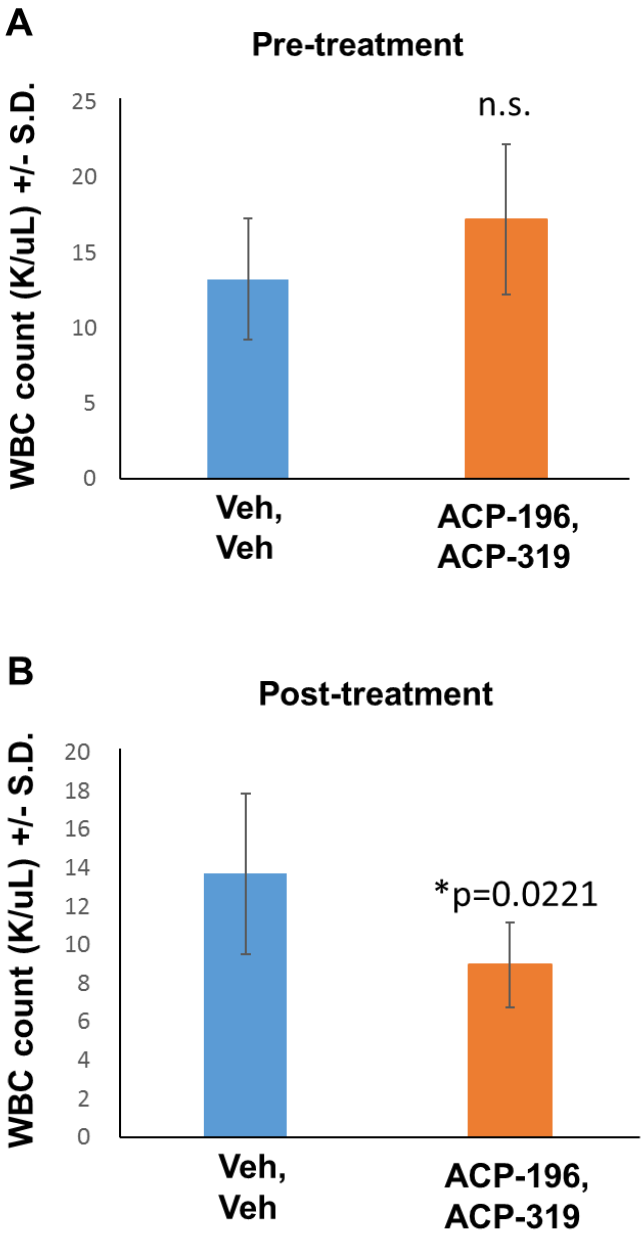

Figure 4.11: BTK and p110δ dual inhibition *in vivo* decreases peripheral blood WBC count in *Shp2*$^{E76K/+}$;LysMcre^{+} mice

(A) The average values of peripheral blood WBC count in vehicle group and treatment group prior to treatment. (B) The average values of peripheral blood WBC count in vehicle-treated and 20mg/kg inhibitor-treated mice at the end of 21 days of treatment, n=7 per group, *p=0.0221 comparing the inhibitor-treated mice to vehicle-treated mice, statistical analyses performed by unpaired, two-tailed, Student's t-test.

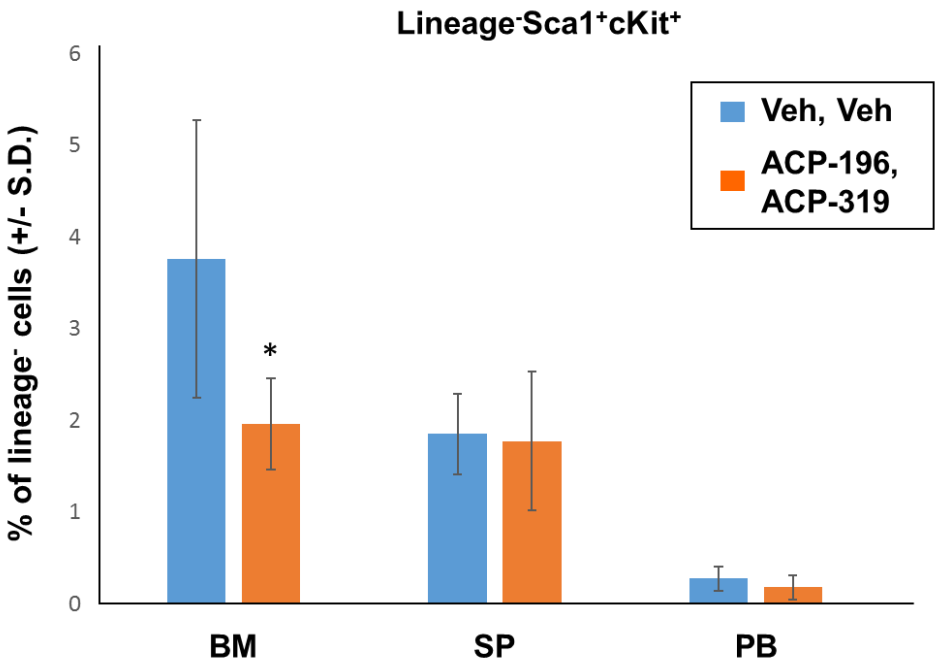

Figure 4.12: BTK and p110δ dual inhibition *in vivo* decreases Lin$^-$Sca1$^+$Kit$^+$ progenitor cells in the bone marrow of *Shp2*$^{E76K/+}$;LysMcre$^+$ mice

Average percentage of Lin$^-$Sca1$^+$Kit$^+$ (LSK) cells in bone marrow (BM), spleen (SP), and peripheral blood (PB), n=7 per group, *p=0.0114 comparing LSK cells in the bone marrow of 20mg/kg inhibitor-treated mice to vehicle-treated mice, statistical analyses performed by unpaired, two-tailed, Student's t-test.

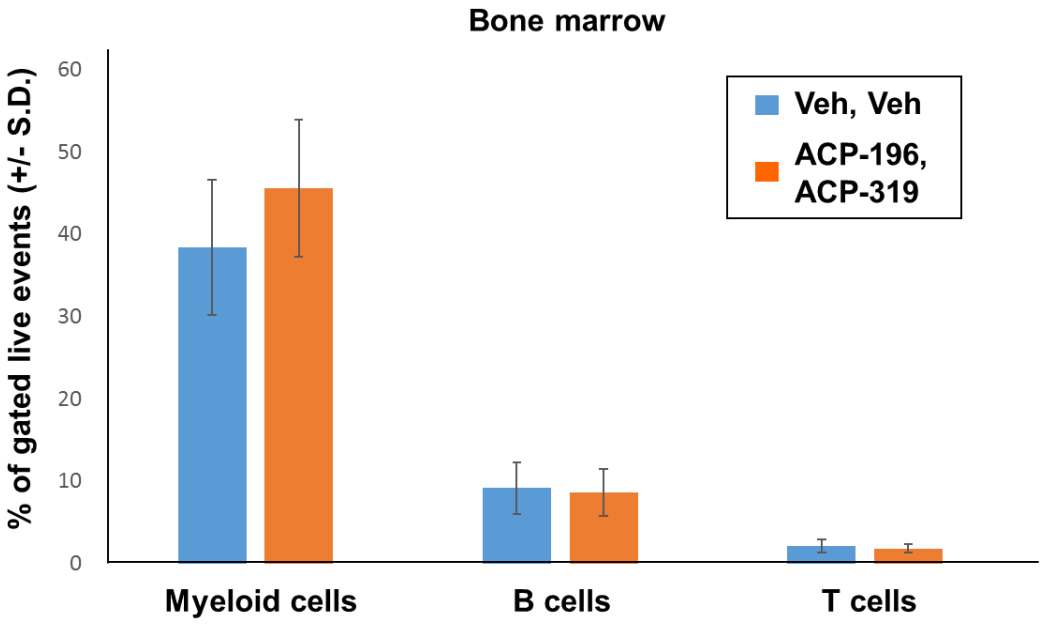

Figure 4.13: BTK and p110δ dual inhibition *in vivo* does not affect terminally differentiated hematopoietic cell populations in the bone marrow of *Shp2*$^{E76K/+}$;LysMcre^{+} mice

Average percentage of bone marrow myeloid cells (Gr1^{+}Mac1^{+}), B cells (B220^{+}), and T cells (CD4^{+}CD8^{+}) gated on live events, n=7 per treatment group.

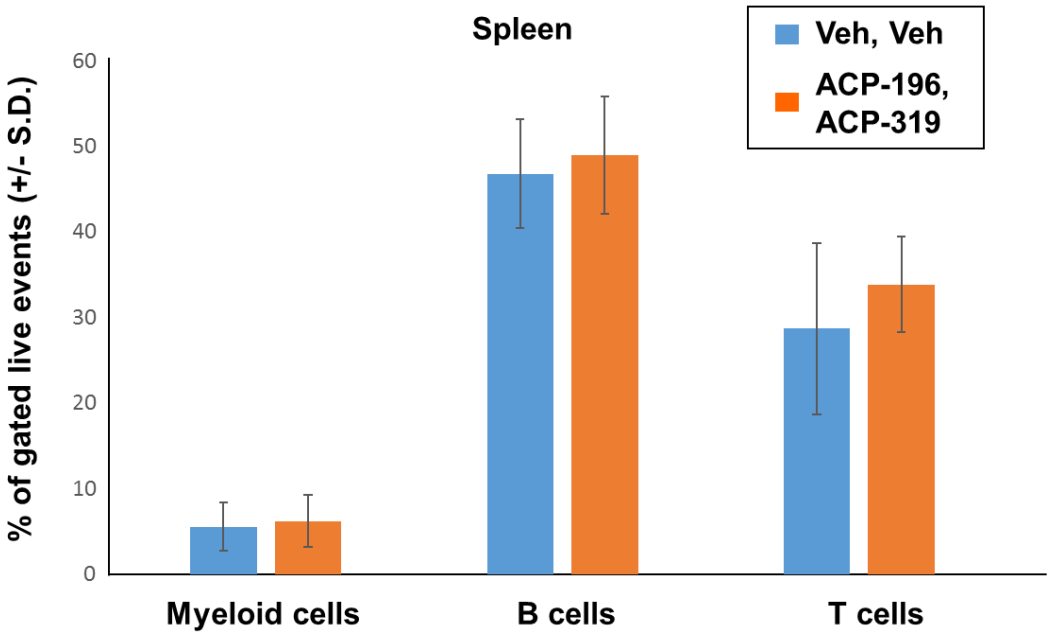

Figure 4.14: BTK and p110δ dual inhibition *in vivo* does not affect terminally differentiated hematopoietic cell populations in the spleen of *Shp2*$^{E76K/+}$;LysMcre^{+} mice

Average percentage of spleen myeloid cells (Gr1^{+}Mac1^{+}), B cells (B220^{+}), and T cells (CD4^{+}CD8^{+}) gated on live events, n=7 per treatment group.

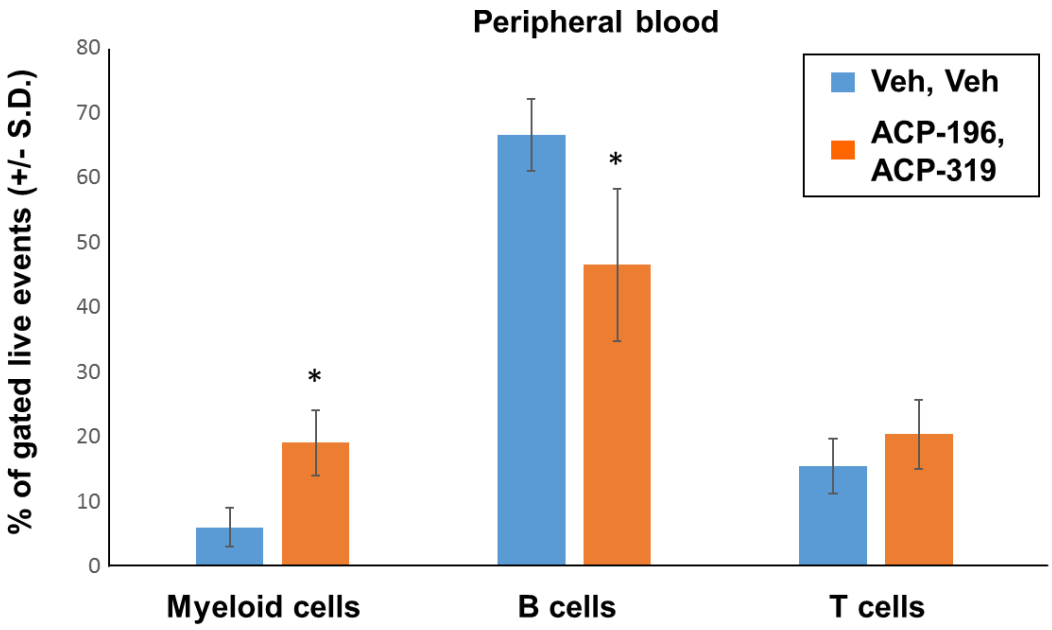

Figure 4.15: BTK and p110δ dual inhibition *in vivo* increases terminally differentiated myeloid cells and decreases B cells in the peripheral blood of *Shp2*$^{E76K/+}$;LysMcre^{+} mice

Average percentage of peripheral blood myeloid cells (Gr1^{+}Mac1^{+}), B cells (B220^{+}), and T cells (CD4^{+}CD8^{+}) gated on live events, n=7 per treatment group, *p=0.0002 comparing the percentage of myeloid cells in the peripheral blood of 20mg/kg inhibitor-treated mice to vehicle-treated mice, *p=0.0015 comparing the percentage of B cells in the peripheral blood of 20mg/kg inhibitor-treated mice to vehicle-treated mice, statistical analyses performed by unpaired, two-tailed, Student's t-test.

Discussion

In recent years, BTK has emerged as a target of intense interest in the field of lymphoid malignancies. Because it was identified as the defective protein in X-linked agammaglobulinemia in 1993, much is already known about BTK's structure and its signaling in the context of the B cell receptor. For example, it is known to be phosphorylated after BCR cross-linking, and its activation is promoted by recruitment to the plasma membrane by $PI(3,4,5)P_3$, which is produced by PI3K. Beyond BCR signaling, there have been some suggestions that BTK plays a role in myeloid diseases as well. Thus, BTK came to our attention as a possible signaling molecule that may cooperate with p110δ to promote GOF Shp2-induced myeloid leukemia.

First, we evaluated the importance of BTK in GM-CSF-stimulated signaling in GOF Shp2-expressing myeloid cells. We found that BTK activation is upregulated in GOF Shp2-expressing bone marrow-derived macrophages compared to WT Shp2 (Figure 4.1). We were then able to verify that the p110δ-to-BTK signaling pathway was intact by showing that inhibition of p110δ caused a dose-dependent decrease in BTK phosphorylation (Figure 4.2). We also demonstrated that, while BTK inhibition alone only modestly induced signaling changes, the inhibition of BTK and p110δ together cooperatively reduced the phosphorylation of Akt and Erk in GOF Shp2-expressing macrophages in response to GM-CSF stimulation (Figure 4.3). Consistent with these biochemical results, BTK inhibition alone did not affect proliferation of $Shp2^{E76K}$-expressing bone marrow LDMNCs in [^{3}H]-thymidine incorporation assays, but it

cooperated with p110δ inhibition to further reduce hyperproliferation in response to GM-CSF (Figure 4.4).

Next we moved our studies with the BTK and p110δ inhibitors to $Shp2^{E76K}$;$LysMcre^{+}$ mice *in vivo*. We initially used 15mg/kg of each inhibitor and saw promising but statistically non-significant trends in prolonged survival and decreased leukemia progression compared to vehicle treatment (Figures 4.5-4.9). Therefore, we repeated our experiments using the increased dose of 20mg/kg of each inhibitor. With the increased dosing, there was significantly reduced splenomegaly and leukocytosis in the treatment group versus the vehicle group (Figures 4.10-4.11). We also found fewer bone marrow LSK progenitor cells and a corresponding increase in mature myeloid cells in the peripheral blood (Figures 4.12 and 4.15). These findings are consistent with what we have seen using the other p110δ inhibitor, GS-9820, administered at 30mg/kg (Chapter Three, Figures 3.1, 3.3, and 3.6). A probable explanation for this shift in cell populations is due to p110δ and/or BTK inhibition causing a disruption in the bone marrow tumor cell niche and inducing myeloid cell maturation. We also saw significantly decreased terminally differentiated B cells in the peripheral blood (Figure 4.15). This observation is likely due to the inhibition of BTK signaling, which has been well-documented to be crucial for normal B cell differentiation and maturation.

The first generation BTK inhibitor ibrutinib has had great success in a variety of B cell leukemias and lymphomas ever since its accelerated FDA approval in 2013 for relapsed mantle cell lymphoma. However, it also has significant activity against a number of other kinases, leading to side effects and discontinuation in patients. Second-

generation BTK inhibitors, such as acalabrutinib (ACP-196), bring the promise of having the same effectiveness as ibrutinib but fewer side effects and reduced toxicity. We have shown in our pre-clinical mouse model that ACP-196 effectively blocks the phosphorylation of BTK in bone marrow-derived macrophages. Another problem that has arisen during ibrutinib treatment is the development of resistance, which is an inherent drawback of many monotherapies. The idea of using combined BTK and p110δ inhibition has been proposed for the treatment of B cell malignancies, and clinical trials to test such a strategy have already begun. Our studies show that ACP-196 can cooperate with the p110δ inhibitor, ACP-319, to correct GM-CSF hypersensitivity *in vitro* and to decrease leukemia progression *in vivo*. A drug combination strategy is advantageous because it allows a lower dose of each drug to be used to attain high efficacy with less risk of toxicity. This concept is demonstrated in our studies by the similar responses we observed in the $Shp2^{E76K}$;$LysMcre^{+}$ mice after *in vivo* treatment with 30mg/kg of GS-9820 compared with 20mg/kg each of ACP-319 plus ACP-196.

CHAPTER FIVE

BCAP IS HYPERPHOSPHORYLATED AND CONNECTS BTK SIGNALING TO PI3K IN GAIN-OF-FUNCTION MUTANT SHP2-EXPRESSING MYELOID CELLS

Introduction

With the importance of BTK established in gain-of-function (GOF) Shp2-induced myeloid leukemia, we wished to further explore the mechanism of how BTK promotes leukemogenesis. We were intrigued by our finding that, unlike in BCR signaling, neither the BTK inhibitor nor the p110δ inhibitor changed the levels of phospho-PLCγ2 in bone marrow-derived macrophages (Chapter Four, Figure 4.2). PLCγ2 is the known downstream direct target of BTK in B cell receptor (BCR) signaling that connects BTK to Erk activation. Thus, although BTK inhibition cooperated with p110δ inhibition to further decrease both Erk and Akt phosphorylation compared to p110δ inhibition alone in GOF Shp2-expressing myeloid cells, the effect of BTK inhibition appeared to be independent of phospho-PLCγ2. Therefore, we were interested in finding how, if not by way of phospho-PLCγ2, BTK may be signaling in order to promote GM-CSF-stimulated Akt and Erk phosphorylation and hyperproliferation in GOF Shp2-expressing myeloid cells.

In the literature on BCR signaling, we found that another direct target of BTK phosphorylation is B cell adaptor for PI3K (BCAP). The mouse BCAP protein has three YxxM motifs that, once phosphorylated, bind to proteins at their SH2 domains. A known binding target of phospho-BCAP is PI3K, specifically the N-SH2 domain of the p85α regulatory subunit. In fact, BCAP was first discovered as a novel protein that binds to the N-terminal SH2 domain of p85α from chicken DT40 B cells (Okada, Maeda 2000). This

BCAP-p85α association promotes PI3K activity both by increasing the PI3K catalytic domain's kinase activity and by recruiting PI3K to the plasma membrane where it can access its substrate, $PI(4,5)P_2$ (Fruman, Snapper 1999). Thus, BCAP facilitates the activation of Akt via the canonical PI3K-Akt pathway, as well as Erk activation by cross-talk between signaling pathways.

There are four different protein isoforms of BCAP encoded by the *Pik3ap1* gene by way of alternative splicing and posttranslational modification mechanisms. The full-length transcript, BCAP-L, has been found to be more important than the truncated BCAP-S for PI3K activation in myeloid cells. In a study of BCAP's ability to activate PI3K in the context of toll-like receptor signaling, Ni et. al used bone marrow-derived macrophages lacking Syk expression, as Syk is another molecule known to be activated by BCR signaling and functions to activate BCAP in B cells. Ni et. al made the surprising observation of increased BCAP phosphorylation in these $Syk^{-/-}$ macrophages, which is the opposite of what occurs in B cells. In the bone marrow-derived macrophages, the increase in phosphorylation occurred specifically in the two full-length BCAP isoforms, which led to more BCAP association with p85α as visualized by co-immunoprecipitation. Furthermore, the authors found that the isolated membrane fraction from macrophages stimulated with lipopolysaccharide (LPS) also demonstrated the full-length BCAP isoforms being specifically phosphorylated (Ni, MacFarlane 2012).

After B cells, the cells with the second highest expression levels of BCAP are macrophages (Okada, Maeda 2000). Several studies, including the above-mentioned one by Ni et. al, have recently been published that provide evidence that BCAP plays an

important role in myeloid cells as well as B cells. A phosphoproteomics screen using *Btk*$^{-/-}$*Tec*$^{-/-}$ bone marrow-derived macrophages found decreased phosphorylation in several proteins, including BCAP (Tampella, Kerns 2015). Since BCAP's ability to activate PI3K and Akt has been well-documented in B cells (Castello, Gaya 2013, Qin and Chock 2003), and because Tampella et. al identified BCAP as being activated downstream of BTK in bone marrow-derived macrophages, we hypothesized that BCAP may be the connecting molecule between BTK and Akt/Erk activation in our GOF Shp2-expressing myeloid cells (Figure 5.1).

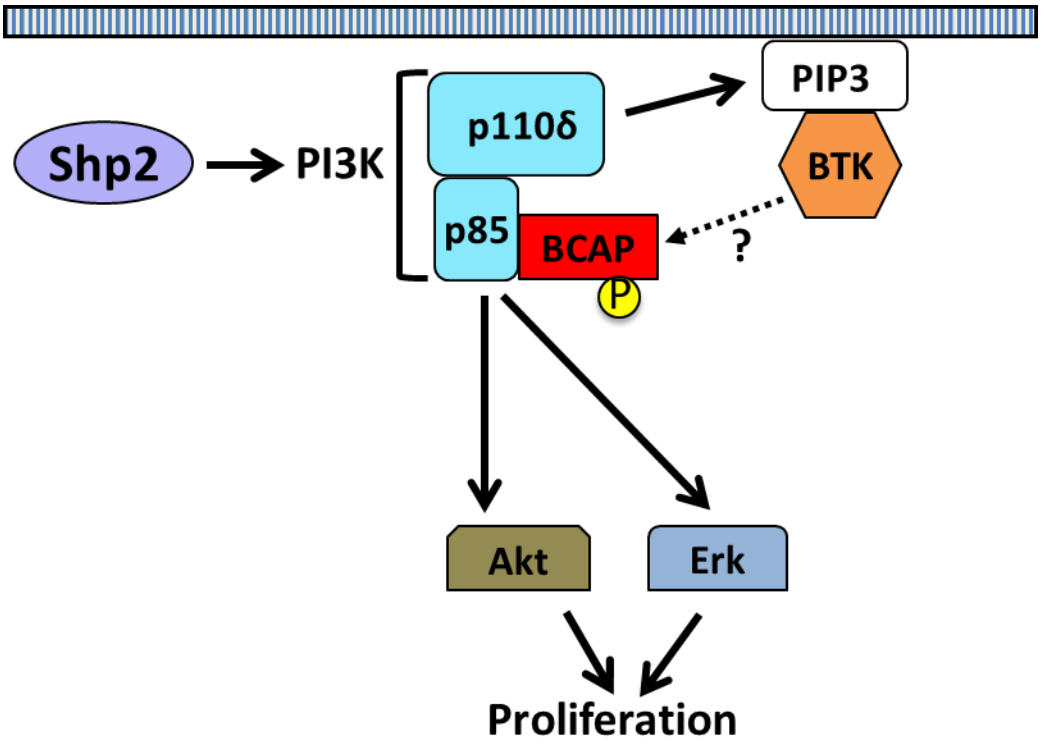

Figure 5.1: Schematic of proposed signaling pathway explaining the ability of BTK to activate Akt and Erk in *Shp2*$^{E76K/+}$;LysMcre^{+} myeloid cells

We hypothesized that BTK phosphorylates BCAP, allowing BCAP binding to p85α and promotion of PI3K catalytic activity, thus leading to increased activation of Akt and Erk downstream.

Results

Phosphorylation of the full-length BCAP isoforms is increased in response to GM-CSF stimulation and decreased by BTK inhibition in gain-of-function mutant Shp2^{E76K} bone marrow-derived macrophages

In order to investigate if BCAP plays a role in connecting BTK to Akt/Erk in GOF Shp2-expressing myeloid cells, we first examined its activation in response to GM-CSF stimulation in bone marrow-derived macrophages from *Shp2$^{E76K/+}$*;LysMcre^{+} mice. Because there is no commercially available anti-phospho-BCAP antibody, we used the strategy of pulling down total BCAP protein by immunoprecipitation, and then probing with an anti-phospho-tyrosine antibody. Based on the kinetics of Akt activation in mutant Shp2-expressing macrophages (Yang, Li 2008), we initially conducted these experiments using 1 hour of GM-CSF stimulation and saw no differences in BCAP phosphorylation compared to baseline (data not shown). We referred again to the paper describing the initial discovery of BCAP and saw that the authors found tyrosine phosphorylation to peak at 1 minute following BCR stimulation in DT40 chicken B cells, and then return to basal levels by 30 minutes (Okada, Maeda 2000). Therefore, we performed a time course experiment testing 10 minutes and 30 minutes of GM-CSF stimulation.

After immunoprecipitation for BCAP and blotting for phospho-tyrosine, we observed the four isoforms corresponding to BCAP-S (BCAP1/BCAP2) and BCAP-L (BCAP3/BCAP4), as well as a larger band that potentially could be BCAP5 or BCAP6, which were previously reported to be less prevalent and not visible until after BCR

stimulation (Okada, Maeda 2000). In WT Shp2 macrophages, there was increased phosphorylation of both BCAP-S and BCAP-L isoforms at 10 minutes, with phosphorylation levels slightly decreased at 30 minutes (Figure 5.2, lanes 3, 4, and 5). However, in $Shp2^{E76K}$-expressing macrophages, we saw a different pattern of baseline and GM-CSF-stimulated BCAP phosphorylation. Baseline BCAP phosphorylation was higher in the GOF Shp2-expressing cells compared to the WT Shp2-expressing cells, and following GM-CSF stimulation, phospho-BCAP was specifically increased in the full-length isoforms (Figure 5.2, lanes 6, 7, and 8). In the mutant Shp2 myeloid cells, we also saw that phosphorylation peaked earlier at 10 minutes and somewhat decreased after 30 minutes of GM-CSF stimulation.

Our findings are consistent with those observed in DT40 chicken B cells that BCAP3/BCAP4 has five fold more tyrosine phosphorylation than BCAP1/BCAP2 following BCR stimulation (Okada, Maeda 2000). As mentioned previously, BCAP3/BCAP4 seem to be more important than BCAP1/BCAP2 for binding to and activating PI3K (Ni, MacFarlane 2012). Thus, our results imply that there may be more BCAP-induced activation of PI3K in macrophages expressing GOF Shp2 compared to WT Shp2.

Having seen that BCAP is activated in mutant Shp2-expressing macrophages, we next wanted to interrogate the BTK-to-BCAP signaling pathway. Based on the B cell signaling pathway, we hypothesized that BTK phosphorylates BCAP, which would allow binding to p85α and promotion of PI3K activity, thus activating Akt and Erk (Figure 5.1). To test the hypothesis that BCAP is a BTK substrate in GOF Shp2-expressing myeloid

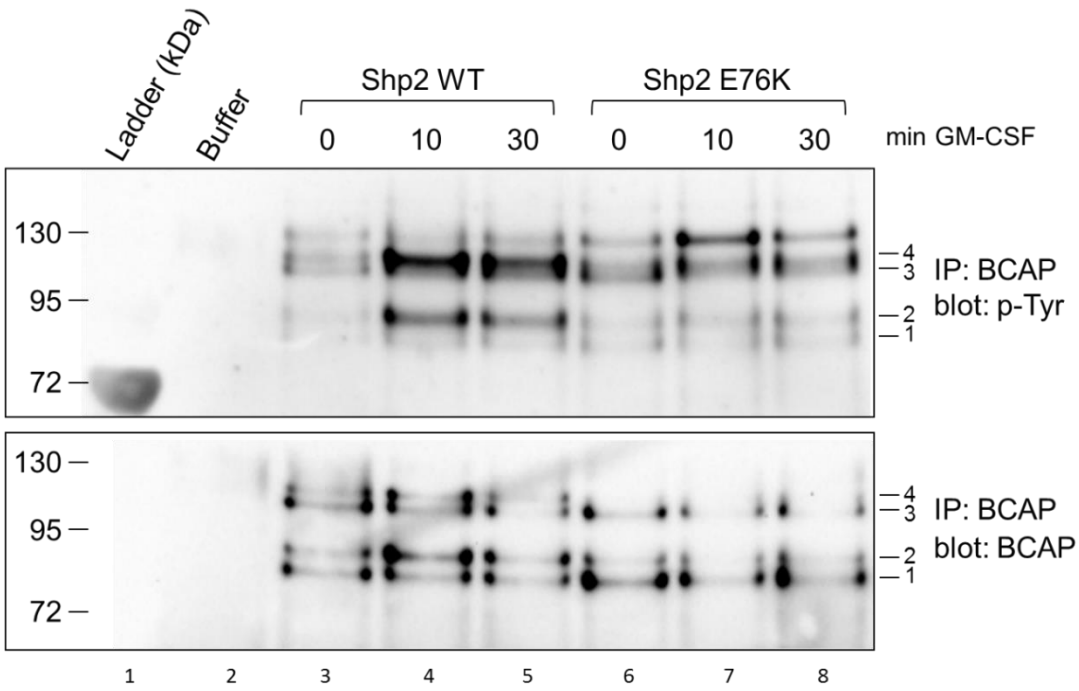

Figure 5.2: BCAP phosphorylation is increased by GM-CSF stimulation specifically in the full-length isoforms in bone marrow-derived macrophages from *Shp2*$^{E76K/+}$;LysMcre^{+} mice

Bone marrow-derived macrophages expressing WT Shp2 or Shp2^{E76K} were treated with 10ng/mL of GM-CSF for 0, 10, or 30 minutes before lysing. Protein lysates were subjected to immunoprecipitation (IP) with anti-BCAP antibody followed by immunoblotting with anti-phospho-tyrosine. 390mg of protein lysis were loaded per lane and IP was performed with 5µg/mL of the anti-BCAP antibody.

cells, we used the BTK inhibitor ACP-196 to treat Shp2^{E76K}-expressing macrophages that were stimulated with GM-CSF for 10 minutes. With 0.5μM and 1μM concentrations of ACP-196, we observed a dose-dependent decrease in BCAP phosphorylation, indicating that BTK is responsible for phosphorylating BCAP in GOF Shp2-expressing myeloid cells (Figure 5.3, lanes 3, 4, and 5).

Total BCAP expression is increased in gain-of-function mutant Shp2-expressing macrophages compared to WT Shp2-expressing macrophages

Given the variable phosphorylation pattern of BCAP in GOF Shp2-expressing cells compared to WT Shp2-expressing cells, we investigated if total BCAP expression is also altered in mutant Shp2-expressing cells. We tested this by retrovirally transducing WT Shp2 or Shp2^{E76K} tagged with GFP into bone marrow LDMNCs isolated from WT mice. GFP^{+} cells were sorted using fluorescence activated cell sorting and plated in media containing 25ng/mL of macrophage colony-stimulating factor to obtain macrophages expressing WT Shp2 or Shp2^{E76K}. In both primary bone marrow-derived macrophages retrovirally transduced with Shp2^{E76K} and primary bone marrow-derived macrophages isolated from *Shp2$^{E76K/+}$*;LysMcre^{+} mice (data not shown), we found increased BCAP protein levels compared to WT Shp2-expressing control cells (Figure 5.4).

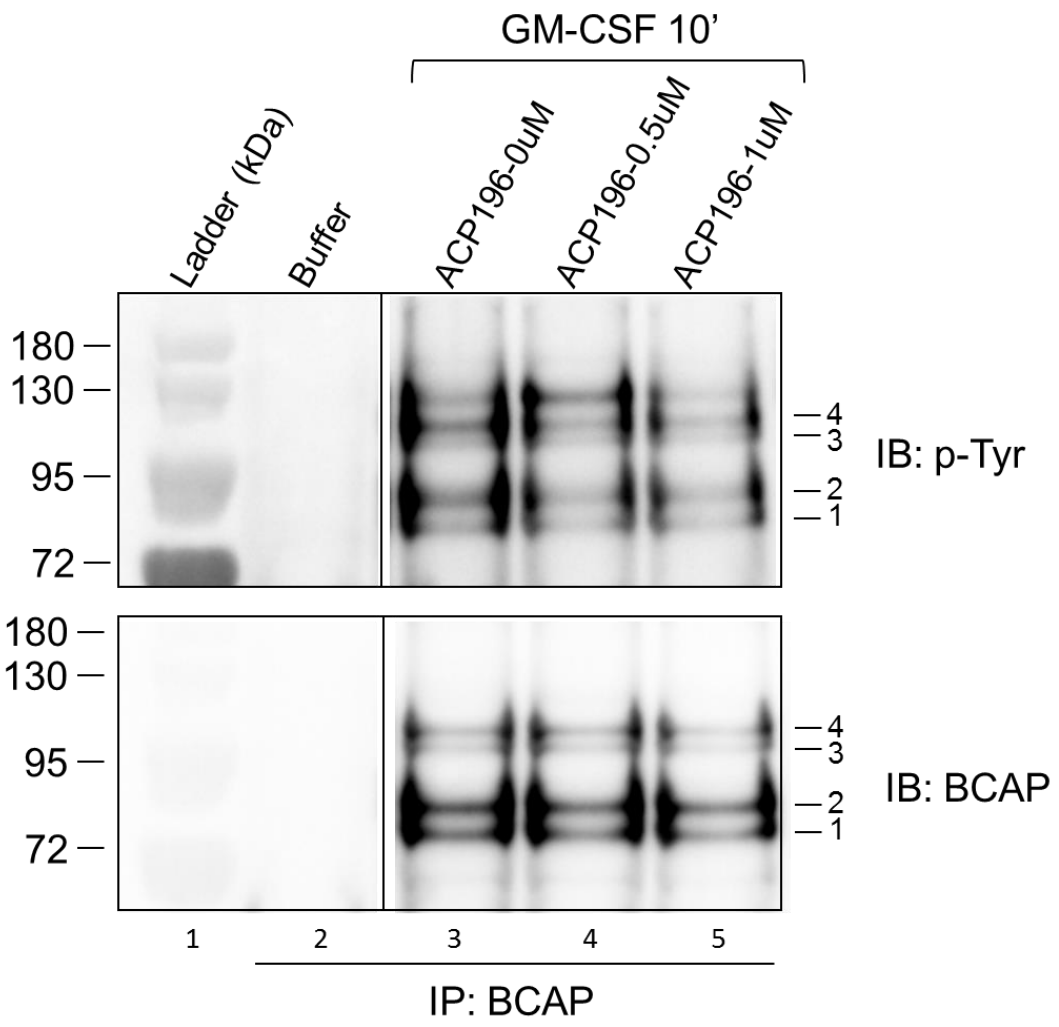

Figure 5.3: BCAP phosphorylation is decreased by ACP-196 in a dose-dependent manner in bone marrow-derived macrophages from *Shp2$^{E76K/+}$*;LysMcre^{+} mice

Bone marrow-derived macrophages expressing Shp2^{E76K} were treated with 10ng/mL of GM-CSF for 10 minutes with 0µM, 0.5µM, or 1µM ACP-196 before lysing. Protein lysates were subjected to immunoprecipitation (IP) with anti-BCAP antibody followed by immunoblotting (IB) with anti-phospho-tyrosine. 650mg of protein lysis were loaded per lane and IP was performed with 5ug/mL of the anti-BCAP antibody.

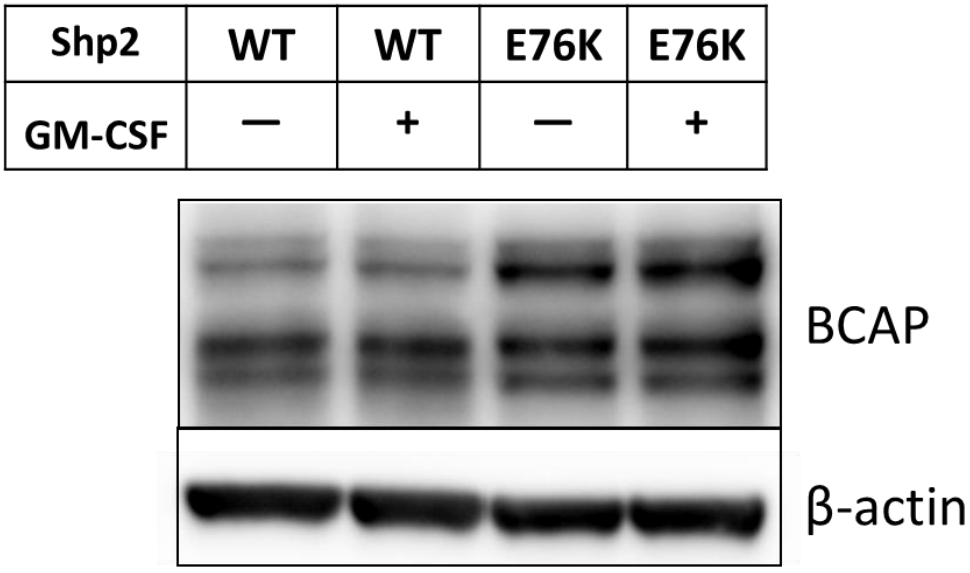

Figure 5.4: BCAP expression is increased in bone marrow-derived macrophages expressing Shp2^{E76K}

Primary bone marrow low-density mononuclear cells were isolated from WT mice, transduced with either WT Shp2-GFP or Shp2^{E76K}-GFP constructs, and sorted for GFP^{+} cells. The GFP^{+} cells were differentiated into macrophages and treated with or without 10ng/mL of GM-CSF for 10 minutes before lysing. Immunoblot shows total BCAP levels with β-actin used as a loading control.

Mutagenesis of the SH2 domains of p85α leads to decreased interaction with BCAP in gain-of-function mutant Shp2-expressing cells

Next, we wanted to further investigate the interaction between BCAP and the p85α regulatory subunit of PI3K in GOF Shp2-expressing and WT Shp2-expressing cells. As mentioned previously, BCAP was first isolated by binding to the N-SH2 domain of p85α (Okada, Maeda 2000). However, studies have shown that the N-terminal and the C-terminal SH2 domains can both bind with high affinity to similar phospho-tyrosine sequences (Songyang, Shoelson 1993). In addition to examining potential differences in the interaction between p85α and BCAP in cells expressing GOF Shp2 and WT Shp2, we wanted to test if mutation of the p85α SH2 domains differentially affected the p85α-BCAP interaction in GOF Shp2-expressing compared to WT Shp2-expressing cells. As the first step, we explored the consequences of complete loss of SH2 domain binding ability in the context of mutant or WT Shp2 expression.

To perform these experiments, we generated cell lines ectopically expressing p85α, Shp2, and BCAP. We utilized WT and mutant p85α plasmid constructs previously generated in our lab. These constructs were created by site-directed mutagenesis to render the p85α N-SH2 and C-SH2 domains unable to bind to phospho-tyrosine residues using the R358A and R649A mutations, respectively (Rordorf-Nikolic, Van Horn 1995, Yu, Wjasow 1998). These p85α mutant constructs were fused to yellow fluorescent protein (YFP) in order to track p85α expression. For Shp2 expression, we utilized previously generated Shp2 constructs (WT or E76K) that contain the neomycin resistance (neoR) cassette (Chan, Leedy 2005). Finally, we created a novel plasmid construct containing

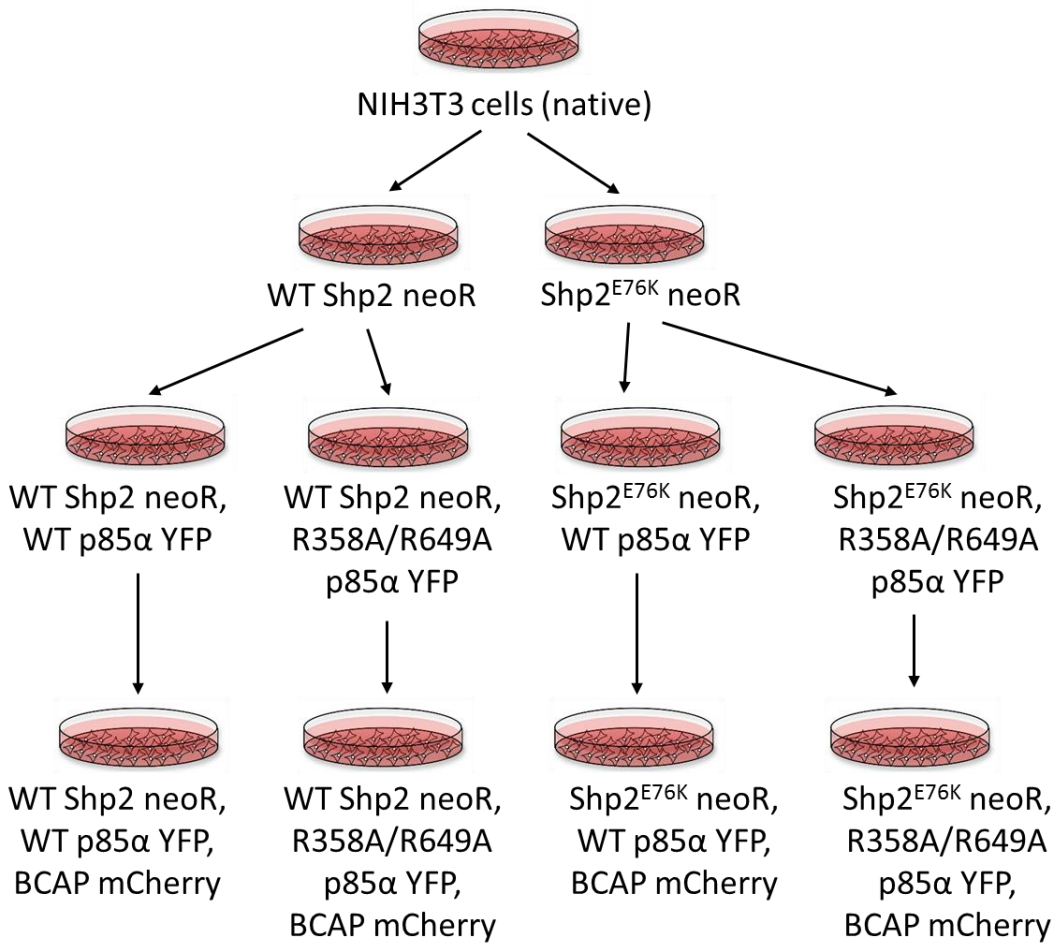

Figure 5.5: Schematic of transduction strategy used to generate NIH3T3 cells expressing three proteins-of-interest: Shp2, p85α, and BCAP.

Serial transduction and selection were performed to obtain NIH3T3 cells stably expressing WT Shp2 or Shp2^{E76K}, WT or R358A/R649A p85α, and BCAP. Shp2 was selected for using neomycin-containing media, p85α was sorted for YFP positivity, and BCAP was sorted for mCherry positivity.

full-length BCAP in tandem with mCherry. In a stepwise fashion, we introduced the constructs into NIH3T3 cells followed by selection in order to generate the following stable cell lines: 1) WT Shp2, WT p85α, BCAP; 2) WT Shp2, R358A/R649A p85α, BCAP; 3) $Shp2^{E76K}$, WT p85α, BCAP; and 4) $Shp2^{E76K}$, R358A/R649A p85α, BCAP (Figure 5.5). We collected protein lysates from each of the exponentially growing cell lines and performed co-immunoprecipitation assays to compare the amount of p85α-BCAP interaction in GOF Shp2-expressing cells and WT Shp2-expressing cells.

From these studies, we did not see a difference in the BCAP-p85α interaction between WT Shp2- and GOF Shp2-expressing cells (Figure 5.6A, compare lanes 2 and 4). In both the WT Shp2- and GOF Shp2-expressing cells, we found reduced interaction between BCAP and p85α in the cells expressing the double mutant R358A/R649A p85α construct compared to WT p85α (Figure 5.6A, compare lanes 2 and 3, and lanes 4 and 5). A western blot on the same protein lysates demonstrated essentially equal quantification/loading of samples and consistent levels of expression in p85α and BCAP between the four cell lines, although the two samples with p85α R358A/R649A may have had slightly higher levels of the p85α construct compared to the WT p85α samples (Figure 5.6B). This confirms that BCAP contains the motifs necessary for binding to the SH2 domains of p85α and validates our cell model system for the use of studying this interaction. Future studies will include co-immunoprecipitation assays using the p85α SH2 domain single mutants. Any differences will tell us which (if either) of the two SH2 domains are more vital for BCAP binding.

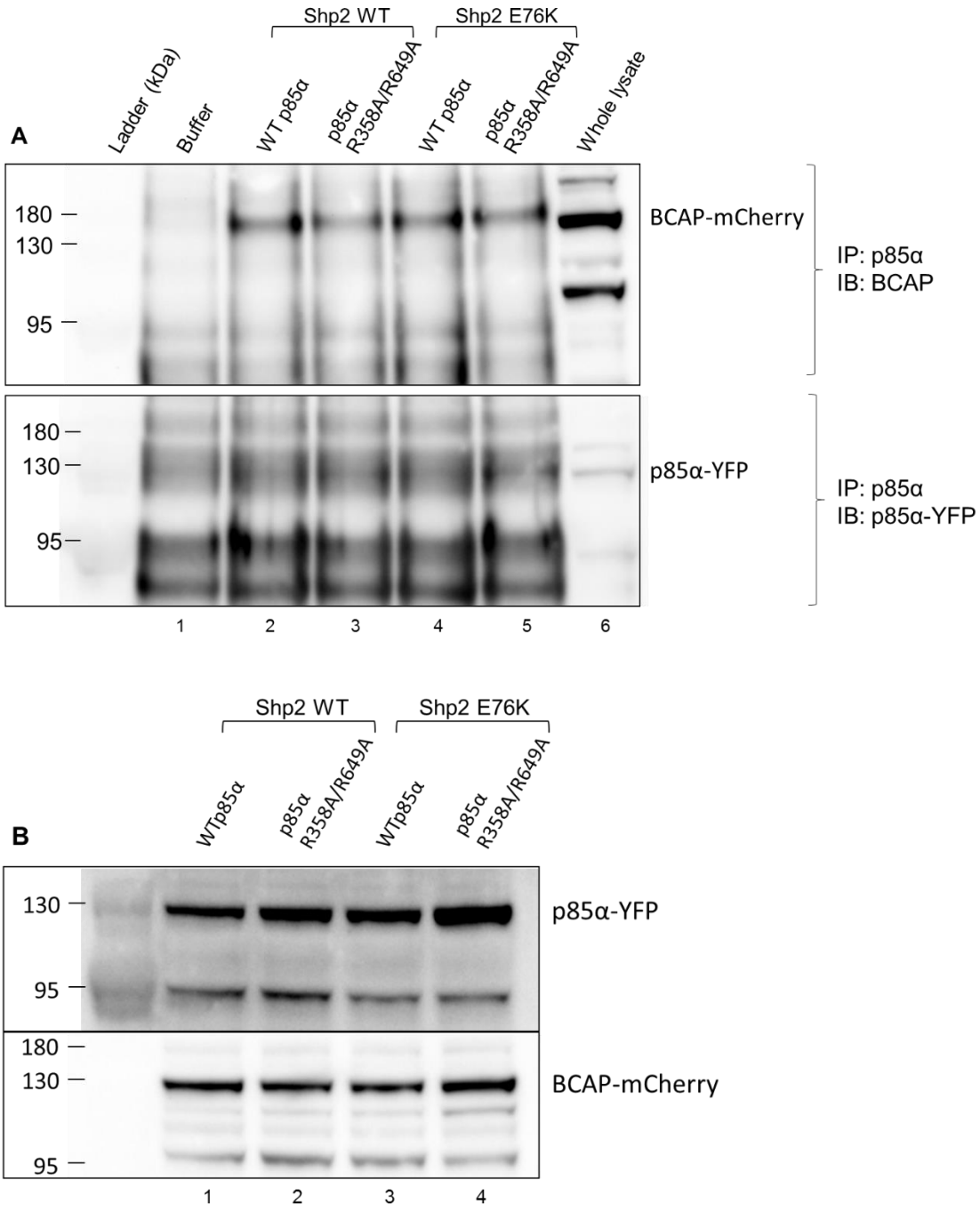

Figure 5.6: BCAP interaction with p85α is decreased by mutagenesis of both SH2 domains

(A) Protein lysates were collected from each of the stably expressing NIH3T3 cell lines and were subjected to immunoprecipitation (IP) with anti-p85α antibody followed by immunoblotting (IB) with anti-BCAP. 950mg of protein lysate was used for each IP using a 1:25 dilution of the anti-p85α antibody. (B) Western blots probing for p85α-YFP (~110kDa) or BCAP-mCherry (~130kDa) using lysates from each NIH3T3 cell line.

Discussion

From our initial biochemistry studies using a BTK inhibitor in GOF Shp2-expressing macrophages, we found that BTK promotes Akt and Erk phosphorylation in a phospho-PLCγ2 independent manner (Chapter Four, Figure 4.2). Because PLCγ2 is known to be directly phosphorylated by BTK in B cells, which then promotes Erk activation, we addressed the unanswered question of how BTK signals to the downstream effectors Akt and Erk in GOF Shp2-expressing macrophages. Upon review of the literature on the BCR signaling pathway, we found that an alternative direct target of BTK is B cell adaptor for PI3K (BCAP). As its name suggests, BCAP is an adaptor protein that interacts with the p85α regulatory subunit of PI3K. BCAP contains three YxxM motifs that, once phosphorylated, can bind to p85α and enhance PI3K catalytic activity. As PI3K-to-Akt is a classical signaling pathway and PI3K is known to cross-talk with other pathways to promote Erk activation (Aksamitiene, Kiyatkin 2012), we hypothesized that BCAP phosphorylation may serve as a phospho-PLCγ2-independent means of BTK-induced hyperactivation of Akt and Erk in GOF Shp2-expressing macrophages.

First, to establish the importance of BCAP in bone marrow-derived macrophages expressing mutant Shp2, we measured the GM-CSF-stimulated phosphorylation of BCAP. We visualized the four isoforms of BCAP and saw increased pan-BCAP phosphorylation following GM-CSF in the WT Shp2 cells. However, in the $Shp2^{E76K}$-expressing macrophages, we saw increased phosphorylation specifically in BCAP3 and BCAP4 isoforms (Figure 5.2). This finding is intriguing because it has been previously

shown in macrophages that the full-length BCAP isoforms play a more important role in PI3K activation compared to the shorter isoforms. Ni et. al found that BCAP3/BCAP4 were selectively phosphorylated and correspondingly led to increased interaction with p85α in cells lacking Syk expression. Additionally, although BCAP is predominantly found in the cytoplasm, once activated, it translocates to the plasma membrane, where it recruits PI3K to its lipid substrate. Ni et. al observed that the full length BCAP3/BCAP4 isoforms, rather than the shorter BCAP1/BCAP2 isoforms, were preferentially phosphorylated and associated with the membrane fraction in LPS-stimulated macrophages (Ni, MacFarlane 2012). Thus, our finding that the larger BCAP isoforms are more hyper-phosphorylated in the GOF Shp2-expressing macrophages is consistent with these previous data indicating that activation of the two larger BCAP isoforms are responsible for PI3K activation.

Next, we tested if BTK activity leads to increased BCAP phosphorylation in myeloid cells. We had already found that the BCR signaling pathway is not faithfully reproduced in myeloid cells, as BTK inhibition does not reduce the phosphorylation of PLCγ2. This lack of an effect of BTK inhibition on PLCγ2 phosphorylation is either because PLCγ2 is not a BTK substrate in myeloid cells, or because an alternative pathway is upregulated that compensates for BTK inhibition. Therefore, verifying that BTK inhibition alters BCAP phosphorylation was crucial for implicating BCAP function in BTK signaling in myeloid cells. We used two different concentrations of the Acerta Pharma BTK inhibitor, ACP-196, and demonstrated a dose-dependent decrease in BCAP phosphorylation in $Shp2^{E76K}$-expressing macrophages (Figure 5.3). This finding confirms

that BTK does signal to BCAP in myeloid cells as it does in B cells and strengthens the hypothesis that BCAP may connect BTK to Akt and Erk activation. Studies using the stably expressing NIH3T3 cell lines further confirmed that BCAP interacts with the regulatory subunit of PI3K, p85α, and that one or both of the p85α SH2 domains are necessary for the BCAP-p85α interaction. These data collectively support a signaling mechanism involving a positive feedback loop: PI3K activation of BTK via Plekstrin Homology domain binding to $PI(3,4,5)P_3$, BTK phosphorylation of BCAP, phospho-BCAP interaction with p85α leading to PI3K catalytic activation, and subsequent augmentation of PI3K-dependent activation of BTK (Figure 5.1). Characterization of this signaling mechanism in GOF Shp2-expressing myeloid cells corroborates the biochemical and functional findings that dual p110δ and BTK inhibition works cooperatively *in vitro* and *in vivo* (Chapter Four) and validates the rationale for using this inhibitor strategy for the treatment of GOF Shp2-induced myeloid leukemia in order to simultaneously block two targets in this positive feedback loop.

We were initially surprised at the finding that there was no apparent increase in p85α-BCAP interaction in the $Shp2^{E76K}$-expressing cells compared to the WT Shp2-expressing cells (Figure 5.6). We expected to see increased interaction, which may account for increased BCAP stability and increased total BCAP expression found in cells expressing GOF Shp2 (Figure 5.4). However, these results were obtained from studies using NIH3T3 cells, a mouse fibroblast cell line, which does not express endogenous BTK or BCAP, as NIH3T3 are a non-hematopoietic cell line. Therefore, this model system lacks hyperactive BTK, which is needed to hyperphosphorylate BCAP and potentially

produce an enhanced interaction with p85α compared to WT Shp2 cells. To carry these studies forward, we will focus on the interaction of endogenous p85α and BCAP in WT Shp2- and GOF Shp2-expressing hematopoietic cells to determine if an increased interaction between BCAP and p85α may account for the increased total BCAP expression found in GOF Shp2-expressing macrophages (Figure 5.4).

CHAPTER SIX

MICE WITH COMBINED MUTANT Shp2^{D61Y} AND DNMT3A HAPLOINSUFFICIENCY HAVE RAPID DEVELOPMENT OF MYELOPROLIFERATIVE NEOPLASM

Introduction

Loss of DNA methyltransferase 3A (DNMT3A) activity has been shown to lead to hematopoietic stem cell differentiation defects and the development of myeloid malignancies. *DNMT3A* is commonly mutated in myeloid diseases, with mutations found in over 20% of acute myeloid leukemia (AML) patients (Ley, Ding 2010). For AML patients, 60% of those with a *DNMT3A* mutation are heterozygous at Arginine 882 (R882), a dominant negative mutation that results in less than 80% enzymatic activity (Kim, Zhao 2013). The remaining patients usually exhibit compound heterozygous or homozygous mutations.

In contrast to AML, individuals with clonal hematopoiesis of indeterminate potential (CHIP) commonly bear a loss-of-function mutation in only one copy of *DNMT3A* (Xie, Lu 2014) and mutations in R882 are rare in this preleukemic state (Young, Challen 2016). These otherwise normal individuals are at an increased risk of developing MDS/AML due to acquisition of a second driver mutation (Jaiswal, Fontanillas 2014) and tend to have a poor overall prognosis (Ley, Ding 2010). Thus, although DNMT3A protein function must be almost completely lost in order to result in malignancy (Mayle, Yang 2015), heterozygous loss-of-function mutations are often found combined with a driver mutation during the course of development of frank leukemia. Furthermore, *Dnmt3a*

haploinsufficiency alone with no other lesions is sufficient for mice to develop myeloid malignancies when aged to 18-24 months (Cole, Russler-Germain 2017).

We studied the effects of *Dnmt3a* haploinsufficiency combined with *Ptpn11*^{D61Y}, a gain-of-function mutation encoding oncogenic Shp2, which is the most commonly mutated gene in JMML (Chan, Kalaitzidis 2009). Concurrent mutations in both *DNMT3A* and *PTPN11*, albeit rare, have been reported in AML (Chen, Chen 2015, Hou, Kuo 2012) and in JMML patients (Stieglitz, Mazor 2017, Stieglitz, Taylor-Weiner 2015). Clinical outcomes in JMML vary considerably from spontaneous regression to rapid progression. In an effort to better predict prognosis and guide treatment strategies, Stieglitz et. al have shown that JMML cases with secondary mutations have much poorer prognosis and require aggressive treatment (Stieglitz, Taylor-Weiner 2015). The authors recently discovered that DNA methylation status of the genome is predictive of patient outcome as well (Stieglitz, Mazor 2017). Because of the need to better understand the mechanisms of disease in JMML, especially when involving alterations in DNA methylation, we studied the combined effects of *Ptpn11* and *Dnmt3a* mutations in a mouse model of JMML.

Results

Dnmt3a$^{+/-}$;D61Y *double mutant mice have accelerated disease progression in comparison to control and single mutant mice*

We crossed *Ptpn11*$^{D61Y/+}$;Mx1-cre^{+} mice (Chan, Kalaitzidis 2009) with *Dnmt3a*$^{+/-}$ mice (Yu, Zhou 2012) to produce Mx1-cre^{-} (WT), *Dnmt3a*$^{+/-}$*;Ptpn11*$^{+/+}$*;*Mx1-cre^{+}

(*Dnmt3a*$^{+/-}$), *Dnmt3a*$^{+/+}$;*Ptpn11*$^{D61Y/+}$;Mx1-cre^{+} (*D61Y*), and *Dnmt3a*$^{+/-}$;*Ptpn11*$^{D61Y/+}$;Mx1-cre^{+} (*Dnmt3a*$^{+/-}$;*D61Y*) mice. Six cohorts of mice, with 1 to 4 mice of each genotype, were treated with polyI:polyC to knockout one copy of *Dnmt3a* and to knock-in the mutant *Ptpn11*^{D61Y} allele. All mice were followed until the *Dnmt3a*$^{+/-}$;*D61Y* mice became moribund and the entire cohort was euthanized for analysis, which occurred at an average of 24 weeks after polyI:polyC treatment. We found that at the time when the *Dnmt3a*$^{+/-}$;*D61Y* mice appeared moribund (thin, hunched, increased respiratory rate and effort, abdominal distension, ruffled fur, pale extremities), the Mx1-cre^{-} or single mutant mice of the same cohort remained healthy. Upon euthanasia, the *Dnmt3a*$^{+/-}$;*D61Y* mice showed obvious splenomegaly and the spleen to body weight percentage was significantly increased compared to the other three genotypes (Figure 6.1A). In addition to splenomegaly, the double mutant mice also showed significantly higher peripheral blood WBC counts compared to WT or *Dnmt3a*$^{+/-}$ mice (Figure 6.1B).

Dnmt3a$^{+/-}$;D61Y *mice have increased myeloid cells in the periphery and increased granulocyte macrophage progenitors in the bone marrow*

Flow cytometric analysis of the spleen and peripheral blood to assess the frequency of Gr1^{+}Mac1^{+} myeloid cells revealed a significantly higher percentage of these mature myeloid cells in the *Dnmt3a*$^{+/-}$;*D61Y* mice compared to WT and *Dnmt3a*$^{+/-}$ mice in the spleen, and compared to WT mice in the peripheral blood (Figure 6.2 and 6.3). In contrast, the myeloid cell frequencies in the single mutant mice were not statistically different from WT mice except for *D61Y* mice in the peripheral blood (Figure 6.3A). The

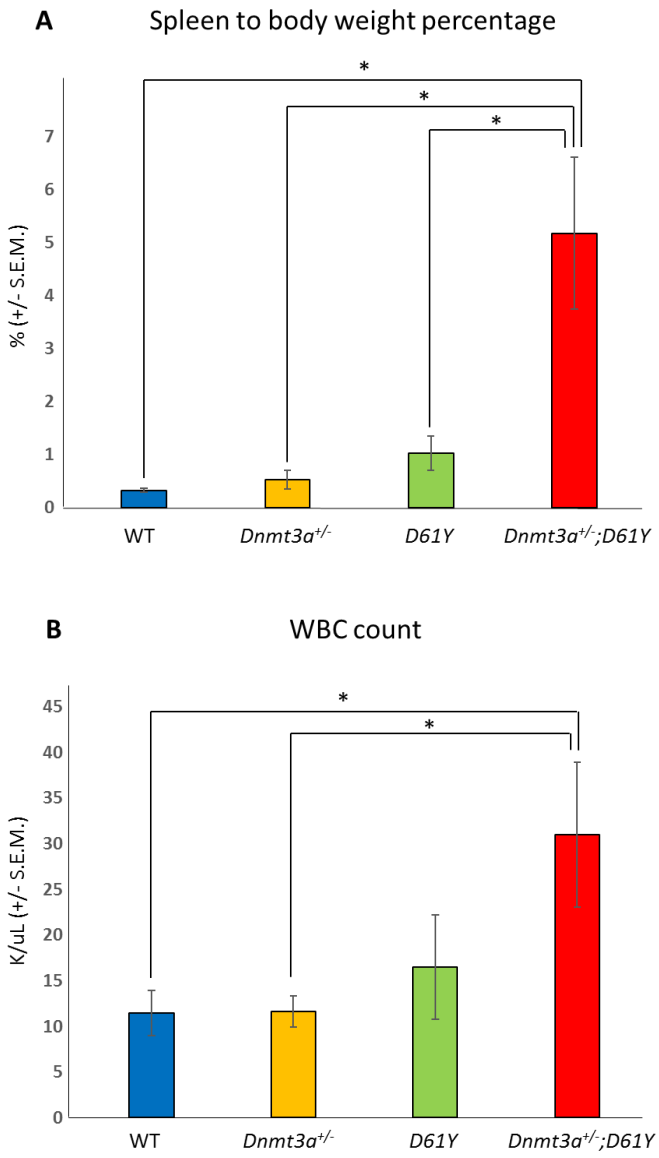

Figure 6.1: *Dnmt3a$^{+/-}$;D61Y* mice show splenomegaly and leukocytosis at the time of death

(A) Average spleen to body weight ratio of mice at the time of euthanasia; n=13 for WT, n=9 for *Dnmt3a$^{+/-}$*, n=10 for *D61Y*, n=6 for *Dnmt3a$^{+/-}$;D61Y*, *p<0.0001 comparing *Dnmt3a$^{+/-}$;D61Y* to WT, *p=0.003 comparing *Dnmt3a$^{+/-}$;D61Y* to *Dnmt3a$^{+/-}$*, *p=0.003 comparing *Dnmt3a$^{+/-}$;D61Y* to *D61Y*; statistical analyses performed by unpaired, two-tailed, Student's t-test. (B) Average WBC count in peripheral blood of mice immediately prior to euthanasia; n=8 for WT, n=7 for *Dnmt3a$^{+/-}$*, n=5 for *D61Y*, n=5 for *Dnmt3a$^{+/-}$;D61Y*; *p=0.0157 comparing *Dnmt3a$^{+/-}$;D61Y* to WT, *p=0.018 comparing *Dnmt3a$^{+/-}$;D61Y* to *Dnmt3a$^{+/-}$*; statistical analyses performed by unpaired, two-tailed, Student's t-test.

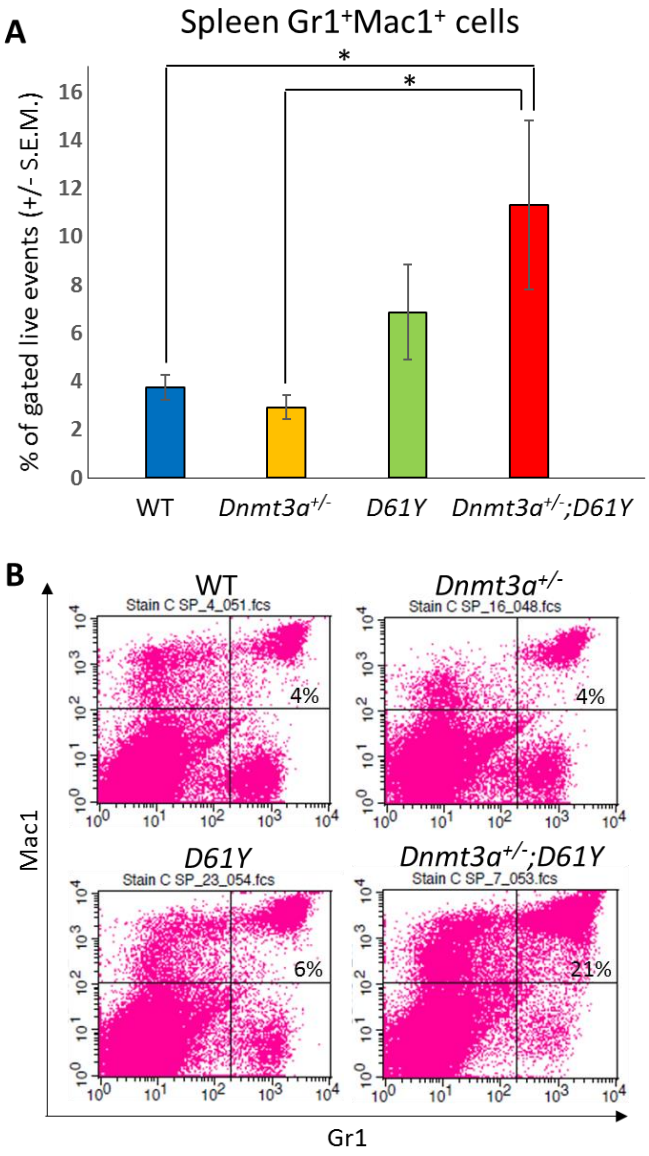

Figure 6.2: *Dnmt3a$^{+/-}$;D61Y* mice have increased Gr1^{+}Mac1^{+} myeloid cells in the spleen at the time of death

(A) Spleen average percentage of myeloid cells (Gr1^{+}Mac1^{+}) gated on live events and (B) representative flow diagrams; n=10 for WT, n=7 for *Dnmt3a$^{+/-}$*, n=9 for *D61Y*, n=5 for *Dnmt3a$^{+/-}$;D61Y*, *p=0.0095 comparing *Dnmt3a$^{+/-}$;D61Y* to WT, *p=0.0177 comparing *Dnmt3a$^{+/-}$;D61Y* to *Dnmt3a$^{+/-}$*; statistical analyses performed by unpaired, two-tailed, Student's t-test.

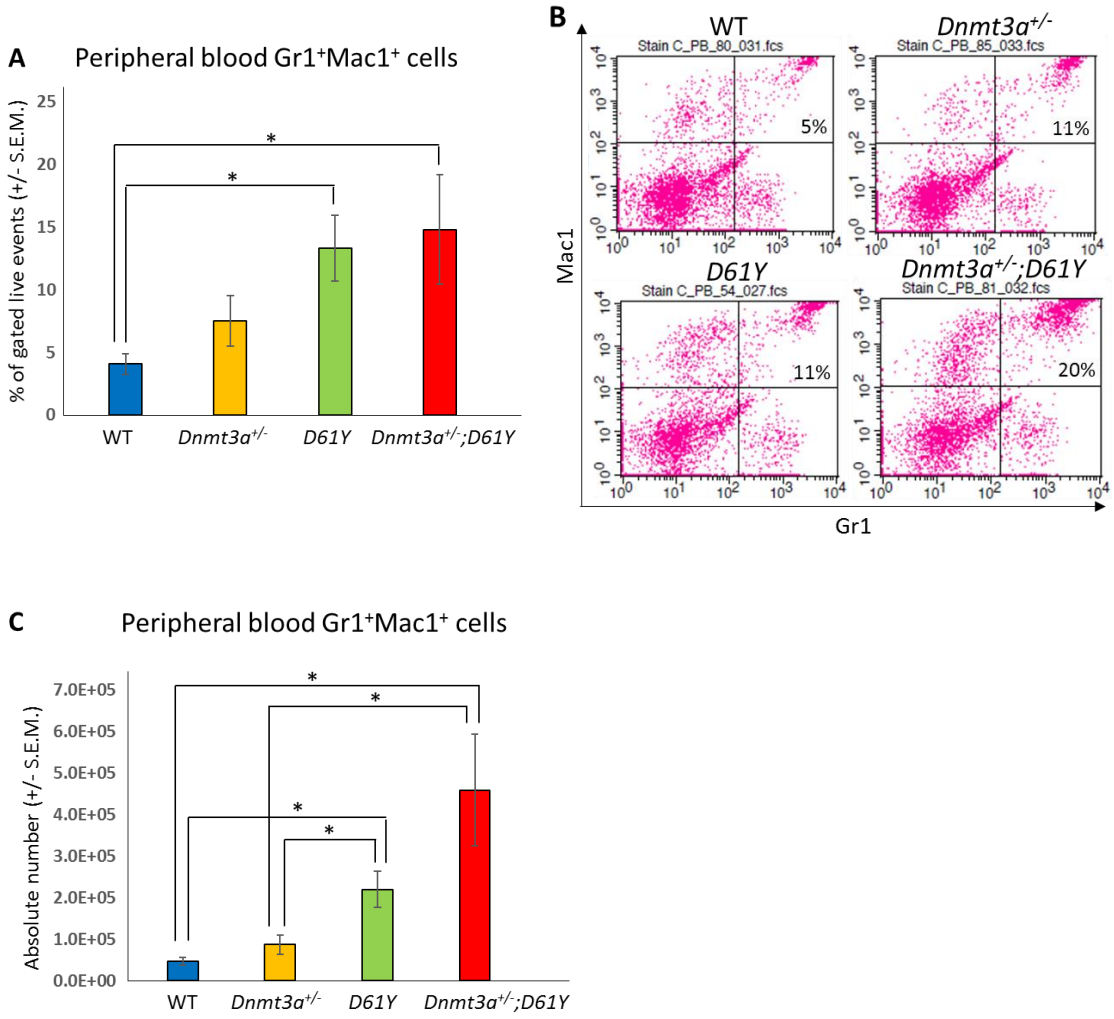

Figure 6.3: *Dnmt3a$^{+/-}$;D61Y* mice have increased Gr1^{+}Mac1^{+} myeloid cells in the peripheral blood at the time of death

(A) Peripheral blood average percentage of myeloid cells (Gr1^{+}Mac1^{+}) gated on live events and (B) representative flow diagrams; n=12 for WT, n=9 for *Dnmt3a$^{+/-}$*, n=9 for *D61Y*, n=5 for *Dnmt3a$^{+/-}$;D61Y*, *p=0.0025 comparing *Dnmt3a$^{+/-}$;D61Y* to WT, *p=0.0009 comparing *D61Y* to WT; statistical analyses performed by unpaired, two-tailed, Student's t-test. (C) Peripheral blood average absolute number of myeloid cells (Gr1^{+}Mac1^{+}) calculated by multiplying percentage and WBC count; n=12 for WT, n=9 for *Dnmt3a$^{+/-}$*, n=9 for *D61Y*, n=5 for *Dnmt3a$^{+/-}$;D61Y*, *p=0.0002 comparing *Dnmt3a$^{+/-}$;D61Y* to WT, *p=0.0034 comparing *Dnmt3a$^{+/-}$;D61Y* to *Dnmt3a$^{+/-}$*, *p=0.0003 comparing *D61Y* to WT, *p=0.0159 comparing *D61Y* to *Dnmt3a$^{+/-}$;* statistical analyses performed by unpaired, two-tailed, Student's t-test.

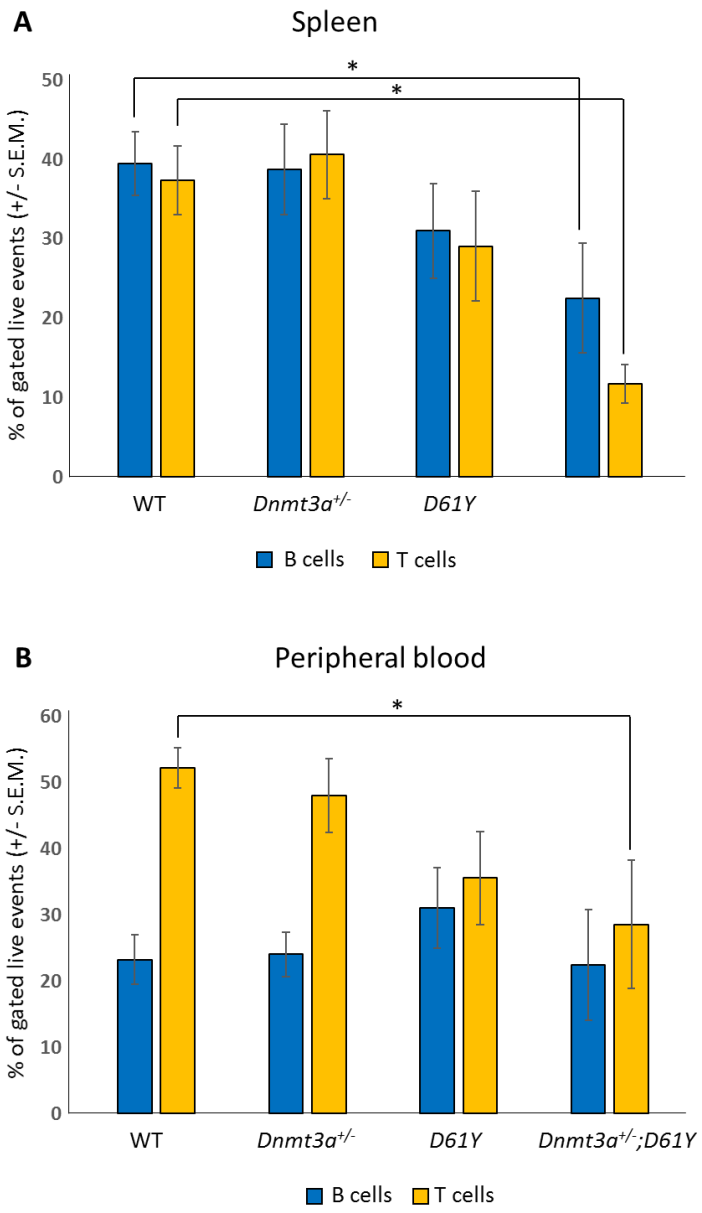

Figure 6.4: *Dnmt3a$^{+/-}$;D61Y* mice have decreased B cells and T cells in the periphery at the time of death

(A) Spleen average percentage of B cells (CD19^{+} or B220^{+}) and T cells (CD4^{+} or CD8^{+}) gated on live events; n=13 for WT, n=9 for *Dnmt3a$^{+/-}$*, n=9 for *D61Y*, n=6 for *Dnmt3a$^{+/-}$;D61Y*, *p=0.0386 comparing *Dnmt3a$^{+/-}$;D61Y* to WT B cells, *p=0.0013 comparing *Dnmt3a$^{+/-}$;D61Y* to WT T cells; statistical analyses performed by unpaired, two-tailed, Student's t-test. (B) Peripheral blood average percentage of B cells (CD19^{+} or B220^{+}) and T cells (CD4^{+} or CD8^{+}) gated on live events; n=12 for WT, n=9 for *Dnmt3a$^{+/-}$*, n=9 for *D61Y*, n=5 for *Dnmt3a$^{+/-}$;D61Y*, *p=0.0071 comparing *Dnmt3a$^{+/-}$;D61Y* to WT T cells; statistical analyses performed by unpaired, two-tailed, Student's t-test.

absolute number of $Gr1^{+}Mac1^{+}$ cells were also significantly greater in double mutant mice relative to the WT and *Dnmt3a*$^{+/-}$ mice (Figure 6.3C). In contrast to the increase in myeloid cells, the T and B cells were decreased in the spleen and peripheral blood of *Dnmt3a*$^{+/-}$*;D61Y* mice relative to other groups (Figure 6.4A and 6.4B).

In an effort to explain the increase in mature myeloid cells in the double mutant mice, we performed flow cytometric analysis on bone marrow cells from all four genotypes to assess the number of granulocyte macrophage progenitors (GMPs). As seen in Figure 6.5, *Dnmt3a*$^{+/-}$*;D61Y* mice showed a significant increase in the absolute number of GMPs compared to WT and *Dnmt3a*$^{+/-}$ mice. The double mutant mice also had significantly more absolute numbers of megakaryocyte erythrocyte progenitors (MEPs) compared to WT mice, but no significant differences in common myeloid progenitors (CMPs) were observed among any of the four groups (Figure 6.5).

Dnmt3a$^{+/-}$;D61Y *mice have signs of anemia and increased erythroid progenitors in the spleen*

The double mutant mice also showed signs of anemia, with significant decreases in peripheral red blood cell counts, hemoglobin levels, as well as hematocrits relative to WT mice (Figure 6.6). Consistent with these observations, within the erythroid lineage, the $CD36^{+}CD71^{+}$ erythroid progenitors (EPs) were significantly increased in the spleens of the *Dnmt3a*$^{+/-}$*;D61Y* mice, suggesting compensatory erythropoiesis (Figure 6.7). Although EP frequency was not increased in the *Dnmt3a*$^{+/-}$*;D61Y* bone marrow

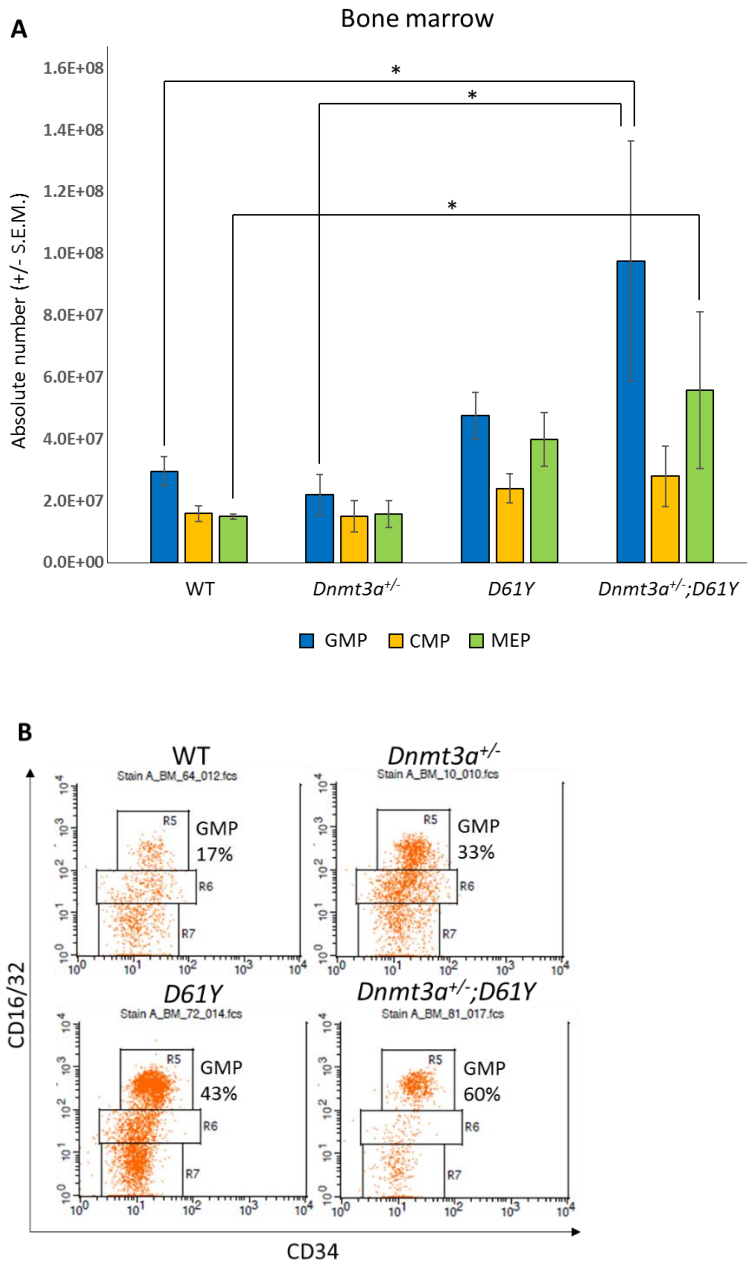

Figure 6.5: *Dnmt3a$^{+/-}$;D61Y* mice have increased GMPs and MEPs in the bone marrow at the time of death

(A) Absolute numbers of granulocyte monocyte progenitors (GMPs), common myeloid progenitors (CMPs), and megakaryocyte erythrocyte progenitors (MEPs) in bone marrow, gated on lineage$^-$cKit$^+$Sca1$^-$ events and (B) representative flow diagrams; n=10 for WT, n=6 for *Dnmt3a$^{+/-}$*, n=6 for *D61Y*, n=4 for *Dnmt3a$^{+/-}$;D61Y*, *p=0.0159 comparing *Dnmt3a$^{+/-}$;D61Y* GMPs to WT GMPs, *p=0.0445 comparing *Dnmt3a$^{+/-}$;D61Y* GMPs to *Dnmt3a$^{+/-}$* GMPs, *p=0.0186 comparing *Dnmt3a$^{+/-}$;D61Y* MEPs to WT MEPs; statistical analyses performed by unpaired, two-tailed, Student's t-test.

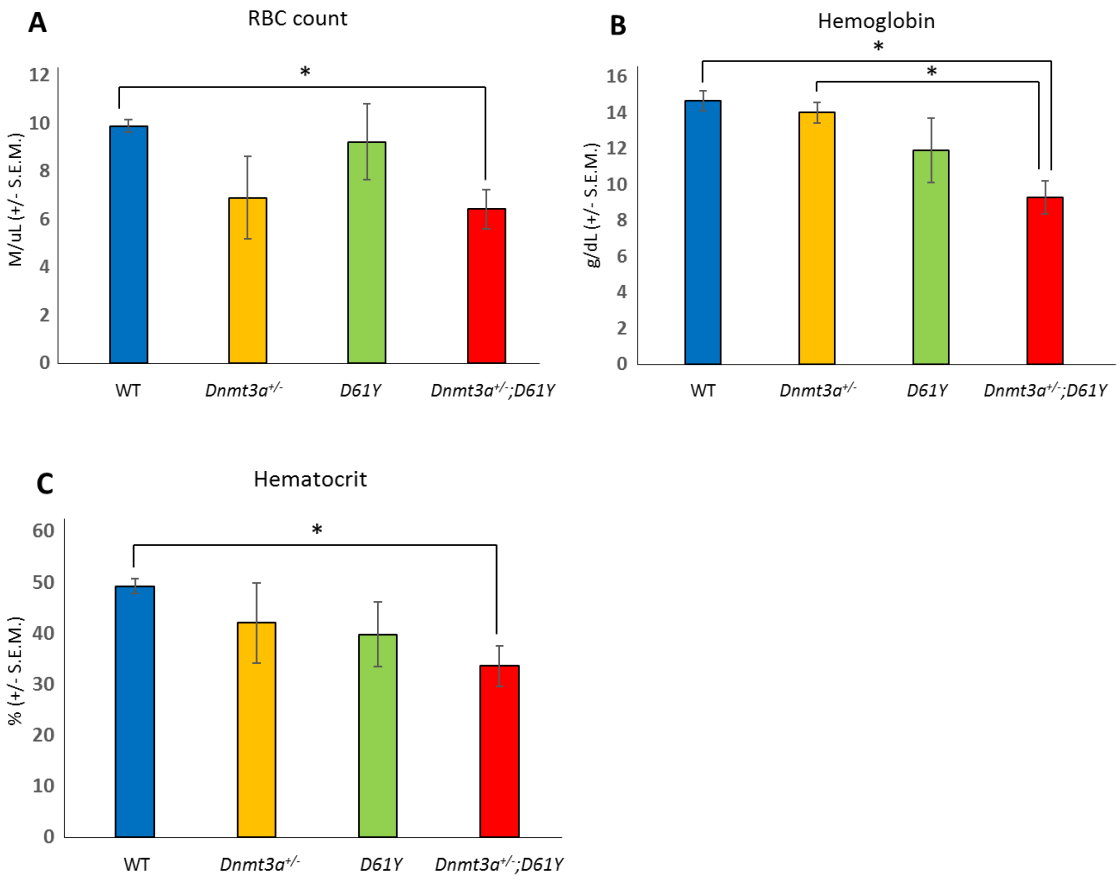

Figure 6.6: *Dnmt3a$^{+/-}$;D61Y* mice have anemia as indicated by peripheral blood measurements immediately prior to euthanasia

(A) Average peripheral blood red blood cell (RBC) count in mice immediately prior to euthanasia; n=8 for WT, n=7 for *Dnmt3a$^{+/-}$*, n=5 for *D61Y*, n=5 for *Dnmt3a$^{+/-}$;D61Y*, *p=0.0005 comparing *Dnmt3a$^{+/-}$;D61Y* to WT. (B) Average peripheral blood hemoglobin values in mice immediately prior to euthanasia; n=8 for WT, n=6 for *Dnmt3a$^{+/-}$*, n=5 for *D61Y*, n=5 for *Dnmt3a$^{+/-}$;D61Y*, *p=0.0002 comparing *Dnmt3a$^{+/-}$;D61Y* to WT, *p=0.0016 comparing *Dnmt3a$^{+/-}$;D61Y* to *Dnmt3a$^{+/-}$*. (C) Average peripheral blood hematocrit values in mice immediately prior to euthanasia; n=8 for WT, n=7 for *Dnmt3a$^{+/-}$*, n=5 for *D61Y*, n=5 for *Dnmt3a$^{+/-}$;D61Y*, *p=0.001 comparing *Dnmt3a$^{+/-}$;D61Y* to WT, statistical analyses performed by unpaired, two-tailed, Student's t-test.

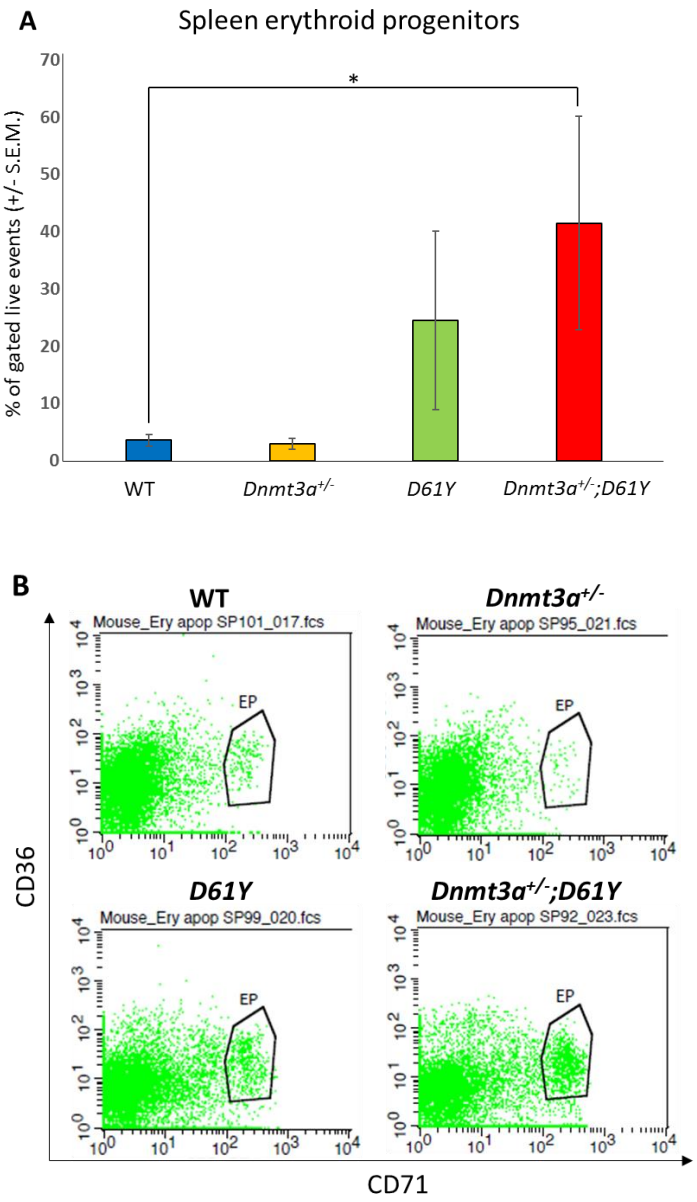

Figure 6.7: *Dnmt3a$^{+/-}$;D61Y* mice have compensatory erythropoiesis in the spleen

(A) Average percentage of erythroid progenitors ($CD36^{+}CD71^{+}$) in spleen gated on live events, with (B) representative flow diagrams; n=6 for WT, n=4 for *Dnmt3a$^{+/-}$*, n=3 for *D61Y*, n=3 for *Dnmt3a$^{+/-}$;D61Y*; *p=0.0177 comparing *Dnmt3a$^{+/-}$;D61Y* to WT, statistical analyses performed by unpaired, two-tailed, Student's t-test.

compartment (data not shown), the increased splenic erythropoiesis may explain the increased bone marrow MEP numbers.

Discussion

Individuals with CHIP often have partial loss of *DNMT3A* enzyme activity, but how this affects the development and progression of leukemia when combined with a second driver mutation is not known. We observed that mice with heterozygous loss of *Dnmt3a* combined with a gain-of-function Shp2 mutation, *D61Y*, develop more rapid disease progression and earlier mortality. Mice expressing $Shp2^{D61Y}$ do not usually succumb to leukemia until 45 weeks after induction of expression (Chan, Kalaitzidis 2009) and mice with *Dnmt3a* haploinsufficiency not develop disease until approximately 80 weeks (Cole, Russler-Germain 2017). We found that mice with the two mutations together become moribund much earlier at 24 weeks, indicating that they cooperate to promote myeloid leukemia progression and to shorten survival.

The most marked phenotypic changes we observed in the *Dnmt3a*$^{+/-}$*;D61Y* mice were splenomegaly, mature myeloid cell expansion in the periphery, as well as increased GMPs in the bone marrow. These mice also exhibited signs of anemia, perhaps due to defects in erythrocyte cell maturation in the bone marrow. In support of this notion, MEPs in the bone marrow of compound mutant mice were increased and there were more erythroid progenitors present in the spleen, which most likely contributed to the splenomegaly in these mice.

The disease course of JMML also exhibits pronounced splenomegaly, sometimes even in the absence of highly elevated WBC count. It has been previously reported that

mice with *Dnmt3a*$^{-/-}$ combined with *Kras*$^{G12D/+}$ mutation, another common mutation found in JMML patients, developed stress erythropoiesis in the spleen (Chang, You 2015). Perhaps one reason JMML patients develop extreme splenomegaly is compensatory splenic erythropoiesis, as observed in the *Dnmt3a*$^{+/-}$*;D61Y* mice in this study.

Because *DNMT3A* and *PTPN11* mutations are found in combination in AML and JMML patients, our double mutant mice provide a novel clinically relevant model for developing and evaluating therapies for myeloid leukemia. In AML, the presence of a *DNMT3A* mutation led to significantly shortened overall survival (Ley, Ding 2010). For JMML, a disease with poor prognosis, there is currently no established decision-making process for determining which patients would be candidates for experimental therapies. However, it is known that the number of mutations present at diagnosis is strongly correlated with survival when comparing patients who have 0-1 mutations to those with 2 or more mutations (Stieglitz, Taylor-Weiner 2015). Further work must be done to find the importance of having specifically the *DNMT3A* and *PTPN11* genes mutated together, but these are two commonly mutated genes in myeloid leukemia that we have now shown leads to accelerated disease.

The mechanism of how *Dnmt3a* loss cooperates with driver mutations to accelerate disease progression is still unknown, but this *Dnmt3a*$^{+/-}$*;D61Y* mouse model will be useful to explore this question. Perhaps the changes in methylation caused by reduced DNMT3A activity lead to epigenetic changes that alter the normal transcription of tumor suppressor genes needed to dampen Shp2 signaling. Future work performing a

genome-wide transcriptional analysis would help to elucidate the mechanism of enhanced myeloid leukemia observed in the double mutant mice.

CHAPTER SEVEN

DISCUSSION

Juvenile myelomonocytic leukemia (JMML) is a disease with a poor prognosis that urgently needs effective therapies. There are currently no chemotherapies that can improve overall or event-free survival, and allogeneic hematopoietic stem cell transplant has high therapy-induced morbidity as well as a high relapse rate of 50% (Loh 2011). SHP2 is the most commonly mutated protein in JMML patients, with gain of function (GOF) mutations in *PTPN11* making up 35% of all cases (Chan, Cooper 2009). One of the classic features of JMML is progenitor hypersensitivity to GM-CSF with hyperactivation of the RAS/MAPK signaling pathway. However, our laboratory has shown that the PI3K/AKT pathway is also important, since AKT (as well as ERK) is hyper-phosphorylated in GOF Shp2 cells after GM-CSF stimulation. Importantly, our lab also found that p110δ is a hematopoietic-specific PI3K catalytic subunit that promotes GOF Shp2-induced leukemia (Goodwin, Li 2014). These studies were done using genetic inactivation of *Pik3cd* and p110δ-specific pharmacologic inhibition *in vitro*, and we wanted to take the next step in making these findings applicable to JMML patients by performing *in vivo* pharmacologic studies.

We treated *Shp2*$^{E76K/+}$;LysMcre^{+} mice with the specific and potent p110δ inhibitor, GS-9820, and found significantly reduced splenomegaly and prolonged survival compared to the vehicle-treated controls (Figures 3.1 and 3.8), indicating that the reduced activation of Akt and Erk and the reduced cell hyperproliferation observed *in vitro* translates into substantial improvements *in vivo*. We also found that there were

significantly decreased phenotypically-defined progenitor cells in the bone marrow (Figure 3.3) and a corresponding increase in mature myeloid cells in the peripheral blood (Figure 3.6), suggesting that inhibition of p110δ induces myeloid differentiation.

Having demonstrated that p110δ inhibition can treat GOF Shp2-induced leukemia, we next wanted to further the therapeutic impact of our findings by identifying other signaling molecules that cooperate with p110δ to promote Shp2 signaling. Because mechanisms of cancer resistance include upregulation of downstream molecules and compensatory pathways, single-agent chemotherapy is unlikely to be effective in JMML patients. We observed this in our GS-9820-treated mice, as they eventually became moribund and succumbed to the same disease as their vehicle-treated counterparts (Figures 3.10-3.12). Thus, we decided to study downstream molecules in the p110δ signaling pathway that might be able to compensate for loss of p110δ activity. We identified Bruton's tyrosine kinase (BTK) as a molecule-of-interest because it is known in B cell receptor (BCR) signaling to become activated downstream of PI3K. Ibrutinib, the first BTK inhibitor, obtained accelerated FDA approval and BTK has recently emerged in the field of lymphoid malignancies as a very successful therapeutic target for a variety of B cell malignancies.

We used a second-generation BTK inhibitor, acalabrutinib (ACP-196), and another specific p110δ inhibitor, ACP-319, to explore the role that BTK plays in a GOF Shp2-induced myeloid leukemia. Our results showed that, while BTK inhibition alone failed to reduce proliferation of GOF Shp2-expressing cells, dual inhibition of BTK and p110δ cooperatively decreased the phosphorylation of Akt and Erk in bone marrow-

derived macrophages from mutant Shp2-expressing mice and cooperatively decreased the hyperproliferation of cells stimulated with GM-CSF (Figure 4.3 and 4.4). *In vivo*, we initially used 15mg/kg doses of each drug and saw promising yet statistically insignificant trends in prolonged survival, decreased splenomegaly, and decreased peripheral blood WBC counts (Figures 4.5, 4.7, and 4.8). However, when we increased the dosing to 20mg/kg for each drug, we observed highly significant reductions in spleen size and leukocytosis (Figures 4.10 and 4.11). Similar to the study we performed using the p110δ inhibitor alone, the treated mice ultimately died of the same leukemia as the vehicle-treated mice (Figure 4.6 and data not shown). Thus, the drug treatment would need to be continued beyond the 21 days in order to obtain a sustained effect. The dosing regimen likely could be decreased from twice per day to once per day or less during this maintenance phase to attain prolonged suppression of myeloproliferation.

Similar to our GS-9820 study, we also observed fewer phenotypically-defined progenitors in the bone marrow and more terminally differentiated myeloid cells in the peripheral blood in mice treated with dual BTK and p110δ inhibition (Figures 4.12 and 4.15). Again, this finding implies that the combination of BTK and p110δ inhibition disrupts the tumor cell niche in the bone marrow and promotes myeloid cell maturation. This observation is consistent with what is seen in lymphoid diseases, where ibrutinib has disruptive effects on the tumor microenvironment and promotes peripheral distribution of the lymphoid leukemia cells due to BTK being an integral component of chemokine receptor signaling and supporting B cell homing to the lymph nodes and spleen.

The lack of efficacy observed with the BTK inhibitor alone may be due to TEC being able to compensate for BTK loss in mice (Ellmeier, Jung 2000). Ellmeier et. al generated *Tec*$^{-/-}$*Btk*$^{-/-}$ mice and compared their phenotype to *Btk*$^{-/-}$ mice, concluding that TEC worked together with BTK to allow for normal B cell development. The authors postulated that the ability of TEC to partially compensate for BTK could explain the differences between X-linked immunodeficiency (XID) in mice and X-linked agammaglobulinemia (XLA) in humans. Both XID and XLA are due to loss-of-function mutations in *Btk* and *BTK*, respectively, but the murine XID has less severe B cell depletion (Cancro, Sah 2001). Therefore, it is possible that the use of ACP-196 in patients with myeloid diseases will show a superior response compared to that observed in mice because humans seemingly have a higher reliance on BTK signaling.

Next, we wanted to further explore the mechanism of BTK signaling in myeloid cells. Our biochemistry data had shown that PLCγ2 is not essential for BTK-dependent activation of Erk (Figures 4.2 and 4.3). We were intrigued by this observation, as it implied that BTK signals to Erk in myeloid cells in a phospho-PLCγ2-independent manner and in a fashion distinct from that described in BCR signaling. However, an alternative BTK downstream target that activates PI3K in B cells is B cell adaptor for PI3K (BCAP). We wanted to test if BCAP could be the connector between BTK and PI3K, thus leading to Akt and Erk activation (Figure 5.1). We performed immunoprecipitation assays to pull down total BCAP in bone marrow-derived macrophages and immunoblotted for phospho-tyrosine. In response to GM-CSF stimulation, there was selective phosphorylation of the two full-length BCAP isoforms in the *Shp2*^{E76K}-expressing cells

(Figure 5.2). These are the BCAP isoforms previously defined to be more important for binding to and recruitment of PI3K to the plasma membrane, suggesting that GOF Shp2-expressing cells have more BCAP-induced activation of PI3K. We also showed that treatment with ACP-196 reduced the phosphorylation of BCAP in a dose-dependent manner, suggesting that BTK-to-BCAP signaling is intact in macrophages (Figure 5.3). In order to study the mechanism of p85α-BCAP interaction, we used p85α constructs with specific sites mutated in the N-SH2 and C-SH2 domains to ablate the ability to bind to phospho-tyrosine residues. We transduced these p85α constructs, along with Shp2 and BCAP constructs, into NIH3T3 cells to study their interactions. We found that, compared to WT, the mutated p85α constructs had less binding to BCAP, confirming that BCAP binds to the SH2 domains of p85α (Figure 5.6). This gives more insight into the mechanism of BCAP-p85α interaction and informs on a strategy to potentially disrupt this binding.

Finally, we explored the consequences of combining a GOF $Shp2^{D61Y}$ mutation with heterozygous loss of *Dnmt3a*. JMML patients with more than one mutation have significantly poorer survival, and our mouse model reflects this observation as the double mutant mice became moribund at only 24 weeks of age with a myeloproliferative neoplasm. In comparison to control and single mutant mice, the *Dnmt3a;D61Y* mice had increased splenomegaly and leukocytosis (Figure 6.1), myeloid expansion in the spleen and peripheral blood (Figures 6.2 and 6.3), and more granulocyte macrophage progenitors (GMPs) in the bone marrow (Figure 6.5). We also observed a novel phenotype of defective erythrocyte differentiation, which led to

anemia in the *Dnmt3a;D61Y* mice with significantly reduced red blood cell count, hemoglobin, and hematocrit levels (Figure 6.6). In response, we observed evidence of compensatory erythropoiesis, as there was an increased proportion of erythroid progenitors in the spleens of the double mutant mice (Figure 6.7). *DNMT3A* is one of the first genes mutated in the development of preleukemia, and loss-of-function in HSCs leads to increased self-renewal and expansion of the mutated stem cells. JMML patients bearing secondary mutations, such as having mutated *DNMT3A* in addition to a *PTPN11* mutation, have a much poorer prognosis. It is still unknown how DNMT3A loss can cause enhanced disease in the context of GOF SHP2. One possibility is that the altered methylation pattern leads to aberrant repression of tumor suppressor genes and/or increased expression of oncogenes. We have shown that the *Dnmt3a;D61Y* mice exhibit the phenotype of accelerated leukemia and can be used as a model for the investigation of the mechanism of DNMT3A.

Overall Conclusions and Significance

Juvenile myelomonocytic leukemia (JMML) is a rare childhood leukemia that urgently needs better therapies. Gain-of-function mutations in *PTPN11*, which encodes for the protein tyrosine phosphatase SHP2, are the most frequent mutations found in JMML patients. Downstream of SHP2 signaling, PI3K/AKT has recently been recognized to be as important as the RAF/MEK/ERK pathway for promoting leukemogenesis, particularly the hematopoietic-specific subunit p110δ (Goodwin, Li 2014). However, because single-agent cancer therapy is limited by resistance development, as evidenced

by the example of imatinib (Reddy and Aggarwal 2012), we looked for other signaling molecules that cooperate with p110δ to promote GOF Shp2 signaling. Lymphoid malignancy studies have demonstrated that Bruton's tyrosine kinase (BTK) is a key player in cancer, with the inhibitor ibrutinib having much success recently in a variety of B cell lymphomas and leukemias. BTK may soon make the leap into the myeloid malignancies field as an important target. A study done in acute myeloid leukemia (AML) showed that BTK is constitutively phosphorylated in a majority of AML patient samples and that ibrutinib has good efficacy against AML blast proliferation *in vitro* (Rushworth, Murray 2014).

Our studies here in GOF Shp2-expressing myeloid cells suggest that BTK has a significant role in myeloid malignancies as well. We used ACP-196, a second-generation inhibitor with less off-target binding than ibrutinib, to show that BTK inhibition cooperates with p110δ inhibition to reduce Akt/Erk hyperphosphorylation and hyperproliferation in response to GM-CSF. The dual inhibition also proved effective *in vivo*, with a significant decrease in splenomegaly and leukocytosis, and (with lower drug doses) trends towards prolonged survival. These experiments were done in mice with mutant Shp2 under the control of the lysozyme 2 promoter, limiting the expression specifically to the myeloid cells. These findings provide the first evidence that BTK inhibition can be effective as a combination treatment with p110δ inhibition to treat mutant Shp2-induced myeloproliferative neoplasm (MPN). It is also significant to note that we used $Shp2^{E76K/+}$;LysMcre^{+} mice for both the single-agent p110δ inhibitor experiment and for the drug combination experiment. We observed a similar response

in both groups of treated mice, but the dose we used to obtain a response was less in the drug combination (20mg/kg) than the single-therapy p110δ inhibitor (30mg/kg).

The effect of BTK inhibition on the microenvironment is also relevant to our findings. Despite the significant effect of the two-inhibitor combination, we did not see any improvement for ACP-196 alone. Thus, perhaps the mechanism of ACP-196 *in vivo* is to disrupt the nurturing tumor microenvironment, as ibrutinib does in chronic lymphocytic leukemia (CLL) patients. By doing so, the leukemic cells are more vulnerable and susceptible to the effects of the p110δ drug. The microenvironment of JMML patients is suspected to be abnormal because of the high relapse rate after hematopoietic stem cell transplant. A recent paper also found that having a GOF *Ptpn11* mutation expressed in the bone marrow's non-hematopoietic microenvironmental cells alone was sufficient for mice to fully develop MPN (Dong, Yu 2016). Therefore, testing microenvironment-altering drugs may be a new strategy worth pursuing for JMML.

An alternative explanation for the lack of effect with BTK inhibition alone can be seen from our proposed signaling pathway. We show evidence that BTK may form a positive feedback loop with PI3K by way of B cell adaptor for PI3K (BCAP). Because PI3K is hyperactivated due to GOF Shp2 (Goodwin, Li 2014), inhibiting BTK alone is not sufficient to reduce this high level of p110δ activity. However, once p110δ activity is curtailed by the inhibitor ACP-319, PI3K may be more dependent on BTK phosphorylation of BCAP for recruitment to the cell membrane and continued activation. Therefore, the addition of a BTK inhibitor can now make a significant difference on the phosphorylation of downstream effectors and cell hyperproliferation.

The idea that BTK may be part of a positive feedback loop by way of BCAP phosphorylation to promote PI3K and its own activation gives some insight into the mechanism of action of the dual inhibition of BTK and p110δ.

Our finding that full length BCAP (BCAP-L) is more important than shortened BCAP (BCAP-S) for activating PI3K may be explained by the BCAP protein structure. Perhaps the Toll-IL-1 receptor (TIR) domain at the N-terminal end of BCAP-L, which is absent from BCAP-S, allows BCAP-L to better associate with p85α and recruit PI3K to the plasma membrane. Toll-like receptor (TLR) signaling is known to activate PI3K, which then inhibits proinflammatory events and thus negatively regulates TLR signaling as a negative feedback loop (Hazeki, Nigorikawa 2007). It is known that BCAP-S cannot negatively regulate inflammation because it lacks the TIR domain. In fact, BCAP-S is a positive regulator of inflammation, so perhaps the TIR domain is necessary in order to bind to PI3K (Matsumura, Oyama 2010). Furthermore, in response to lipopolysaccharide (LPS), an activator of TLR signaling, there is increased tyrosine-phosphorylated BCAP at the membrane. Therefore, TLR signaling either phosphorylates BCAP already present at the membrane, or it causes translocation of the constitutively phosphorylated BCAP in the cytoplasm to the membrane (Ni, MacFarlane 2012). Thus, it seems that the TIR domain may be important for membrane recruitment of PI3K as well.

A case report was recently published that strengthens the idea that BTK and PI3K are two intimately linked signaling partners. BTK loss causes X-linked agammaglobulinemia, but in this referenced case, a child was diagnosed with autosomal recessive agammaglobulinemia (Tang, Upton 2017). Rather than a loss-of-function

mutation in BTK, the patient had homozygous mutations in the *PIK3R1* gene, which encodes p85α. This observation suggests that p85α is a crucial component of BTK signaling, as the complete loss of p85α phenocopies the complete loss of BTK.

Finally, our results from crossing *Dnmt3a*$^{+/-}$ and *D61Y* mice provides further proof that multiple mutations lead to a more aggressive disease, consistent with that observed in JMML patients (Stieglitz, Taylor-Weiner 2015). Although the prognosis of JMML patients is variable, it is now known that secondary mutations and hypermethylation states are associated with poorer survival. Even though mutations in *DNMT3A* are loss-of-function and lead to hypomethylation of focal CpG sites, Stieglitz et. al found that all JMML patient samples bearing secondary mutations were globally hypermethylated (Stieglitz, Mazor 2017). It remains unknown why some JMML patients experience spontaneous resolution while others relapse soon after allogeneic HSCT. Perhaps the reason some patients relapse following transplantation is due to incomplete ablation of HSCs bearing *DNMT3A* mutations. These HSCs have been shown in mice to have increased self-renewal and will out-compete the normal donor HSCs (Challen, Sun 2011). If the leukemic clone in a JMML patient had acquired both mutant *PTPN11* and *DNMT3A*, then this stem cell would expand even after allogeneic HSCT. Perhaps the addition of azacitidine or another hypomethylating agent to the treatment regimen would be beneficial to patients.

To summarize, we have proposed and provided evidence that p110δ and BTK form a positive feedback loop with BCAP to drive their own activity and promote GOF

Shp2-induced leukemogenesis. We have also shown that the dual inhibition of p110δ and BTK is more effective than inhibition with either alone.

Future Directions

An important future experiment is to determine if BCAP knockdown leads to reduced phosphorylation of Akt and Erk in myeloid cells, which would cement the link between BCAP and these downstream effectors. To begin work on this, we have transduced BCAP shRNA into bone marrow low-density mononuclear cells expressing $Shp2^{E76K}$. We are testing which shRNA results in the best knockdown of BCAP. Once this experimental model is optimized, we will use immunoblotting to look at phospho-Akt and phospho-Erk, and [^{3}H]-thymidine assays to measure cell proliferation. If BCAP is indeed responsible for connecting BTK to PI3K, then we expect to see a reduction in all of these measures upon knockdown of BCAP expression.

We will also continue our work on the mechanism of BCAP-p85α interaction. We already have a validated system in NIH3T3 cells in which we have shown that p85α constructs with both SH2 domains mutated have decreased BCAP binding. The next step is to test the effect of single SH2 domain mutations on the interaction. Because only the N-SH2 domain has been previously shown to bind to BCAP, we may find that mutating the C-SH2 domain has no effect. However, it is believed that both SH2 domains can bind to similar phospho-tyrosine sequences, so it is more likely that we will find each domain to be involved in BCAP binding, although we do not know to what degree. This would be vital information were we to attempt to disrupt the BCAP-PI3K binding in the future.

Another important question is whether other driver mutations of JMML also rely on p110δ and BTK to the same extent as Shp2^{E76K}-induced JMML. We have focused our attention on the *Shp2*$^{E76K/+}$;LysMcre^{+} mice, as *PTPN11* is the most frequent mutation in patients and this mouse model is conducive to *in vivo* studies because of its consistent disease development. However, another 65% of JMML cases involve mutations in other genes, including *KRAS*, *NF1*, and *CBL*. Mouse models using these other driver genes could be used to repeat the same *in vitro*, and perhaps the *in vivo*, studies that we have shown here. This would potentially expand the applicability of our findings to more JMML patients and may bring the utility of p110δ and BTK inhibitors to other myeloid malignancies as well.

Thus far, our work has been a purely pharmacologic approach. Although this is more realistic to patient situations than genetic studies, a genetically modified mouse lacking BTK or BCAP would provide results without the potential confounding off-target effects. Therefore, we predict that crossing GOF Shp2 mice with *Btk*$^{-/-}$ and the kinase-dead p110δ$^{D910A/D910A}$ mice would yield an even stronger cooperative effect on the correction of leukemia. A *Pik3ap1*$^{-/-}$ mouse would also prove very useful to demonstrate BCAP's involvement in the BTK/PI3K signaling pathway.

Finally, many questions remain unanswered about how *Dnmt3a* loss in mice expressing GOF Shp2 leads to accelerated leukemia development. One important experiment is to perform a genome-wide transcriptional analysis, which would clarify if the aberrant methylation due to mutant *Dnmt3a* directly affects Shp2 signaling. Two possible epigenetic consequences of loss of DNMT3A activity are that signaling

molecules upstream or downstream of Shp2 are upregulated, or that there is downregulation of proteins normally needed to dampen Shp2 signaling. An *in vivo* study including azacitidine in the treatment of *Dnmt3a*$^{+/-}$;*D61Y* mice, perhaps in combination with a p110δ and/or BTK inhibitor, would further elucidate the role of DNMT3A in the progression of JMML and other myeloid malignancies.

The results of our experiments show that the combined inhibition of p110δ and BTK effectively reduces the leukemia progression of GOF Shp2-induced JMML. Targeting both proteins at once is likely effective because it interrupts the positive feedback loop that they form with BCAP. It also allows a lower dose of each drug to be used compared to a single-agent p110δ inhibitor. These observations expand the role of BTK beyond B cell lymphoid malignancies into myeloid leukemia. In this regard, the p110δ/BTK dual inhibition strategy may be useful in conjunction with a methylating agent and in a variety of other malignancies as well.

REFERENCES

Aksamitiene E, Kiyatkin A, and Kholodenko BN. Cross-talk between mitogenic Ras/MAPK and survival PI3K/Akt pathways: a fine balance. Biochem Soc Trans. 2012; 40: 139-46.

Akutagawa J, Huang T, Epstein I, Chang T, Quirindongo-Crespo M, Cottonham C, Dail M, Slusher B, Friedman L, Sampath D, and Braun B. Targeting the PI3K/Akt pathway in murine MDS/MPN driven by hyperactive Ras. Leukemia. 2016; 30: 1335-43.

Arber DA, Orazi A, Hasserjian R, Thiele J, Borowitz MJ, Beau MML, Bloomfield CD, Cazzola M, and Vardiman JW. The 2016 revision to the World Health Organization classification of myeloid neoplasms and acute leukemia. Blood. 2016; 127: 2391-405.

Balakrishnan K, Peluso M, Fu M, Rosin NY, Burger JA, Wierda WG, Keating MJ, Faia K, O'Brien S, Kutok JL, and Gandhi V. The phosphoinositide-3-kinase (PI3K)-delta and gamma inhibitor, IPI-145 (Duvelisib), overcomes signals from the PI3K/AKT/S6 pathway and promotes apoptosis in CLL. Leukemia. 2015; 29: 1811-22.

Barr AJ. Protein tyrosine phosphatases as drug targets: strategies and challenges of inhibitor development. Future Med Chem. 2010; 2: 1563-76.

Barr P, Robak T, Owen CJ, Tedeschi A, Bairey O, Bartlett NL, Burger J, Hillmen P, Coutre S, Devereux S, Grosicki S, McCarthy H, Li J, et al. Updated Efficacy and Safety from the Phase 3 Resonate-2 Study: Ibrutinib As First-Line Treatment Option in Patients 65 Years and Older with Chronic Lymphocytic Leukemia/Small Lymphocytic Leukemia. Blood. 2016; 128: 234.

Battersby A, Csiszar A, Leptin M, and Wilson R. Isolation of proteins that interact with the signal transduction molecule Dof and identification of a functional domain conserved between Dof and vertebrate BCAP. J Mol Biol. 2003; 329: 479-93.

Baylin SB and Herman JG. DNA hypermethylation in tumorigenesis: epigenetics joins genetics. Trends Genet. 2000; 16: 168-74.

Bentires-Alj M, Paez JG, David FS, Keilhack H, Halmos B, Naoki K, Maris JM, Richardson A, Bardelli A, Sugarbaker DJ, Richards WG, Du J, Girard L, et al. Activating mutations of the noonan syndrome-associated SHP2/PTPN11 gene in human solid tumors and adult acute myelogenous leukemia. Cancer Res. 2004; 64: 8816-20.

Bergstraesser E, Hasle H, Rogge T, Fischer A, Zimmermann M, Noellke P, and Niemeyer CM. Non-hematopoietic stem cell transplantation treatment of juvenile myelomonocytic leukemia: A retrospective analysis and definition of response criteria. Pediatric Blood & Cancer. 2006; 49: 629-33.

Bradshaw JM. The Src, Syk, and Tec family kinases: distinct types of molecular switches. Cell Signal. 2010; 22: 1175-84.

Brown J, Byrd J, Coutre S, Benson D, Flinn I, Wagner-Johnston N, Spurgeon S, Kahl B, Bello C, Webb H, Johnson D, Peterman S, Li D, et al. Idelalisib, an inhibitor of phosphatidylinositol 3-kinase p110δ, for relapsed/refractory chronic lymphocytic leukemia. Blood. 2014; 123: 3390-97.

Brown JR. Ibrutinib in chronic lymphocytic leukemia and B cell malignancies. Leuk Lymphoma. 2014; 55: 263-9.

Burger JA, Keating MJ, Wierda WG, Hartmann E, Hoellenriegel J, Rosin NY, de Weerdt I, Jeyakumar G, Ferrajoli A, Cardenas-Turanzas M, Lerner S, Jorgensen JL, Nogueras-Gonzalez GM, et al. Safety and activity of ibrutinib plus rituximab for patients with high-risk chronic lymphocytic leukaemia: a single-arm, phase 2 study. Lancet Oncol. 2014; 15: 1090-9.

Burger JA, Tedeschi A, Barr PM, Robak T, Owen C, Ghia P, Bairey O, Hillmen P, Bartlett NL, Li J, Simpson D, Grosicki S, Devereux S, et al. Ibrutinib as Initial Therapy for Patients with Chronic Lymphocytic Leukemia. N Engl J Med. 2015; 373: 2425-37.

Butterworth S, Overduin M, and Barr AJ. Targeting protein tyrosine phosphatase SHP2 for therapeutic intervention. Future Med Chem. 2014; 6: 1423-37.

Byrd JC, Brown JR, O'Brien S, Barrientos JC, Kay NE, Reddy NM, Coutre S, Tam CS, Mulligan SP, Jaeger U, Devereux S, Barr PM, Furman RR, et al. Ibrutinib versus ofatumumab in previously treated chronic lymphoid leukemia. N Engl J Med. 2014; 371: 213-23.

Byrd JC, Furman RR, Coutre SE, Flinn IW, Burger JA, Blum KA, Grant B, Sharman JP, Coleman M, Wierda WG, Jones JA, Zhao W, Heerema NA, et al. Targeting BTK with ibrutinib in relapsed chronic lymphocytic leukemia. N Engl J Med. 2013; 369: 32-42.

Byrd JC, Harrington B, O'Brien S, Jones JA, Schuh A, Devereux S, Chaves J, Wierda WG, Awan FT, Brown JR, Hillmen P, Stephens DM, Ghia P, et al. Acalabrutinib (ACP-196) in Relapsed Chronic Lymphocytic Leukemia. N Engl J Med. 2016; 374: 323-32.

Cancro MP, Sah AP, Levy SL, Allman DM, Schmidt MR, and Woodland RT. xid mice reveal the interplay of homeostasis and Bruton's tyrosine kinase-mediated selection at multiple stages of B cell development. Int Immunol. 2001; 13: 1501-14.

Cantley LC. The phosphoinositide 3-kinase pathway. Science. 2002; 296: 1655-7.

Carter M, Cox K, Blakemore S, Turaj A, Oldham R, Dahal L, Tannheimer S, Forconi F, Packham G, and Cragg M. PI3Kδ inhibition elicits anti-leukemic effects through Bim-dependent apoptosis. Leukemia. 2017; 31: 1423-33.

Castello A, Gaya M, Tucholski J, Oellerich T, Lu KH, Tafuri A, Pawson T, Wienands J, Engelke M, and Batista FD. Nck-mediated recruitment of BCAP to the BCR regulates the PI(3)K-Akt pathway in B cells. Nat Immunol. 2013; 14: 966-75.

Challen GA, Sun D, Jeong M, Luo M, Jelinek J, Berg JS, Bock C, Vasanthakumar A, Gu H, Xi Y, Liang S, Lu Y, Darlington GJ, et al. Dnmt3a is essential for hematopoietic stem cell differentiation. Nat Genet. 2011; 44: 23-31.

Chan G, Kalaitzidis D, Usenko T, Kutok JL, Yang W, Mohi MG, and Neel BG. Leukemogenic Ptpn11 causes fatal myeloproliferative disorder via cell-autonomous effects on multiple stages of hematopoiesis. Blood. 2009; 113: 4414-24.

Chan RJ, Cooper T, Kratz CP, Weiss B, and Loh ML. Juvenile Myelomonocytic Leukemia: A Report from the 2nd International JMML Symposium. Leukemia Research. 2009; 33: 355-62.

Chan RJ and Feng GS. PTPN11 is the first identified proto-oncogene that encodes a tyrosine phosphatase. Blood. 2007; 109: 862-7.
Chan RJ, Leedy MB, Munugalavadla V, Voorhorst CS, Li Y, Yu M, and Kapur R. Human somatic PTPN11 mutations induce hematopoietic-cell hypersensitivity to granulocyte-macrophage colony-stimulating factor. Blood. 2005; 105: 3737-42.
Chang Y, Jou S, Lin D, Lu M, and Lin K. Second allogeneic hematopoietic stem cell transplantation for juvenile myelomonocytic leukemia: case report and literature review. Journal of Pediatric Hematology/Oncology. 2004; 26: 190-93.
Chang YI, You X, Kong G, Ranheim EA, Wang J, Du J, Liu Y, Zhou Y, Ryu MJ, and Zhang J. Loss of Dnmt3a and endogenous Kras(G12D/+) cooperate to regulate hematopoietic stem and progenitor cell functions in leukemogenesis. Leukemia. 2015; 29: 1847-56.
Chen L, Chen W, Mysliwski M, Serio J, Ropa J, Abulwerdi FA, Chan RJ, Patel JP, Tallman MS, Paietta E, Melnick A, Levine RL, Abdel-Wahab O, et al. Mutated Ptpn11 alters leukemic stem cell frequency and reduces the sensitivity of acute myeloid leukemia cells to Mcl1 inhibition. Leukemia. 2015; 29: 1290-300.
Chen YN, LaMarche MJ, Chan HM, Fekkes P, Garcia-Fortanet J, Acker MG, Antonakos B, Chen CH, Chen Z, Cooke VG, Dobson JR, Deng Z, Fei F, et al. Allosteric inhibition of SHP2 phosphatase inhibits cancers driven by receptor tyrosine kinases. Nature. 2016; 535: 148-52.
Clausen BE, Burkhardt C, Reith W, Renkawitz R, and Forster I. Conditional gene targeting in macrophages and granulocytes using LysMcre mice. Transgenic Res. 1999; 8: 265-77.
Cole CB, Russler-Germain DA, Ketkar S, Verdoni AM, Smith AM, Bangert CV, Helton NM, Guo M, Klco JM, O'Laughlin S, Fronick C, Fulton R, Chang GS, et al. Haploinsufficiency for DNA methyltransferase 3A predisposes hematopoietic cells to myeloid malignancies. J Clin Invest. 2017; 127: 3657-74.
Crank MC, Grossman JK, Moir S, Pittaluga S, Buckner CM, Kardava L, Agharahimi A, Meuwissen H, Stoddard J, Niemela J, Kuehn H, and Rosenzweig SD. Mutations in PIK3CD can cause hyper IgM syndrome (HIGM) associated with increased cancer susceptibility. J Clin Immunol. 2014; 34: 272-6.
de Gorter DJ, Beuling EA, Kersseboom R, Middendorp S, van Gils JM, Hendriks RW, Pals ST, and Spaargaren M. Bruton's tyrosine kinase and phospholipase Cgamma2 mediate chemokine-controlled B cell migration and homing. Immunity. 2007; 26: 93-104.
Deng C, Lipstein MR, Scotto L, Jirau Serrano XO, Mangone MA, Li S, Vendome J, Hao Y, Xu X, Deng SX, Realubit RB, Tatonetti NP, Karan C, et al. Silencing c-Myc translation as a therapeutic strategy through targeting PI3Kdelta and CK1epsilon in hematological malignancies. Blood. 2017; 129: 88-99.
Dimopoulos MA, Trotman J, Tedeschi A, Matous JV, Macdonald D, Tam C, Tournilhac O, Ma S, Oriol A, Heffner LT, Shustik C, Garcia-Sanz R, Cornell RF, et al. Ibrutinib for patients with rituximab-refractory Waldenstrom's macroglobulinaemia (iNNOVATE): an open-label substudy of an international, multicentre, phase 3 trial. Lancet Oncol. 2017; 18: 241-50.

Dong L, Yu W-M, Zheng H, Loh ML, Bunting ST, Pauly M, Huang G, Zhou M, Broxmeyer HE, Scadden DT, and Qu C-K. Leukaemogenic effects of Ptpn11 activating mutations in the stem cell microenvironment. Nature. 2016; 539: 304-08.

Dong L, Yu WM, Zheng H, Loh ML, Bunting ST, Pauly M, Huang G, Zhou M, Broxmeyer HE, Scadden DT, and Qu CK. Leukaemogenic effects of Ptpn11 activating mutations in the stem cell microenvironment. Nature. 2016; 539: 304-08.

Dreyling M, Jurczak W, Jerkeman M, Silva RS, Rusconi C, Trneny M, Offner F, Caballero D, Joao C, Witzens-Harig M, Hess G, Bence-Bruckler I, Cho SG, et al. Ibrutinib versus temsirolimus in patients with relapsed or refractory mantle-cell lymphoma: an international, randomised, open-label, phase 3 study. Lancet. 2016; 387: 770-8.

Dreyling M, Morschhauser F, Bouabdallah K, Bron D, Cunningham D, Assouline SE, Verhoef G, Linton K, Thieblemont C, Vitolo U, Hiemeyer F, Giurescu M, Garcia-Vargas J, et al. Phase II study of copanlisib, a PI3K inhibitor, in relapsed or refractory, indolent or aggressive lymphoma. Ann Oncol. 2017; 28: 2169-78.

Duggan JM, Buechler MB, Olson RM, Hohl TM, and Hamerman JA. BCAP inhibits proliferation and differentiation of myeloid progenitors in the steady state and during demand situations. Blood. 2017; 129: 1503-13.

Ellmeier W, Jung S, Sunshine MJ, Hatam F, Xu Y, Baltimore D, Mano H, and Littman DR. Severe B cell deficiency in mice lacking the tec kinase family members Tec and Btk. J Exp Med. 2000; 192: 1611-24.

Emanuel P. Juvenile myelomonocytic leukemia and chronic myelomonocytic leukemia. Leukemia. 2008; 2008: 1335-42.

Epling-Burnette PK and Loughran TP, Jr. Suppression of farnesyltransferase activity in acute myeloid leukemia and myelodysplastic syndrome: current understanding and recommended use of tipifarnib. Expert Opin Investig Drugs. 2010; 19: 689-98.

Flinn I, Jäger U, Offner F, Cymbalista F, Hallek M, Caligaris-Cappio F, Delgado J, Hillmen P, Davids MS, Wright DD, Essell JH, Baker BW, Cosolo W, et al. DUO: A phase 3 trial of the PI3K-δ,γ inhibitor IPI-145 versus ofatumumab in patients with relapsed or refractory chronic lymphocytic leukemia or small lymphocytic lymphoma. Journal of Clinical Oncology. 2014; 32: TPS7122-TPS22.

Fruman D, Chiu H, Hopkins B, Bagrodia S, Cantley L, and Abraham R. The PI3K Pathway in Human Disease. Cell. 2017; 170: 605-35.

Fruman DA. Regulatory subunits of class IA PI3K. Curr Top Microbiol Immunol. 2010; 346: 225-44.

Fruman DA, Meyers RE, and Cantley LC. Phosphoinositide kinases. Annu Rev Biochem. 1998; 67: 481-507.

Fruman DA, Snapper SB, Yballe CM, Davidson L, Yu JY, Alt FW, and Cantley LC. Impaired B cell development and proliferation in absence of phosphoinositide 3-kinase p85alpha. Science. 1999; 283: 393-7.

Furlan I, Batz C, Flotho C, Mohr B, Lubbert M, Suttorp M, and Niemeyer CM. Intriguing response to azacitidine in a patient with juvenile myelomonocytic leukemia and monosomy 7. Blood. 2009; 113: 2867-8.

Furman RR, Sharman JP, Coutre SE, Cheson BD, Pagel JM, Hillmen P, Barrientos JC, Zelenetz AD, Kipps TJ, Flinn I, Ghia P, Eradat H, Ervin T, et al. Idelalisib and rituximab in relapsed chronic lymphocytic leukemia. N Engl J Med. 2014; 370: 997-1007.

Garcia Fortanet J, Chen CH, Chen YN, Chen Z, Deng Z, Firestone B, Fekkes P, Fodor M, Fortin PD, Fridrich C, Grunenfelder D, Ho S, Kang ZB, et al. Allosteric Inhibition of SHP2: Identification of a Potent, Selective, and Orally Efficacious Phosphatase Inhibitor. J Med Chem. 2016; 59: 7773-82.

Gaynon PS, Angiolillo AL, Carroll WL, Nachman JB, Trigg ME, Sather HN, Hunger SP, Devidas M, and Children's Oncology G. Long-term results of the children's cancer group studies for childhood acute lymphoblastic leukemia 1983-2002: a Children's Oncology Group Report. Leukemia. 2010; 24: 285-97.

Genovese G, Jaiswal S, Ebert BL, and McCarroll SA. Clonal hematopoiesis and blood-cancer risk. N Engl J Med. 2015; 372: 1071-2.

Gharbi SI, Zvelebil MJ, Shuttleworth SJ, Hancox T, Saghir N, Timms JF, and Waterfield MD. Exploring the specificity of the PI3K family inhibitor LY294002. Biochem J. 2007; 404: 15-21.

Goodwin CB, Li XJ, Mali RS, Chan G, Kang M, Liu Z, Vanhaesebroeck B, Neel BG, Loh ML, Lannutti BJ, Kapur R, and Chan RJ. PI3K p110delta uniquely promotes gain-of-function Shp2-induced GM-CSF hypersensitivity in a model of JMML. Blood. 2014; 123: 2838-42.

Goodwin CB, Li XJ, Mali RS, Chan G, Kang M, Liu Z, Vanhaesebroeck B, Neel BG, Loh ML, Lannutti BJ, Kapur R, and Chan RJ. PI3K p110δ uniquely promotes gain-of-function Shp2-induced GM-CSF hypersensitivity in a model of JMML. Blood. 2014; 123: 2838-42.

Gopal AK, Kahl BS, de Vos S, Wagner-Johnston ND, Schuster SJ, Jurczak WJ, Flinn IW, Flowers CR, Martin P, Viardot A, Blum KA, Goy AH, Davies AJ, et al. PI3Kdelta inhibition by idelalisib in patients with relapsed indolent lymphoma. N Engl J Med. 2014; 370: 1008-18.

Gysin S, Salt M, Young A, and McCormick F. Therapeutic strategies for targeting ras proteins. Genes Cancer. 2011; 2: 359-72.

Halabi S, Sekine E, Verstak B, Gay NJ, and Moncrieffe MC. Structure of the Toll/Interleukin-1 Receptor (TIR) Domain of the B-cell Adaptor That Links Phosphoinositide Metabolism with the Negative Regulation of the Toll-like Receptor (TLR) Signalosome. J Biol Chem. 2017; 292: 652-60.

Hashimoto A, Okada H, Jiang A, Kurosaki M, Greenberg S, Clark EA, and Kurosaki T. Involvement of guanosine triphosphatases and phospholipase C-gamma2 in extracellular signal-regulated kinase, c-Jun NH2-terminal kinase, and p38 mitogen-activated protein kinase activation by the B cell antigen receptor. J Exp Med. 1998; 188: 1287-95.

Hasle H. Myelodysplastic and myeloproliferative disorders of childhood. ASH Education Book. 2016; 2016: 598-604.

Hasle H, Wadsworth LD, Massing BG, McBride M, and Schultz KR. A population-based study of childhood myelodysplastic syndrome in British Columbia, Canada. British Journal of Haematology. 1999; 106: 1027-32.

Hazeki K, Nigorikawa K, and Hazeki O. Role of phosphoinositide 3-kinase in innate immunity. Biol Pharm Bull. 2007; 30: 1617-23.

Hendriks RW, Bredius RG, Pike-Overzet K, and Staal FJ. Biology and novel treatment options for XLA, the most common monogenetic immunodeficiency in man. Expert Opin Ther Targets. 2011; 15: 1003-21.

Honigberg LA, Smith AM, Sirisawad M, Verner E, Loury D, Chang B, Li S, Pan Z, Thamm DH, Miller RA, and Buggy JJ. The Bruton tyrosine kinase inhibitor PCI-32765 blocks B-cell activation and is efficacious in models of autoimmune disease and B-cell malignancy. Proc Natl Acad Sci U S A. 2010; 107: 13075-80.

Hou HA, Kuo YY, Liu CY, Chou WC, Lee MC, Chen CY, Lin LI, Tseng MH, Huang CF, Chiang YC, Lee FY, Liu MC, Liu CW, et al. DNMT3A mutations in acute myeloid leukemia: stability during disease evolution and clinical implications. Blood. 2012; 119: 559-68.

Inagaki J, Fukano R, Nishikawa T, Nakashima K, Sawa D, Ito N, and Okamura J. Outcomes of immunological interventions for mixed chimerism following allogeneic stem cell transplantation in children with juvenile myelomonocytic leukemia. Pediatric Blood & Cancer. 2013; 60: 116-20.

Jaglowski SM, Jones JA, Nagar V, Flynn JM, Andritsos LA, Maddocks KJ, Woyach JA, Blum KA, Grever MR, Smucker K, Ruppert AS, Heerema NA, Lozanski G, et al. Safety and activity of BTK inhibitor ibrutinib combined with ofatumumab in chronic lymphocytic leukemia: a phase 1b/2 study. Blood. 2015; 126: 842-50.

Jaiswal S, Fontanillas P, Flannick J, Manning A, Grauman PV, Mar BG, Lindsley RC, Mermel CH, Burtt N, Chavez A, Higgins JM, Moltchanov V, Kuo FC, et al. Age-related clonal hematopoiesis associated with adverse outcomes. N Engl J Med. 2014; 371: 2488-98.

Jean S and Kiger AA. Classes of phosphoinositide 3-kinases at a glance. J Cell Sci. 2014; 127: 923-8.

Jeong M, Sun D, Luo M, Huang Y, Challen GA, Rodriguez B, Zhang X, Chavez L, Wang H, Hannah R, Kim SB, Yang L, Ko M, et al. Large conserved domains of low DNA methylation maintained by Dnmt3a. Nat Genet. 2014; 46: 17-23.

Khan M, Gibbons JL, and Ferrajoli A. Spotlight on ibrutinib and its potential in frontline treatment of chronic lymphocytic leukemia. Onco Targets Ther. 2017; 10: 1909-14.

Kim SJ, Zhao H, Hardikar S, Singh AK, Goodell MA, and Chen T. A DNMT3A mutation common in AML exhibits dominant-negative effects in murine ES cells. Blood. 2013; 122: 4086-9.

Kim YJ, Sekiya F, Poulin B, Bae YS, and Rhee SG. Mechanism of B-cell receptor-induced phosphorylation and activation of phospholipase C-gamma2. Mol Cell Biol. 2004; 24: 9986-99.

Kracker S, Curtis J, Ibrahim MA, Sediva A, Salisbury J, Campr V, Debre M, Edgar JD, Imai K, Picard C, Casanova JL, Fischer A, Nejentsev S, et al. Occurrence of B-cell

lymphomas in patients with activated phosphoinositide 3-kinase delta syndrome. J Allergy Clin Immunol. 2014; 134: 233-6.
Kratz CP, Niemeyer CM, Castleberry RP, Cetin M, Bergstrasser E, Emanuel PD, Hasle H, Kardos G, Klein C, Kojima S, Stary J, Trebo M, Zecca M, et al. The mutational spectrum of PTPN11 in juvenile myelomonocytic leukemia and Noonan syndrome/myeloproliferative disease. Blood. 2005; 106: 2183-5.
Kuhn R, Schwenk F, Aguet M, and Rajewsky K. Inducible gene targeting in mice. Science. 1995; 269: 1427-9.
LaRochelle J, Fodor M, Ellegast J, Liu X, Vemulapalli V, Mohseni M, Stams T, Buhrlage S, Stegmaier K, LaMarche MJ, Acker MG, and Blacklow S. Identification of an allosteric benzothiazoloprymidone inhibitor of the oncogenic protein tyrosine phosphatase SHP2. Bioorganic & Medicinal Chemistry. 2017.
Lawlor MA and Alessi DR. PKB/Akt: a key mediator of cell proliferation, survival and insulin responses? J Cell Sci. 2001; 114: 2903-10.
Lawrence MS, Stojanov P, Mermel CH, Robinson JT, Garraway LA, Golub TR, Meyerson M, Gabriel SB, Lander ES, and Getz G. Discovery and saturation analysis of cancer genes across 21 tumour types. Nature. 2014; 505: 495-501.
Ley TJ, Ding L, Walter MJ, McLellan MD, Lamprecht T, Larson DE, Kandoth C, Payton JE, Baty J, Welch J, Harris CC, Lichti CF, Townsend RR, et al. DNMT3A mutations in acute myeloid leukemia. N Engl J Med. 2010; 363: 2424-33.
Liu Y, Shreder KR, Gai W, Corral S, Ferris DK, and Rosenblum JS. Wortmannin, a widely used phosphoinositide 3-kinase inhibitor, also potently inhibits mammalian polo-like kinase. Chem Biol. 2005; 12: 99-107.
Locatelli F, Nöllke P, Zecca M, Korthof E, Lanino E, Peters C, Pession A, Kabisch H, Uderzo C, Bonfim CS, Bader P, Dilloo D, Stary J, et al. Hematopoietic stem cell transplantation (HSCT) in children with juvenile myelomonocytic leukemia (JMML): results of the EWOG-MDS/EBMT trial. Blood. 2005; 105: 410-19.
Loh ML. Recent advances in the pathogenesis and treatment of juvenile myelomonocytic leukemia. British Journal of Haematology. 2011; 152: 677-87.
Loh ML, Martinelli S, Cordeddu V, Reynolds MG, Vattikuti S, Lee CM, Wulfert M, Germing U, Haas P, Niemeyer C, Beran ME, Strom S, Lubbert M, et al. Acquired PTPN11 mutations occur rarely in adult patients with myelodysplastic syndromes and chronic myelomonocytic leukemia. Leuk Res. 2005; 29: 459-62.
Loh ML, Reynolds MG, Vattikuti S, Gerbing RB, Alonzo TA, Carlson E, Cheng JW, Lee CM, Lange BJ, Meshinchi S, and Children's Cancer G. PTPN11 mutations in pediatric patients with acute myeloid leukemia: results from the Children's Cancer Group. Leukemia. 2004; 18: 1831-4.
Loh ML, Vattikuti S, Schubbert S, Reynolds MG, Carlson E, Lieuw KH, Cheng JW, Lee CM, Stokoe D, Bonifas JM, Curtiss NP, Gotlib J, Meshinchi S, et al. Mutations in PTPN11 implicate the SHP-2 phosphatase in leukemogenesis. Blood. 2004; 103: 2325-31.
Lorenzana A, Lyons H, Sawaf H, Higgins M, Carrigan D, and Emanuel P. Human herpesvirus 6 infection mimicking juvenile myelomonocytic leukemia in an infant. Journal of Pediatric Hematology/Oncology. 2002; 24: 136-41.

Luo J, Manning BD, and Cantley LC. Targeting the PI3K-Akt pathway in human cancer: rationale and promise. Cancer Cell. 2003; 4: 257-62.

MacFarlane AWt, Yamazaki T, Fang M, Sigal LJ, Kurosaki T, and Campbell KS. Enhanced NK-cell development and function in BCAP-deficient mice. Blood. 2008; 112: 131-40.

Mahajan S, Ghosh S, Sudbeck EA, Zheng Y, Downs S, Hupke M, and Uckun FM. Rational design and synthesis of a novel anti-leukemic agent targeting Bruton's tyrosine kinase (BTK), LFM-A13 [alpha-cyano-beta-hydroxy-beta-methyl-N-(2, 5-dibromophenyl)propenamide]. J Biol Chem. 1999; 274: 9587-99.

Manabe A, Yoshimasu T, Ebihara Y, Yagasaki H, Wada M, Ishikawa K, Hara J, Koike K, Moritake H, Park YD, Tsuji K, and Nakahata T. Viral Infections in Juvenile Myelomonocytic Leukemia: Prevalence and Clinical Implications. Journal of Pediatric Hematology/Oncology. 2004; 26: 636-41.

Mangla A, Khare A, Vineeth V, Panday NN, Mukhopadhyay A, Ravindran B, Bal V, George A, and Rath S. Pleiotropic consequences of Bruton tyrosine kinase deficiency in myeloid lineages lead to poor inflammatory responses. Blood. 2004; 104: 1191-7.

Martinelli S, Carta C, Flex E, Binni F, Cordisco EL, Moretti S, Puxeddu E, Tonacchera M, Pinchera A, McDowell HP, Dominici C, Rosolen A, Di Rocco C, et al. Activating PTPN11 mutations play a minor role in pediatric and adult solid tumors. Cancer Genet Cytogenet. 2006; 166: 124-9.

Matsumura T, Oyama M, Kozuka-Hata H, Ishikawa K, Inoue T, Muta T, Semba K, and Inoue J. Identification of BCAP-(L) as a negative regulator of the TLR signaling-induced production of IL-6 and IL-10 in macrophages by tyrosine phosphoproteomics. Biochem Biophys Res Commun. 2010; 400: 265-70.

Mayle A, Yang L, Rodriguez B, Zhou T, Chang E, Curry CV, Challen GA, Li W, Wheeler D, Rebel VI, and Goodell MA. Dnmt3a loss predisposes murine hematopoietic stem cells to malignant transformation. Blood. 2015; 125: 629-38.

Miklos D, Cutler CS, Arora M, Waller EK, Jagasia M, Pusic I, Flowers ME, Logan AC, Nakamura R, Blazar BR, Li Y, Chang S, Lal I, et al. Ibrutinib for chronic graft-versus-host disease after failure of prior therapy. Blood. 2017.

Miller BW, Przepiorka D, de Claro RA, Lee K, Nie L, Simpson N, Gudi R, Saber H, Shord S, Bullock J, Marathe D, Mehrotra N, Hsieh LS, et al. FDA Approval: Idelalisib Monotherapy for the Treatment of Patients with Follicular Lymphoma and Small Lymphocytic Lymphoma. Clinical Cancer Research. 2015; 21: 1525-29.

Mohi MG and Neel BG. The role of Shp2 (PTPN11) in cancer. Curr Opin Genet Dev. 2007; 17: 23-30.

Moritake H, Ikeda T, Manabe A, Kamimura S, and Nunoi H. Cytomegalovirus infection mimicking juvenile myelomonocytic leukemia showing hypersensitivity to granulocyte–macrophage colony stimulating factor. Pediatric Blood & Cancer. 2009; 53: 1324-26.

Ni M, MacFarlane AWt, Toft M, Lowell CA, Campbell KS, and Hamerman JA. B-cell adaptor for PI3K (BCAP) negatively regulates Toll-like receptor signaling through activation of PI3K. Proc Natl Acad Sci U S A. 2012; 109: 267-72.

Noy A, Vos Sd, Thieblemont C, Martin P, Flowers C, Morschhauser F, Collins GP, Ma S, Coleman M, Peles S, Smith S, Smith A, Munneke B, et al. Single-Agent Ibrutinib Demonstrates Efficacy and Safety in Patients with Relapsed/Refractory Marginal Zone Lymphoma: A Multicenter, Open-Label, Phase 2 Study. Blood. 2016; 128: 1213.

Okada T, Maeda A, Iwamatsu A, Gotoh K, and Kurosaki T. BCAP: the tyrosine kinase substrate that connects B cell receptor to phosphoinositide 3-kinase activation. Immunity. 2000; 13: 817-27.

Okano M, Bell DW, Haber DA, and Li E. DNA methyltransferases Dnmt3a and Dnmt3b are essential for de novo methylation and mammalian development. Cell. 1999; 99: 247-57.

Okkenhaug K, Bilancio A, Farjot G, Priddle H, Sancho S, Peskett E, Pearce W, Meek SE, Salpekar A, Waterfield MD, Smith AJ, and Vanhaesebroeck B. Impaired B and T cell antigen receptor signaling in p110delta PI 3-kinase mutant mice. Science. 2002; 297: 1031-4.

Park H, Wahl MI, Afar DE, Turck CW, Rawlings DJ, Tam C, Scharenberg AM, Kinet JP, and Witte ON. Regulation of Btk function by a major autophosphorylation site within the SH3 domain. Immunity. 1996; 4: 515-25.

Passmore SJ, Chessells JM, Kempski H, Hann IM, Brownbill PA, and Stiller CA. Paediatric myelodysplastic syndromes and juvenile myelomonocytic leukaemia in the UK: a population-based study of incidence and survival. British Journal of Haematology. 2003; 121: 758-67.

Pathak MK and Yi T. Sodium stibogluconate is a potent inhibitor of protein tyrosine phosphatases and augments cytokine responses in hemopoietic cell lines. J Immunol. 2001; 167: 3391-7.

Prabhu SB, Gupta R, and Seth R. Juvenile Myelomonocytic Leukemia Presenting With Coexistent Cytomegalovirus Infection—A Case Report. Journal of Pediatric Hematology/Oncology. 2010; 32: e153-e54.

Qin S and Chock PB. Implication of phosphatidylinositol 3-kinase membrane recruitment in hydrogen peroxide-induced activation of PI3K and Akt. Biochemistry. 2003; 42: 2995-3003.

Qiu W, Wang X, Romanov V, Hutchinson A, Lin A, Ruzanov M, Battaile KP, Pai EF, Neel BG, and Chirgadze NY. Structural insights into Noonan/LEOPARD syndrome-related mutants of protein-tyrosine phosphatase SHP2 (PTPN11). BMC Struct Biol. 2014; 14: 10.

Rawlings DJ, Saffran DC, Tsukada S, Largaespada DA, Grimaldi JC, Cohen L, Mohr RN, Bazan JF, Howard M, Copeland NG, and et al. Mutation of unique region of Bruton's tyrosine kinase in immunodeficient XID mice. Science. 1993; 261: 358-61.

Rawlings DJ, Scharenberg AM, Park H, Wahl MI, Lin S, Kato RM, Fluckiger AC, Witte ON, and Kinet JP. Activation of BTK by a phosphorylation mechanism initiated by SRC family kinases. Science. 1996; 271: 822-5.

Reddy EP and Aggarwal AK. The ins and outs of bcr-abl inhibition. Genes Cancer. 2012; 3: 447-54.

Ronnstrand L, Arvidsson AK, Kallin A, Rorsman C, Hellman U, Engstrom U, Wernstedt C, and Heldin CH. SHP-2 binds to Tyr763 and Tyr1009 in the PDGF beta-receptor and mediates PDGF-induced activation of the Ras/MAP kinase pathway and chemotaxis. Oncogene. 1999; 18: 3696-702.

Rordorf-Nikolic T, Van Horn DJ, Chen D, White MF, and Backer JM. Regulation of phosphatidylinositol 3'-kinase by tyrosyl phosphoproteins. Full activation requires occupancy of both SH2 domains in the 85-kDa regulatory subunit. J Biol Chem. 1995; 270: 3662-6.

Rushworth SA, Murray MY, Zaitseva L, Bowles KM, and MacEwan DJ. Identification of Bruton's tyrosine kinase as a therapeutic target in acute myeloid leukemia. Blood. 2014; 123: 1229-38.

Saito K, Tolias KF, Saci A, Koon HB, Humphries LA, Scharenberg A, Rawlings DJ, Kinet JP, and Carpenter CL. BTK regulates PtdIns-4,5-P2 synthesis: importance for calcium signaling and PI3K activity. Immunity. 2003; 19: 669-78.

Sakaguchi H, Okuno Y, Muramatsu H, Yoshida K, Shiraishi Y, Takahashi M, Kon A, Sanada M, Chiba K, Tanaka H, Makishima H, Wang X, Xu Y, et al. Exome sequencing identifies secondary mutations of SETBP1 and JAK3 in juvenile myelomonocytic leukemia. Nature Genetics. 2013; 45: 937-41.

Sarkissian S and O'Brien S. Second-Generation Brutons Tyrosine Kinase Inhibitors. American Journal of Hematology/Oncology. 2017; 13: 29-34.

Schubbert S, Lieuw K, Rowe SL, Lee CM, Li X, Loh ML, Clapp DW, and Shannon KM. Functional analysis of leukemia-associated PTPN11 mutations in primary hematopoietic cells. Blood. 2005; 106: 311-7.

Shimizu T, Tolcher A, Papadopoulos K, Beeram M, Rasco D, Smith L, Gunn S, Smetzer L, Mays T, Kaiser B, Wick M, Alvarez C, Cavazos A, et al. The Clinical Effect of the Dual-Targeting Strategy Involving PI3K/AKT/mTOR and RAS/MEK/ERK Pathways in Patients with Advanced Cancer. Clinical Cancer Research. 2012; 18: 2316-25.

Shoelson SE, Sivaraja M, Williams KP, Hu P, Schlessinger J, and Weiss MA. Specific phosphopeptide binding regulates a conformational change in the PI 3-kinase SH2 domain associated with enzyme activation. EMBO J. 1993; 12: 795-802.

Smith CI, Baskin B, Humire-Greiff P, Zhou JN, Olsson PG, Maniar HS, Kjellen P, Lambris JD, Christensson B, Hammarstrom L, and et al. Expression of Bruton's agammaglobulinemia tyrosine kinase gene, BTK, is selectively down-regulated in T lymphocytes and plasma cells. J Immunol. 1994; 152: 557-65.

Somoza JR, Koditek D, Villasenor AG, Novikov N, Wong MH, Liclican A, Xing W, Lagpacan L, Wang R, Schultz BE, Papalia GA, Samuel D, Lad L, et al. Structural, biochemical, and biophysical characterization of idelalisib binding to phosphoinositide 3-kinase delta. J Biol Chem. 2015; 290: 8439-46.

Song S, Chew C, Dale BM, Traum D, Peacock J, Yamazaki T, Clynes R, Kurosaki T, and Greenberg S. A requirement for the p85 PI3K adapter protein BCAP in the protection of macrophages from apoptosis induced by endoplasmic reticulum stress. J Immunol. 2011; 187: 619-25.

Songyang Z, Shoelson SE, Chaudhuri M, Gish G, Pawson T, Haser WG, King F, Roberts T, Ratnofsky S, Lechleider RJ, and et al. SH2 domains recognize specific phosphopeptide sequences. Cell. 1993; 72: 767-78.

Speck B, Bortin M, Champlin R, Goldman J, Herzig R, McGlave P, Messner H, Weiner R, and Rimm A. Allogeneic bone-marrow transplantation for chronic myelogenous leukaemia. Lancet. 1984; 1: 665-68.

Stieglitz E, Mazor T, Olshen AB, Geng H, Gelston LC, Akutagawa J, Lipka DB, Plass C, Flotho C, Chehab FF, Braun BS, Costello JF, and Loh ML. Genome-wide DNA methylation is predictive of outcome in juvenile myelomonocytic leukemia. Nat Commun. 2017; 8: 2127.

Stieglitz E, Taylor-Weiner AN, Chang TY, Gelston LC, Wang YD, Mazor T, Esquivel E, Yu A, Seepo S, Olsen S, Rosenberg M, Archambeault SL, Abusin G, et al. The genomic landscape of juvenile myelomonocytic leukemia. Nat Genet. 2015; 47: 1326-33.

Stieglitz E, Troup CB, Gelston LC, Haliburton J, Chow ED, Yu KB, Akutagawa J, Taylor-Weiner AN, Liu YL, Wang Y-D, Beckman K, Emanuel PD, Braun BS, et al. Subclonal mutations in SETBP1 confer a poor prognosis in juvenile myelomonocytic leukemia. Blood. 2015; 125: 516-24.

Stieglitz E, Ward AF, Gerbing RB, Alonzo TA, Arceci RJ, Liu YL, Emanuel PD, Widemann BC, Cheng JW, Jayaprakash N, Balis FM, Castleberry RP, Bunin NJ, et al. Phase II/III trial of a pre-transplant farnesyl transferase inhibitor in juvenile myelomonocytic leukemia: a report from the Children's Oncology Group. Pediatr Blood Cancer. 2015; 62: 629-36.

Sujobert P, Bardet V, Cornillet-Lefebvre P, Hayflick JS, Prie N, Verdier F, Vanhaesebroeck B, Muller O, Pesce F, Ifrah N, Hunault-Berger M, Berthou C, Villemagne B, et al. Essential role for the p110delta isoform in phosphoinositide 3-kinase activation and cell proliferation in acute myeloid leukemia. Blood. 2005; 106: 1063-6.

Tampella G, Kerns HM, Niu D, Singh S, Khim S, Bosch KA, Garrett ME, Moguche A, Evans E, Browning B, Jahan TA, Nacht M, Wolf-Yadlin A, et al. The Tec Kinase-Regulated Phosphoproteome Reveals a Mechanism for the Regulation of Inhibitory Signals in Murine Macrophages. J Immunol. 2015; 195: 246-56.

Tang P, Upton JEM, Barton-Forbes MA, Salvadori MI, Clynick MP, Price AK, and Goobie SL. Autosomal Recessive Agammaglobulinemia Due to a Homozygous Mutation in PIK3R1. J Clin Immunol. 2017.

Tartaglia M and Gelb BD. Noonan syndrome and related disorders: genetics and pathogenesis. Annu Rev Genomics Hum Genet. 2005; 6: 45-68.

Tartaglia M, Kalidas K, Shaw A, Song X, Musat DL, van der Burgt I, Brunner HG, Bertola DR, Crosby A, Ion A, Kucherlapati RS, Jeffery S, Patton MA, et al. PTPN11 mutations in Noonan syndrome: molecular spectrum, genotype-phenotype correlation, and phenotypic heterogeneity. Am J Hum Genet. 2002; 70: 1555-63.

Tartaglia M, Martinelli S, Cazzaniga G, Cordeddu V, Iavarone I, Spinelli M, Palmi C, Carta C, Pession A, Arico M, Masera G, Basso G, Sorcini M, et al. Genetic evidence for lineage-related and differentiation stage-related contribution of somatic PTPN11 mutations to leukemogenesis in childhood acute leukemia. Blood. 2004; 104: 307-13.

Tartaglia M, Mehler EL, Goldberg R, Zampino G, Brunner HG, Kremer H, van der Burgt I, Crosby AH, Ion A, Jeffery S, Kalidas K, Patton MA, Kucherlapati RS, et al. Mutations in PTPN11, encoding the protein tyrosine phosphatase SHP-2, cause Noonan syndrome. Nat Genet. 2001; 29: 465-8.

Tartaglia M, Niemeyer CM, Fragale A, Song X, Buechner J, Jung A, Hahlen K, Hasle H, Licht JD, and Gelb BD. Somatic mutations in PTPN11 in juvenile myelomonocytic leukemia, myelodysplastic syndromes and acute myeloid leukemia. Nat Genet. 2003; 34: 148-50.

Tefferi A and Vardiman J. Classification and diagnosis of myeloproliferative neoplasms: The 2008 World Health Organization criteria and point-of-care diagnostic algorithms. Leukemia. 2008; 22: 14-22.

Thomas JD, Sideras P, Smith CI, Vorechovsky I, Chapman V, and Paul WE. Colocalization of X-linked agammaglobulinemia and X-linked immunodeficiency genes. Science. 1993; 261: 355-8.

Tsukada S, Saffran DC, Rawlings DJ, Parolini O, Allen RC, Klisak I, Sparkes RS, Kubagawa H, Mohandas T, Quan S, and et al. Deficient expression of a B cell cytoplasmic tyrosine kinase in human X-linked agammaglobulinemia. Cell. 1993; 72: 279-90.

Vadas O, Burke JE, Zhang X, Berndt A, and Williams RL. Structural basis for activation and inhibition of class I phosphoinositide 3-kinases. Sci Signal. 2011; 4: re2.

Vanhaesebroeck B, Guillermet-Guibert J, Graupera M, and Bilanges B. The emerging mechanisms of isoform-specific PI3K signalling. Nat Rev Mol Cell Biol. 2010; 11: 329-41.

Vetrie D, Vorechovsky I, Sideras P, Holland J, Davies A, Flinter F, Hammarstrom L, Kinnon C, Levinsky R, Bobrow M, and et al. The gene involved in X-linked agammaglobulinaemia is a member of the src family of protein-tyrosine kinases. Nature. 1993; 361: 226-33.

Walter MJ, Ding L, Shen D, Shao J, Grillot M, McLellan M, Fulton R, Schmidt H, Kalicki-Veizer J, O'Laughlin M, Kandoth C, Baty J, Westervelt P, et al. Recurrent DNMT3A mutations in patients with myelodysplastic syndromes. Leukemia. 2011; 25: 1153-8.

Wang DS and Shaw G. The association of the C-terminal region of beta I sigma II spectrin to brain membranes is mediated by a PH domain, does not require membrane proteins, and coincides with a inositol-1,4,5 triphosphate binding site. Biochem Biophys Res Commun. 1995; 217: 608-15.

Wang ML, Lee H, Chuang H, Wagner-Bartak N, Hagemeister F, Westin J, Fayad L, Samaniego F, Turturro F, Oki Y, Chen W, Badillo M, Nomie K, et al. Ibrutinib in combination with rituximab in relapsed or refractory mantle cell lymphoma: a single-centre, open-label, phase 2 trial. Lancet Oncol. 2016; 17: 48-56.

Woyach JA, Furman RR, Liu TM, Ozer HG, Zapatka M, Ruppert AS, Xue L, Li DH, Steggerda SM, Versele M, Dave SS, Zhang J, Yilmaz AS, et al. Resistance mechanisms for the Bruton's tyrosine kinase inhibitor ibrutinib. N Engl J Med. 2014; 370: 2286-94.

Xie M, Lu C, Wang J, McLellan MD, Johnson KJ, Wendl MC, McMichael JF, Schmidt HK, Yellapantula V, Miller CA, Ozenberger BA, Welch JS, Link DC, et al. Age-related

mutations associated with clonal hematopoietic expansion and malignancies. Nat Med. 2014; 20: 1472-8.
Xu D, Liu X, Yu W-M, Meyerson HJ, Guo C, Gerson SL, and Qu C-K. Non–lineage/stage-restricted effects of a gain-of-function mutation in tyrosine phosphatase Ptpn11 (Shp2) on malignant transformation of hematopoietic cells. Journal of Experimental Medicine. 2011; 208: 1977-88.
Xu D, Liu X, Yu WM, Meyerson HJ, Guo C, Gerson SL, and Qu CK. Non-lineage/stage-restricted effects of a gain-of-function mutation in tyrosine phosphatase Ptpn11 (Shp2) on malignant transformation of hematopoietic cells. J Exp Med. 2011; 208: 1977-88.
Xu Y, Wang Y, Yao A, Xu Z, Dou H, Shen S, Hou Y, and Wang T. Low Frequency Magnetic Fields Induce Autophagy-associated Cell Death in Lung Cancer through miR-486-mediated Inhibition of Akt/mTOR Signaling Pathway. Sci Rep. 2017; 7: 11776.
Yamazaki T, Takeda K, Gotoh K, Takeshima H, Akira S, and Kurosaki T. Essential immunoregulatory role for BCAP in B cell development and function. J Exp Med. 2002; 195: 535-45.
Yang L, Rau R, and Goodell MA. DNMT3A in haematological malignancies. Nat Rev Cancer. 2015; 15: 152-65.
Yang Q, Modi P, Newcomb T, Queva C, and Gandhi V. Idelalisib: First-in-Class PI3K Delta Inhibitor for the Treatment of Chronic Lymphocytic Leukemia, Small Lymphocytic Leukemia, and Follicular Lymphoma. Clin Cancer Res. 2015; 21: 1537-42.
Yang Z, Li Y, Yin F, and Chan RJ. Activating PTPN11 mutants promote hematopoietic progenitor cell-cycle progression and survival. Exp Hematol. 2008; 36: 1285-96.
Yi T, Elson P, Mitsuhashi M, Jacobs B, Hollovary E, Budd TG, Spiro T, Triozzi P, and Borden EC. Phosphatase inhibitor, sodium stibogluconate, in combination with interferon (IFN) alpha 2b: phase I trials to identify pharmacodynamic and clinical effects. Oncotarget. 2011; 2: 1155-64.
Yoshimi A, Mohamed M, Bierings M, Urban C, Korthof E, Zecca M, Sykora K, Duffner U, Trebo M, Matthes-Martin S, Sedlacek P, Klingebiel T, Lang P, et al. Second allogeneic hematopoietic stem cell transplantation (HSCT) results in outcome similar to that of first HSCT for patients with juvenile myelomonocytic leukemia. Leukemia. 2007; 21: 556-60.
You JS and Jones PA. Cancer genetics and epigenetics: two sides of the same coin? Cancer Cell. 2012; 22: 9-20.
Young AL, Challen GA, Birmann BM, and Druley TE. Clonal haematopoiesis harbouring AML-associated mutations is ubiquitous in healthy adults. Nat Commun. 2016; 7: 12484.
Yu J, Wjasow C, and Backer JM. Regulation of the p85/p110alpha phosphatidylinositol 3'-kinase. Distinct roles for the n-terminal and c-terminal SH2 domains. J Biol Chem. 1998; 273: 30199-203.
Yu Q, Zhou B, Zhang Y, Nguyen ET, Du J, Glosson NL, and Kaplan MH. DNA methyltransferase 3a limits the expression of interleukin-13 in T helper 2 cells and allergic airway inflammation. Proc Natl Acad Sci U S A. 2012; 109: 541-6.

Yun S, Vincelette ND, Acharya U, and Abraham I. Risk of Atrial Fibrillation and Bleeding Diathesis Associated With Ibrutinib Treatment: A Systematic Review and Pooled Analysis of Four Randomized Controlled Trials. Clin Lymphoma Myeloma Leuk. 2017; 17: 31-37 e13.

Zhao L and Vogt PK. Class I PI3K in oncogenic cellular transformation. Oncogene. 2008; 27: 5486-96.

CURRICULUM VITAE

Lisa Deng

Education

2018	PhD, Medical and Molecular Genetics Medical Scientist Training Program (MD/PhD) Indiana University, Indianapolis, Indiana Dissertation: The Role of Bruton's Tyrosine Kinase and PI3K p110δ in Mutant Shp2-Induced Juvenile Myelomonocytic Leukemia Co-Advisors: Rebecca J. Chan, MD, PhD and Reuben Kapur, PhD
2011	B.A., Biology: Molecular Biology and Biochemistry Minor: Mathematics Minor: Chinese Language & Culture Washington University in St. Louis, St. Louis, Missouri

Honors and Awards

2017	Indiana University School of Medicine Graduate Student Travel Grant. Pharmacologic Inhibition of PI3K p110δ in Mutant Shp2E76K-Expressing Mice. American Society of Hematology 59th Annual Meeting, Atlanta, GA.
2016	Abstract Travel Award. Evaluation of Bruton's Tyrosine Kinase and PI3K p110δ in Mutant Shp2-Induced Juvenile Myelomonocytic Leukemia. JMML International Symposium, San Diego, CA.
2016	Indiana University School of Medicine Graduate Student Travel Grant. Evaluation of Bruton's Tyrosine Kinase and PI3K p110δ in Mutant Shp2-Induced Juvenile Myelomonocytic Leukemia. JMML International Symposium, San Diego, CA.
2016	Bauer Travel Award. MD/PhD National Student Conference, Keystone, CO.
2015	Jim Heller Travel Grant. The Role of PI3K p110δ in Gain-of-Function Shp2 Neutrophil ROS Production and Myelomonocytic Progenitor Infiltration of Peripheral Tissue. American Medical Women's Association 100th National Meeting.
2013	Top poster presenter, Student Research Program in Academic Medicine
2008-2011	Dean's List, Washington University in St. Louis
2009	Howard Hughes Medical Institute/Washington University Summer Undergraduate Research Fellowship

Publications

Deng L, Richine BM, Virts EL, Jideonwo-Auman VN, Chan RJ, Kapur R. Rapid Development of Myeloproliferative Neoplasm in Mice with Ptpn11D61Y Mutation and Haploinsufficient for Dnmt3a. Oncotarget. 2017 Dec 26; doi:10.18632/oncotarget.23680

Tarnawsky SP, Yoshimoto M, **Deng L**, Chan RJ, Yoder M. Yolk Sac Erythromyeloid Progenitors Expressing Gain-of-Function PTPN11 Have Features Of JMML But Are Not Sufficient To Cause Disease In Mice. Developmental Dynamics. 2017 Oct 4; doi: 10.1002/dvdy.24598.

Deng L, Virts EL, Kapur R, Chan RJ. Pharmacologic inhibition of PI3K p110δ in mutant Shp2E76K-expressing mice. Oncotarget. 2017 Oct 3; doi: 10.18632/oncotarget.21455.

Deng L, Chan RJ. Cleaning up the environment in juvenile myelomonocytic leukemia. Transl Cancer Res. 2017;6(Suppl 1):S36-S38. doi: 10.21037/tcr.2017.02.06.

O'Leary HA, Capitano M, Cooper S, Mantel C, Boswell HS, Kapur R, Ramdas B, Chan RJ, **Deng L**, Qu CK, Broxmeyer HE. DPP4 truncated GM-CSF and IL-3 manifest distinct receptor-binding and regulatory functions compared with their full-length forms. Leukemia. 2017 April 21; doi: 10.1038/leu.2017.98.

Li XJ*, **Deng L***, Brandt SL, Goodwin CB, Ma P, Yang Z, Mali RS, Liu Z, Kapur R, Serezani CH, Chan RJ. Role of p85α in neutrophil extra- and intracellular reactive oxygen species generation. Oncotarget. 2016 Apr 26;7(17): 23096-105.

Pope WH, Anders KR, Baird M, Bowman CA, Boyle MM, Broussard GW, Chow T, Clase KL, Cooper S, Cornely KA, DeJong RJ, Delesalle VA, **Deng L**, Dunbar D, Edgington NP, Ferreira CM, Hafer KW, Hartzog GA, Hatherill JR, Hughes LE, Ipapo K, Krukonis GP, Meier CG, Monti DL, Olm MR, Page ST, Peebles CL, Rinehart CA, Rubin MR, Russell DA, Sanders ER, Schoer M, Shaffer CD, Wherley J, Vazquea E, Yuan H, Zhang C, Cresawn SG, Jacobs-Sera D, Hendrix RW, Hatfull GF. Cluster M mycobacteriophages Bongo, PegLeg, and Rey with unusually large repertoires of tRNA isotypes. J. Virol. 2014 March;88(5): 2461-80.

Pope WT, Jacobs-Sera D, Russell DA, et al. Expanding the diversity of mycobacteriophages: insights into genome architecture and evolution. PLoS ONE. 2011 Jan 27;6(1): e16329.

Oral Presentations

Deng L, Goodwin CB, Chan RJ. Evaluation of Bruton's Tyrosine Kinase and PI3K p110δ in Mutant Shp2-Induced Juvenile Myelomonocytic Leukemia. JMML International Symposium, San Diego, CA. December 1-2, 2016.

Abstracts

Deng L, Virts EL, Kapur R, Chan RJ. Pharmacologic Inhibition of PI3Kδ Prolongs Survival of Mutant Shp2E76K-Expressing Mice. Poster: American Society of Hematology 59th Annual Meeting. December 9, 2017.

Deng L, Goodwin CB, Chan RJ. Evaluation of Bruton's Tyrosine Kinase and PI3K p110δ in Mutant Shp2-Induced Juvenile Myelomonocytic Leukemia. Poster: 31st Annual MD/PhD National Student Conference. Keystone, CO. July 15-17, 2016.

Deng L, Li XJ, Mikan R, Chan RJ. The Role of PI3K p110δ in Gain-of-Function Shp2 Neutrophil ROS Production and Myelomonocytic Progenitor Infiltration of Peripheral Tissue. Poster: American Medical Women's Association 100th National Meeting. Chicago, IL. April 23-26, 2015.

Deng L, Goodwin CB, Chan RJ. JNK and FAK as Targets for Inhibition in Gain-of-Function Shp2-induced Myeloproliferative Disorder. Poster: American Medical Women's Association 99th National Meeting, Washington, D.C. March 13-16, 2014.

Deng L, Goodwin CB, Chan RJ. JNK and FAK as Novel Disease Driving Molecules in Juvenile Myelomonocytic Leukemia. Poster: Student Research Program in Academic Medicine Poster Session, Indianapolis, IN. September 5, 2013.

Deng L, Sasaki Y, Milbrandt J. Regulation of Enzymes in Intracellular NAD^+ Biosynthesis Pathways. Poster: Washington University Spring Undergraduate Research Symposium, St. Louis, MO. 2011.

Deng L, Khan A, Sibley LD. Population Structure of Key Host Transcription Modulator Gene in *Toxoplasma gondii.* Poster: Washington University Fall Undergraduate Research Symposium, St. Louis, MO. 2009.

Barshop W, Anderson A, Alford S, Ng P, Huang V, **Deng L**. Isolation and Characterization of Mycobacteriophage Uncle Howie. Poster: Washington University Spring Undergraduate Research Symposium, St. Louis, MO. 2009.

Grants and Scholarships

2016-2020	NIH/NCI, National Research Service Award F30 CA210518 "Evaluation of Bruton's Tyrosine Kinase and p110 delta in Mutant Shp2-Induced JMML"
2015-2016	T32 HL007910, "Basic Science Studies on Gene Therapy of Blood Diseases." IUSM, Indianapolis, IN
2012-2014, 2018-2020	Indiana University School of Medicine scholarship through the IUSM Scholars Program, awarded based on academic credentials. IUSM, Indianapolis, IN